

AD-A124 304 CARS DIAGNOSTICS OF HIGH PRESSURE COMBUSTION(U) UNITED
TECHNOLOGIES RESEARCH CENTER EAST HARTFORD CT
J H STUFFLEBEAM ET AL. NOV 82 RB2-984888-F

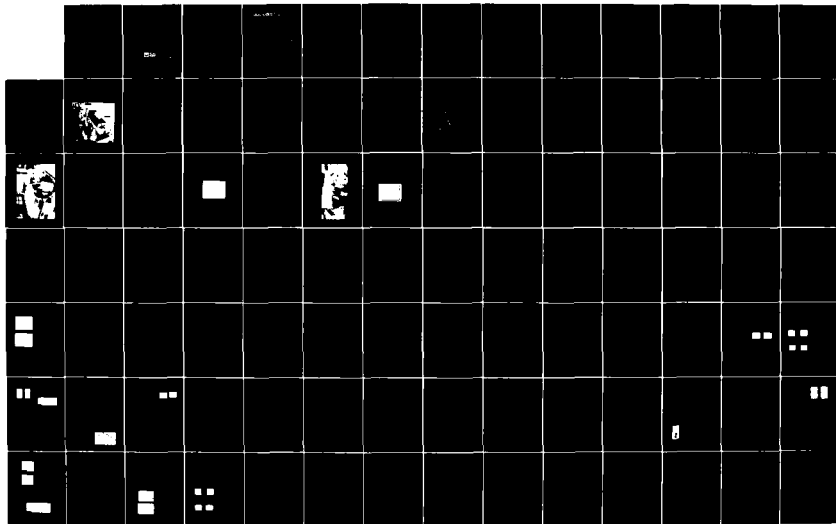
1/2

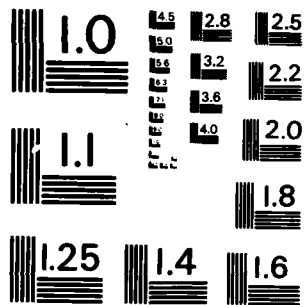
UNCLASSIFIED

ARO-16124.6-CH DAA029-79-C-0008

F/G 21/2

NL





MICROCOPY RESOLUTION TEST CHART
NATIONAL BUREAU OF STANDARDS - 1963 - A

ARO 16124.6-CH

R82-954566-F

12

CARS DIAGNOSTICS OF HIGH PRESSURE COMBUSTION

Final Report

J.H. Stufflebeam
J.A. Shirley
R.J. Hall

November, 1982

U.S. Army Research Office
Contract: DAAG29-79-C-0008



**UNITED
TECHNOLOGIES
RESEARCH
CENTER**

East Hartford, Connecticut 06108

DTIC
FEB 14 1983
H

ADA 124304

DTIC FILE COPY

Approved for Public Release;
Distribution Unlimited

83 02 014 003

83-1-4-1

THE VIEW, OPINIONS, AND/OR FINDINGS CONTAINED IN THIS REPORT ARE THOSE OF THE AUTHOR(S) AND SHOULD NOT BE CONSTRUED AS AN OFFICIAL DEPARTMENT OF THE ARMY POSITION, POLICY, OR DECISION, UNLESS SO DESIGNATED BY OTHER DOCUMENTATION.

**UNITED TECHNOLOGIES
RESEARCH CENTER**



East Hartford, Connecticut 06108

R82-954566-F

CARS Diagnostics of High Pressure Combustion

Final Report

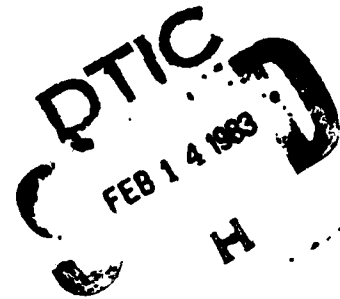
J. H. Stufflebeam
J. A. Shirley
R. J. Hall

November 1982

U. S. Army Research Office
Contract: DAAG29-79-C-0008

United Technologies Research Center
East Hartford, CT 06108

Approved for Public Release;
Distribution Unlimited



REPORT DOCUMENTATION PAGE		READ INSTRUCTIONS BEFORE COMPLETING FORM
1. REPORT NUMBER R82-954566-F	2. GOVT ACCESSION NO. AD-A124 304	3. RECIPIENT'S CATALOG NUMBER
4. TITLE (and Subtitle) CARS DIAGNOSTICS OF HIGH PRESSURE COMBUSTION	5. TYPE OF REPORT & PERIOD COVERED Final Technical Report 2/15/79 to 9/30/82	
	6. PERFORMING ORG. REPORT NUMBER R82-954566-F	
7. AUTHOR(s) J. H. Stufflebeam J. A. Shirley R. J. Hall	8. CONTRACT OR GRANT NUMBER(s) DAAG29-79-C-0008	
9. PERFORMING ORGANIZATION NAME AND ADDRESS United Technologies Research Center East Hartford, CT 06108	10. PROGRAM ELEMENT, PROJECT, TASK AREA & WORK UNIT NUMBERS	
11. CONTROLLING OFFICE NAME AND ADDRESS U. S. Army Research Office P.O. Box 1211 Research Triangle Park, N. C. 27709	12. REPORT DATE November 1982	
	13. NUMBER OF PAGES	
14. MONITORING AGENCY NAME & ADDRESS (if different from Controlling Office)	15. SECURITY CLASS. (of this report) Unclassified	
	15a. DECLASSIFICATION/DOWNGRADING SCHEDULE	
16. DISTRIBUTION STATEMENT (of this Report) Unlimited		
17. DISTRIBUTION STATEMENT (of the abstract entered in Block 20, if different from Report)		
18. SUPPLEMENTARY NOTES		
19. KEY WORDS (Continue on reverse side if necessary and identify by block number) CARS, Coherent Anti-Stokes Raman Spectroscopy, Remote Combustion Diagnostics, High Pressure Combustion Diagnostics, Nitrogen Thermometry, Carbon Dioxide, CARS Spectra, Collisional Narrowing, Picosecond CARS, Concentration Sensitivity Enhancement		
20. ABSTRACT (Continue on reverse side if necessary and identify by block number) Under Contract DAAG29-79-C-0008 sponsored by the Army Research Office, the United Technologies Research Center (UTRC) has conducted basic research investigations into coherent anti-Stokes Raman spectroscopy (CARS). CARS is a remote laser diagnostic technique for temperature and species measurements in hostile combustion environments. As such it possesses considerable relevance to the Army in the general areas of ballistics, propulsion and internal combustion engines.		

UNCLASSIFIED

SECURITY CLASSIFICATION OF THIS PAGE(When Data Entered)

This final report describes the results of the investigations which were conducted in two specific areas. The first area concerns the effects of high pressure, specifically the phenomenon of collisional narrowing, on CARS spectra from which temperature and density information derive. Experimental studies of CARS spectra were conducted in N_2 and CO_2 in a heated, high pressure cell. The experimental spectra were in excellent agreement with the theoretical model developed to describe high pressure CARS spectroscopy. The second area of investigation focused upon the use of picosecond pulses as a means of suppressing the sometimes undesirable nonresonant background which can limit CARS species detectivity. The main purpose of the study was to ascertain whether the background could be suppressed with picosecond pump-probe techniques with less resonant signal loss than accompanies the more widely utilized polarization approach. Using broadband CARS generation and detection, as normally used for time-resolved diagnostics, pump-probe approaches appear to possess little advantage for gas-phase work relative to the simpler polarization techniques. For narrowband CARS work, the results would lead one to infer less signal loss with pump-probe techniques vis-a-vis the polarization methods.

UNCLASSIFIED

SECURITY CLASSIFICATION OF THIS PAGE(When Data Entered)

FOREWORD

This report covers work accomplished under ARO Contract DAAG29-79-C-0008 during the period February 15, 1979 to September 30, 1982. The original contract included provision for studying the high pressure, high temperature CARS spectra of nitrogen and carbon dioxide for the purpose of accurate thermometry in combustion media. Subsequent events mandated an extension to the contract with two aims in mind. First, the study of picosecond pulse techniques in CARS spectroscopy was added for the purpose of resonant signal enhancement over the nonresonant background as a means to improve detectivity. Second, modifications to the UTRC high pressure facility were necessary to allow the acquisition of high pressure and high temperature CARS spectra.

The personnel involved with this contract have had responsibilities for different phases of the work. James F. Verdieck did the high pressure spectroscopy at room temperature for N₂ and CO₂ and also the work in N₂ at elevated temperature up to 30 atmospheres. John H. Stufflebeam continued the high pressure CARS work under the contract extension and obtained the data on N₂ for the conditions of both high pressure and high temperature. Robert J. Hall was responsible for the theoretical aspects of high pressure CARS spectroscopy including the computer analyses employed to model the experimental data. John A. Shirley carried out the picosecond CARS studies. Alan C. Eckbreth, Manager, Chemical Physics, provided the overall direction of the experimental and theoretical aspects of this work.

Accession For	
DTIC GRA&I	<input checked="" type="checkbox"/>
DTIC T.S	<input type="checkbox"/>
Unannounced	<input type="checkbox"/>
Justification	
By _____	
Distribution/ _____	
Availability Codes	
Dist	Avail and/or Special
A	

DTIC
COPY
INSPECTED

CARS Diagnostics of High Pressure Combustion

TABLE OF CONTENTS

	<u>Page</u>
FOREWORD.	iii
SUMMARY	1
INTRODUCTION.	3
HIGH PRESSURE CARS SPECTROSCOPY	5
Experimental Apparatus	5
Experimental Results	5
Theoretical Considerations	13
PICOSECOND CARS INVESTIGATIONS.	19
CARS Nonresonant Susceptibility Effects.	19
N ₂ Delayed CARS Experiments.	21
Theory of Transient Coherent Raman Spectroscopy.	33
Discussion of Results.	41
Conclusions.	42
REFERENCES.	43
APPENDIX A - PUBLICATIONS/PRESENTATIONS UNDER ARO CONTRACT DAAG29-79-C-0008 CARS DIAGNOSTICS OF HIGH PRESSURE COMBUSTION	
APPENDIX B - PARTICIPATING SCIENTIFIC PERSONNEL AND DEGREES AWARDED DURING THIS CONTRACT	
APPENDIX C - COLLISIONAL NARROWING OF THE HIGH PRESSURE CARS SPECTRUM OF N ₂	
APPENDIX D - PRESSURE-INDUCED NARROWING OF THE CARS SPECTRUM OF N ₂	
APPENDIX E - COMBUSTION DIAGNOSTICS BY COHERENT ANTI-STOKES RAMAN SPECTROSCOPY (CARS)	
APPENDIX F - CARS THERMOMETRY IN REACTING SYSTEMS	
APPENDIX G - APPLICATION OF THE ROTATIONAL DIFFUSION MODEL TO GASEOUS N ₂ CARS SPECTRA	
APPENDIX H - SOME APPLICATIONS OF GAS PHASE CARS SPECTROSCOPY	
APPENDIX I - ROTATIONAL DIFFUSION THEORY CALCULATIONS OF HIGH PRESSURE N ₂ AND CO ₂ CARS BANDSHAPES	

R82-954566-F

CARS Diagnostics of High Pressure Combustion

SUMMARY

Under Contract DAAG29-79-C-0008 sponsored by the Army Research Office, the United Technologies Research Center (UTRC) has conducted basic research investigations into coherent anti-Stokes Raman spectroscopy (CARS). CARS is a remote laser diagnostic technique for temperature and species measurements in hostile combustion environments. As such it possesses considerable relevance to the Army in the general areas of ballistics, propulsion and internal combustion engines. This final report describes the results of the investigations which were conducted in two specific areas. The first area concerns the effects of high pressure, specifically the phenomenon of collisional narrowing, on CARS spectra from which temperature and density information derive. Experimental studies of CARS spectra were conducted in N_2 and CO_2 in a heated, high pressure cell. The experimental spectra were in excellent agreement with the theoretical model developed to describe high pressure CARS spectroscopy. The second area of investigation focused upon the use of picosecond pulses as a means of suppressing the sometimes undesirable nonresonant background which can limit CARS species detectivity. The main purpose of the study was to ascertain whether the background could be suppressed with picosecond pump-probe techniques with less resonant signal loss than accompanies the more widely utilized polarization approach. Using broadband CARS generation and detection, as normally used for time-resolved diagnostics, pump-probe approaches appear to possess little advantage for gas-phase work relative to the simpler polarization techniques. For narrowband CARS work, the results would lead one to infer less signal loss with pump-probe techniques vis-a-vis the polarization methods.

INTRODUCTION

High pressure combustion is extremely important in a variety of practical applications of Army relevance such as propulsion, airbreathing and otherwise, ballistics, and diesel engines. Experimental diagnostics of high pressure combustion phenomena are important to gain the understanding required to improve and control these processes. Very little is known about high pressure combustion processes due to the lack of suitable diagnostic techniques. A vast archive of data exists from insertion of thermocouples, pressure transducers, and gas sampling probes into combustion media. However, physical probes are not only confronted with survival considerations, they are of questionable utility since their presence may seriously perturb the phenomena under study. Optical techniques appear ideally suited to diagnosing such phenomena, but many are inappropriate due to poor spatial resolution, weak signal strength, etc. One optical technique, coherent anti-Stokes Raman spectroscopy or CARS, shows considerable promise for diagnosing high pressure combustion phenomena (Refs. 1-4). CARS is spatially-precise (Ref. 5) and its coherent or beamlike nature is quite amenable to the limited optical apertures typical of high pressure combustion chambers. Furthermore, CARS exhibits a nonlinear dependence on molecular number density and increases rapidly in signal strength as the gas density is elevated. CARS has already been shown to be practically applicable, having been demonstrated in gas turbine combustors (Refs. 6-7), internal combustion engines (Ref. 8), propellant flames (Ref. 9), and shock tubes (Ref. 10).

In CARS, incident laser beams at frequencies ω_1 and ω_2 (termed the pump and Stokes, respectively), interact through the third-order, nonlinear electric susceptibility, $\chi^{(3)}$, to produce the coherent CARS radiation at frequency $\omega_3 = 2\omega_1 - \omega_2$. If the frequency difference $\omega_1 - \omega_2$ coincides with a Raman-active vibrational or rotational mode of a certain species, then the CARS radiation is resonantly enhanced and uniquely characteristic of that species. In CARS, measurements of temperature are performed from the spectral shape, i.e., the CARS intensity distribution with frequency (Ref. 11). Species density can be determined from the spectral shape as well in certain concentration ranges, but, in general, density measurements are based upon the strength of the CARS signal (Ref. 12). The intensity of CARS, however, is quite linewidth dependent. As the gas density increases, a variety of linewidth phenomena occur such as pressure broadening, shifting, motional and Dicke narrowing which complicate the calculation of the CARS spectrum. Accurate modeling of high-pressure, high temperature CARS spectra is necessary to extract temperature and density information and, thus, is fundamental to the deployment of the technique as a diagnostic.

For most molecules of combustion interest at atmospheric pressure, the lines are primarily pressure broadened. The isolated linewidths can be expected to broaden linearly with pressure. At pressures where significant line overlap occurs, however, the character of the broadening changes, and the phenomenon of collisional narrowing sets in and thereafter governs the CARS intensity distribution. Under

Army Research Office sponsorship, Contract DAAG29-79-C-0008, UTRC has been investigating the phenomenon of pressure-induced, i.e., collisional, narrowing in N_2 and CO_2 . In N_2 , where most of the effort has been concentrated, excellent progress has been made in modeling collisional narrowing in CARS. At room temperature, CARS spectra of N_2 have been recorded over the pressure range from one to one hundred atmospheres in a specially-designed high pressure cell (Ref. 13). At elevated temperatures, i.e., ~ 1600 K, experiments have also been successfully performed to one hundred atmospheres. Excellent agreement in N_2 has been obtained between the experimental spectra and those predicted by the theory developed under the contract. The CARS spectrum of CO_2 has also been investigated from one to sixty atmospheres at room temperature.

It is also of interest to extend CARS studies to the picosecond time domain and exploit potential increased signal conversion efficiency and possible advantages that time delay techniques afford in suppressing nonresonant background contributions. The reason this approach is attractive is that there may be a relatively small penalty in resonant CARS signal reduction. This contrasts with suppression by polarization orientation in which there is a resonant signal penalty of a factor of 16 (Ref. 12).

In the next section of the report, the results of high pressure CARS studies are presented with the reader referred to the attached appendices for details and experimental spectra. A discussion is also presented that describes the collisional narrowing theory of CARS that was developed under this contract. The subsequent section reviews the objectives and results of the picosecond pulse CARS studies. The work at UTRC, sponsored by ARO, has been received with considerable interest by the technical community and has been publicly presented and/or published on numerous occasions as summarized in Appendix B. A compilation of major papers published by this group as a result of support by the ARO through this contract are included as Appendices C-I at the end of the report.

HIGH PRESSURE CARS SPECTROSCOPY

The objective of work performed under this contract was to extend the applicability of CARS as a diagnostic tool to the regime of high pressure, high temperature combustion media. This was accomplished by the acquisition of high quality, moderate resolution CARS spectra which were used to modify existing (isolated-line) computer models for the prediction of temperature from the CARS spectra of high pressure, high temperature gases. Measurements on nitrogen from one to 100 atmospheres from 300K to over 1600K have been performed as well as measurements on CO₂ from one to 65 atmospheres.

Experimental Apparatus

To obtain fundamental CARS spectroscopic data on the two molecules, a static, internally-heated, high pressure vessel schematically depicted in Fig. 1 was utilized. It is rated for temperatures to 1750K and pressures to 5000 psig.

Figure 2 is a layout of the high pressure CARS apparatus. The output of a Quanta Ray Nd:YAG laser was frequency doubled to generate a horizontally polarized, "primary" pump beam at 5320 Å (ω_1). Residual 1.06 μ was separated from the ω_1 beam in a prism harmonic separator and doubled to generate a secondary beam to pump the broadband Stokes dye laser oscillator. Part of the primary beam (30%) was split off to pump the amplifier of the dye laser, ω_2 . Galilean telescopes were provided to control beam waists and the focal zone locations of ω_1 and ω_2 which were combined collinearly on the dichroic mirror and focused inside the high pressure test cell. CARS, at ω_3 was generated in the focal volume, and all three frequencies ($\omega_1, \omega_2, \omega_3$) were recollimated after exiting the cell. A second dichroic mirror separated ω_3 from ω_1, ω_2 before the signal was incident on the slit of a double, one-meter monochromator with resolution of $\sim 0.4 \text{ cm}^{-1}$. The ω_1 and ω_2 beams were trapped after reflection from the second dichroic. A He-Ne laser is shown in Fig. 2 whose output was coincident with the ω_1, ω_2 path and used for optical alignment. A beamsplitter in the ω_3 leg provided a reference signal to a photomultiplier which was used to normalize the spectrally-dispersed CARS signal from the monochromator. The two signals were ratioed in a boxcar averager to account for variations in laser intensity during the scan of the CARS spectrum. A photograph of the UTRC High Pressure Facility is shown in Fig. 3 with many of the components identified that were described in the previous discussion.

Experimental Results

Using the high pressure facility, studies were performed from 1 to 100 atmospheres and Appendix D contains a reprint which summarizes the 300 K, N₂ CARS spectra obtained from this pressure range. The important result of this work was that the total Q-branch bandwidth has little variation with pressure, an effect

FIG. 1

INTERNALLY HEATED PRESSURE VESSEL FOR CARS DIAGNOSTICS

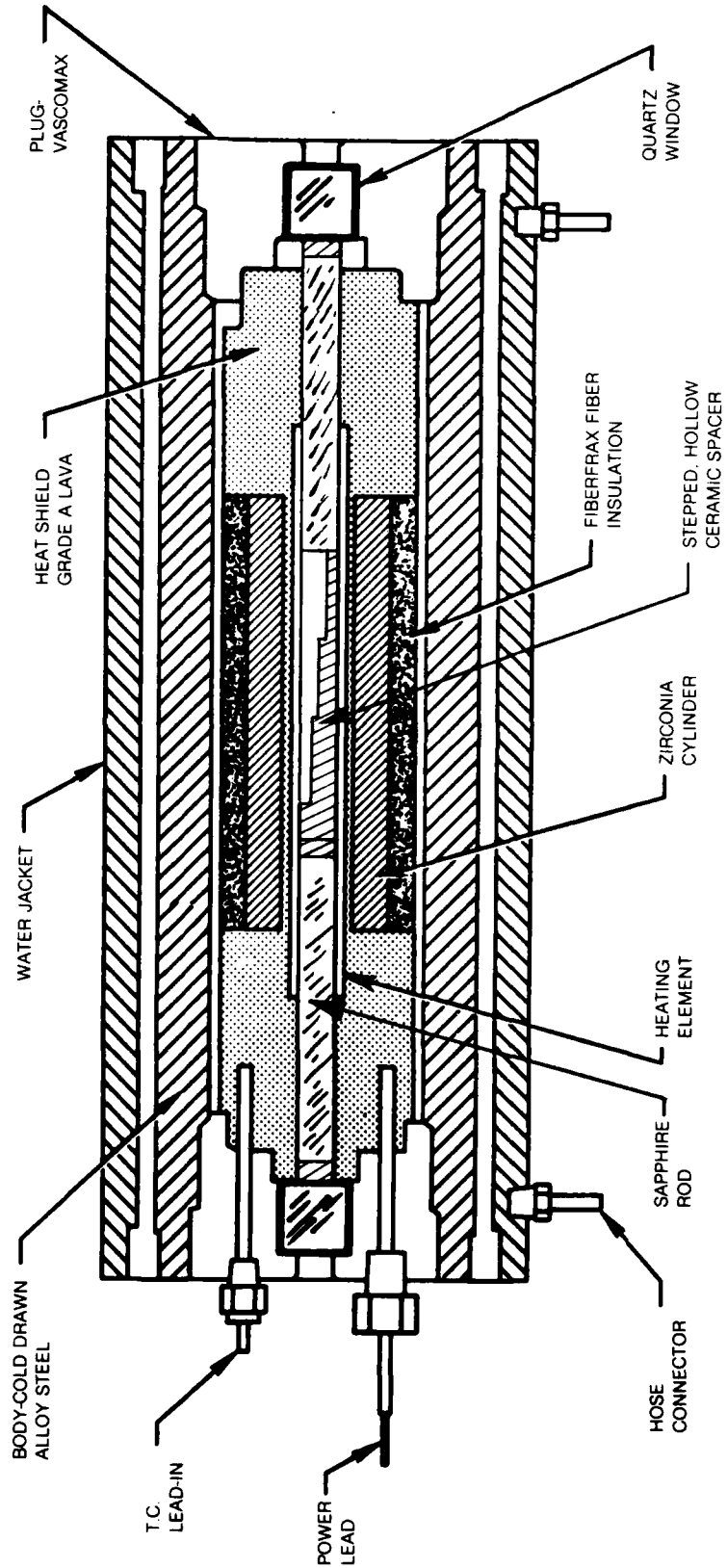
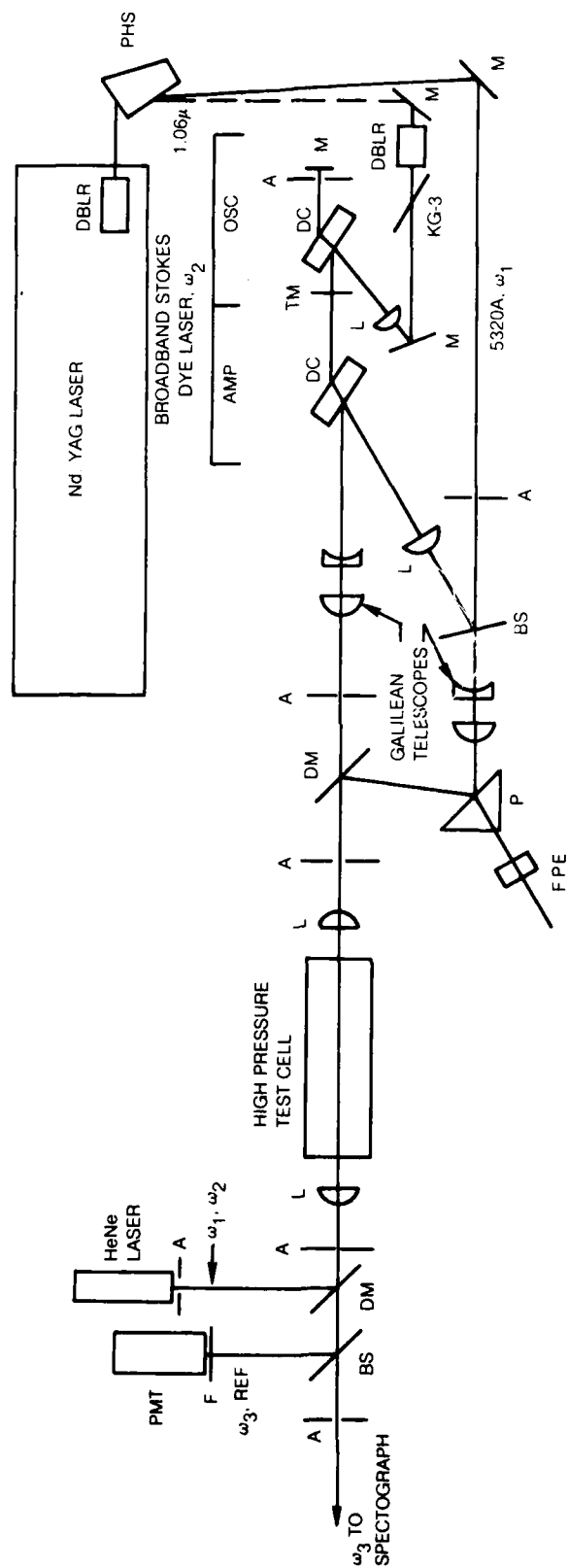


FIG. 2

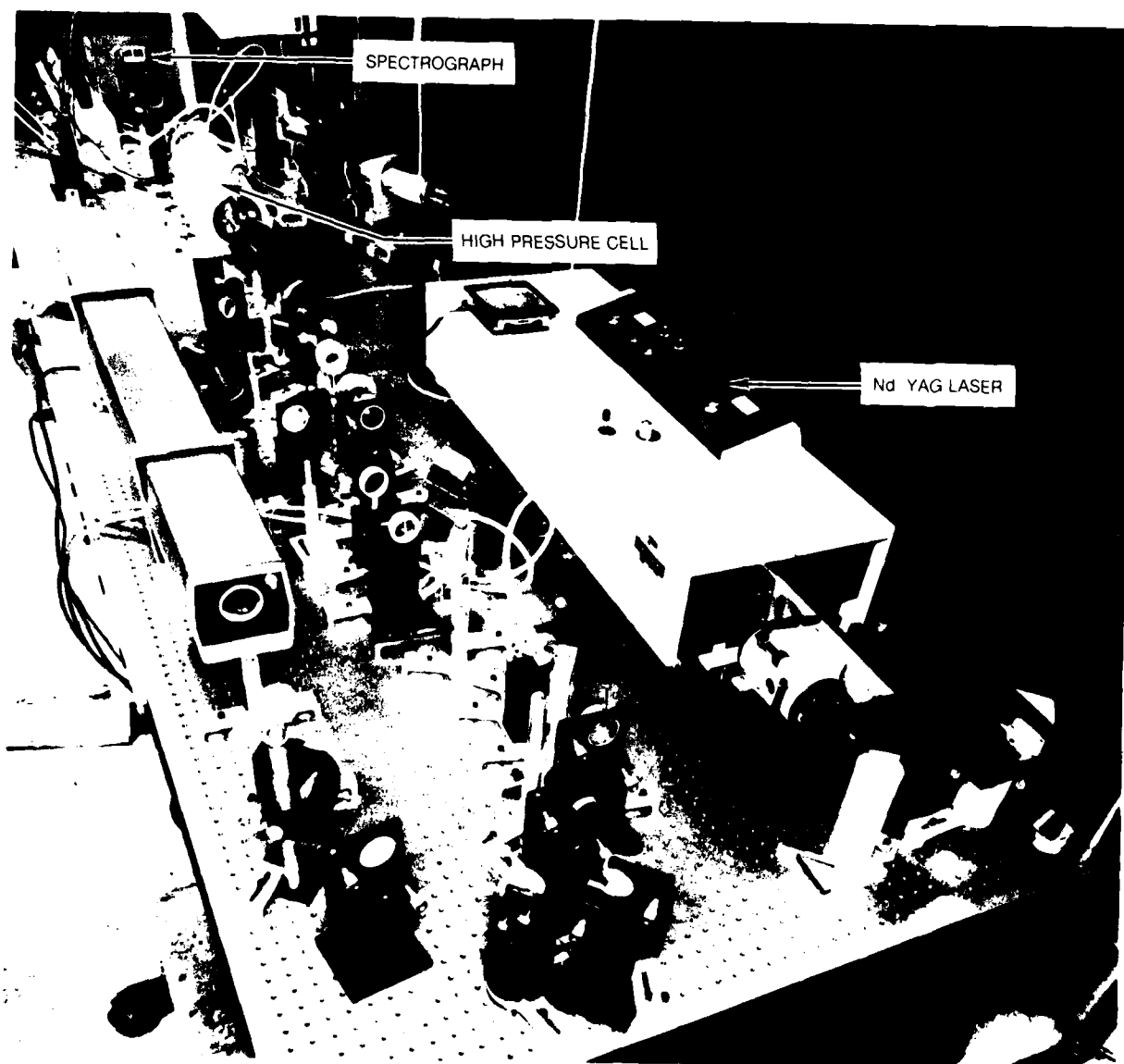
HIGH PRESSURE, HIGH TEMPERATURE CARS EXPERIMENT



- PHS — PRISM HARMONIC SEPARATOR
- F — FILTER
- KG-3 — INFRARED ABSORBING GLASS
- DBLR — FREQUENCY DOUBLER
- FPE — FABRY-PEROT ETALON
- DC — DYE CELL
- PMT — PHOTOMULTIPLIER TUBE

- A — APERTURE
- M — MIRROR
- DM — DICHOIC MIRROR
- TM — PARTIALLY TRANSMITTING MIRROR
- BS — BEAM SPLITTER
- L — LENS
- P — PRISM

HIGH PRESSURE CARS FACILITY



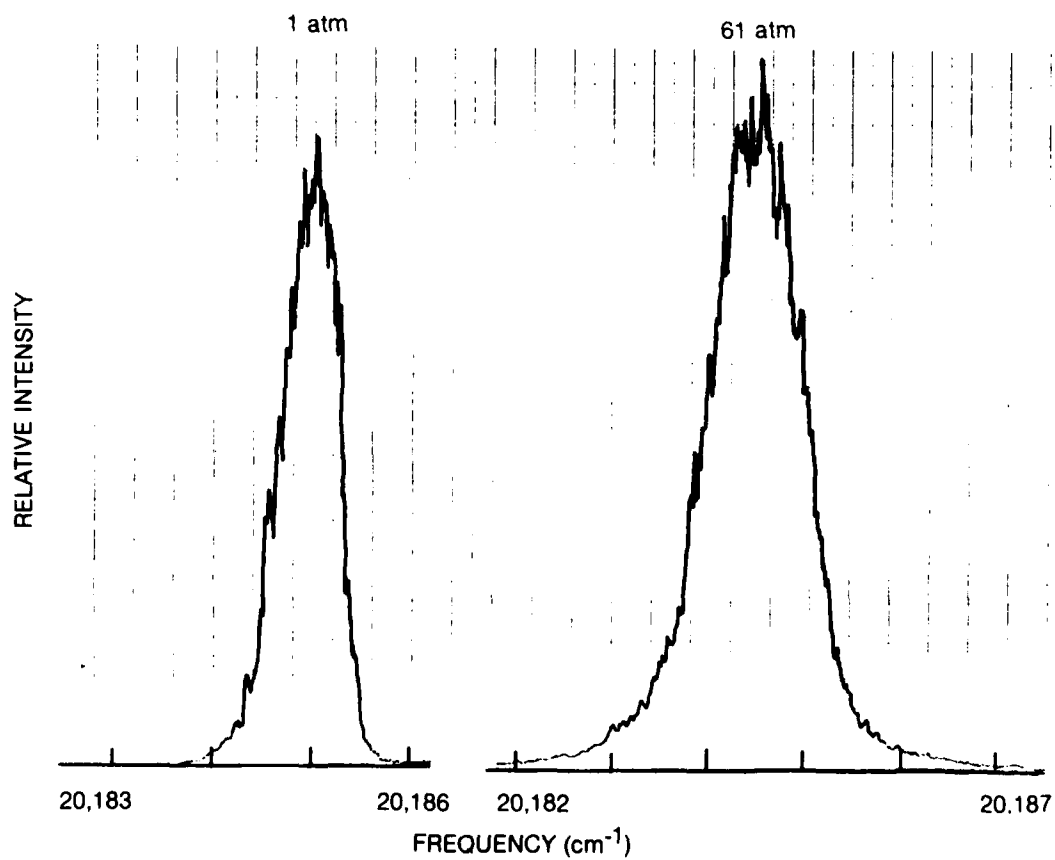
of collisional narrowing. In addition to the discussion of pressure induced narrowing in Appendix D, further developments of this theory are presented in Appendices C and G, as well as in the theoretical section of this report.

Carbon dioxide was also studied with the same high pressure apparatus over the range of 1 to 65 atmospheres. Shown in Fig. 4 are 300 K CARS spectra of the ν_1 , symmetric stretch mode of CO_2 at one and sixty-five atmospheres; again, little broadening of the spectra was evident. Due to the very small rotational spacing of lines in a vibrational band of CO_2 , collisional narrowing is likely to be quite important even at atmospheric pressure. This was supported by the data of Fig. 5 where the pressure dependence of the CO_2 CARS bandwidth is shown to be very weak. Also shown in Fig. 5 is the isolated line prediction of the bandwidth dependence. This model assumes isolated rotational lines broaden linearly with pressure and no interference effects occur as lines overlap. Since bandwidth is used as a parameter to predict temperature, this pressure effect clearly has a large impact on thermometry. The slight discrepancy between the rotational diffusion model predictions and the experimental bandwidth is commented upon in the section on Theoretical Considerations, later in this report.

Studies were also performed at high temperature over the pressure range previously stated. Details of the experiments and spectra in N_2 at 8 and 30 atmospheres, 1630 K are described in Appendices E, F, H. The theoretical comparisons based on the theory of collisional narrowing agree very closely with the experimental data. Also shown and discussed in these same appendices are high temperature CO_2 spectra taken from a CO/air flame at 1620 K, one atmosphere. The high temperature CO_2 spectra exhibited several "hot bands", strongly dependent on temperature and very useful for thermometry. The agreement between theory and experiment was fairly good and has improved as more reliable data on rotational spectral constants have become available.

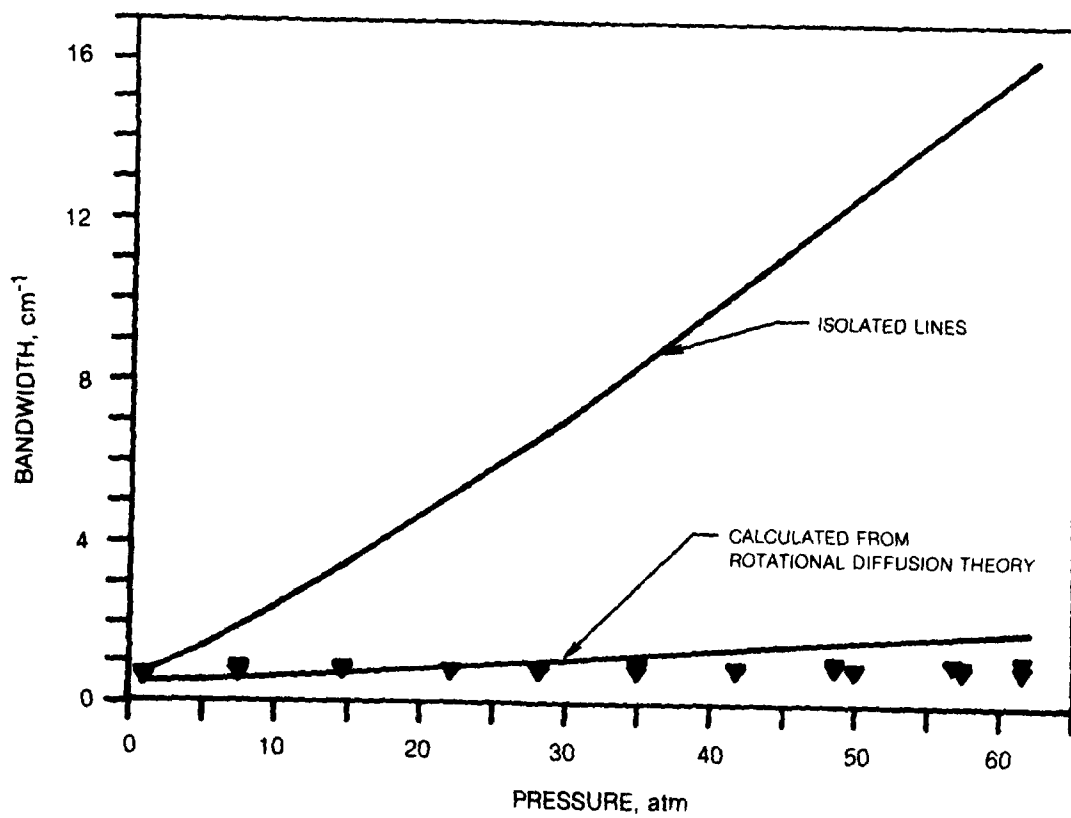
At elevated temperature, and pressures above 30 atmospheres, considerable experimental difficulties were encountered in attempts to acquire high quality CARS spectra. These difficulties are briefly summarized below, together with the modifications necessary to overcome them. The initial design of the high pressure cell did not include the sapphire rods shown in Fig. 1. With the cell mounted horizontally, density gradients induced by buoyancy led to refractive steering of the optical rays and the laser beams did not propagate through the cell. Instead, they were steered into the cell side wall. By orienting the optical axis vertically, i.e., aligned with the gravitational field which is responsible for the buoyancy effects, the laser beams could be propagated through the cell, and indeed, one could look through the cell. However, buoyancy forces again led to two different problems. First, buoyancy-driven turbulent convection cells were established which seriously perturbed the optical phase of the propagating laser beams and led to a time-varying combination of steering, focusing and defocusing. At high pressures and high temperatures, the N_2 in the cell literally took on the appearance of a stirred "oil and vinegar" solution. Much of the laser beam coherence and, hence, its focusability

ν_1 CO₂ LINEWIDTH VS PRESSURE



CO₂ BANDWIDTH VS PRESSURE

0.4 cm⁻¹ RESOLUTION



was destroyed. Second, a strong and highly-peaked temperature distribution was produced whose spatial profile was pressure dependent as determined by thermocouple measurements. At the constant pressure prevailing in the cell, the temperature distribution, which peaked slightly above the center of the cell, led to a concomitant density distribution. The density was highest to the outer edges of the cell near the windows and lowest near the middle of the cell. Ascertaining the temperature at any specific location in the cell was easily solved by placing a stepped ceramic liner into the cell (see Fig. 1) allowing the optical pyrometer to focus on any particular step and, thus, a particular location. However, to generate CARS at a specific temperature location required the CARS measurement to be spatially-precise. The normally-employed collinear phase matching was confronted with its classic limitation (Ref. 5). Namely, most of the CARS signal was generated from the cooler, high density outer regions and not from the hot, low density inner zone where measurements at high temperature were desired. Thus, in examining high temperature CARS spectra in N_2 with increasing pressure, the "hot band" in the N_2 CARS spectrum was found to "disappear". Although this could be physically real, it was suspected that the spatial resolution of the collinearly phase-matched CARS was degrading with increasing pressure. This smearing out of the resolution resulted in (actually from) greater CARS generation from the cooler, high density regions and a spectrum not representative of the small, high temperature region.

Due to the limited optical aperture of the high pressure cell, only very closely packed, from an angular sense, crossed-beam phase-matching schemes were possible. A two-beam, folded BOXCARS approach was attempted in which, in the near field, the Stokes laser beam is inserted inside the annular ω_1 beam (Ref. 14). In principle, this would avoid ω_1 , ω_2 beam overlap except in the focal region, obviating the difficulties of collinear CARS and leading to good spatial resolution. Unfortunately, due to the severe refractive index fluctuations, the Stokes laser could not be confined within the inner annular region of the pump. Rather, beam overlap occurred and one obtained a rather haphazard series of collinearly phase-matched interactions with poor spatial resolution. Indeed, signal strength observations did not demonstrate a pressure dependence anywhere near quadratic, indicating that only a fraction of the respective beams were wave mixing from a geometric sense. Visual observations of the laser beams emerging from the high pressure cell at high temperature also illustrated that the laser beam integrity had been greatly deteriorated with the laser light highly dispersed and fluctuating quite severely spatially (of the order of a beam diameter).

In an effort to retain use of the high pressure cell, sapphire rods were obtained and inserted into the cell at locations shown in Fig. 1 to restrict the gaseous sample to approximately 7 cm. By restricting the optical path of the lasers through the gaseous sample, the deterioration of the laser beams was greatly reduced, and hence, the spatial precision of the phase matching was improved. Additionally, the gaseous sample should have been considerably more uniform. However, experiments indicated that turbulence still inhibited reliable CARS generation with the cell in the vertical position. It was subsequently found, though, that with the cell mounted horizontally and the sapphire rods in place, the "gas lens" effect was reduced

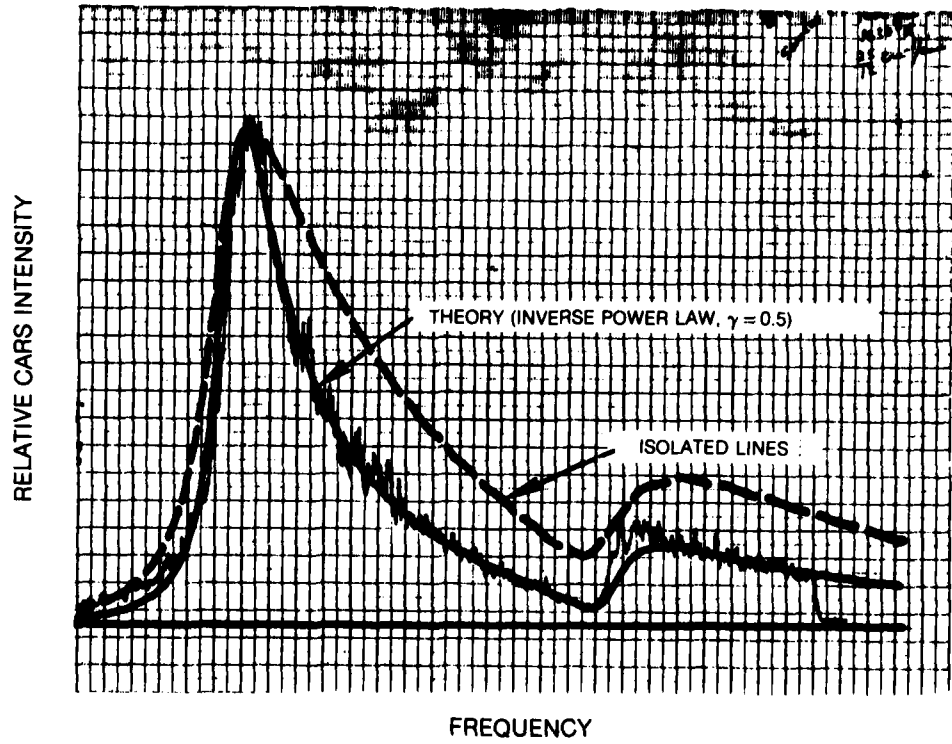
significantly. The laser beams would propagate completely through the cell even for the most severe case of high temperature and high pressure, and CARS generation was observed. However, optical damage to the sapphire rods was often problematical.

It was determined that the optical damage was the result of time-dependent, thermal lensing in the absorptive neutral density filters used to attenuate the pump and Stokes lasers. At high gas pressures it is necessary to attenuate the lasers to avoid gas breakdown and stimulated Raman gain which would interfere with and perturb the CARS signal. As the filters absorb energy, they heat up nonuniformly and "lens" with the result that the focal point of the laser beam shifts. Another approach would be to lower the flashlamp energy input to the Nd:YAG laser, thus lowering the output power; however, the Nd:YAG rods also exhibit thermal lensing and the laser must be operated at a constant setting to maintain unvarying beam divergence and constancy of the focal location. The simple solution was to achieve the desired attenuation through a Fresnel reflection ($\sim 1.5\%$) from a flat surface. A prism was used for this purpose, as shown in Fig. 1, to avoid the back surface reflection which would result from a plane parallel element. Incorporating this modification and the cell mounted horizontally with the sapphire rods, high quality CARS spectra were generated at high pressure and high temperature as shown in Fig. 6. This was the first time spectra have been acquired at these elevated pressures and temperatures from a static cell. The 103 atmosphere, 1630 K data showed a prominent hot band, confirming the suspicions about the effect of turbulence and spatial resolution discussed previously. It also allowed verification of the collisional narrowing theory in the regime of simultaneous high temperature and pressure. As seen in Fig. 6, the theoretical fit is excellent. A further discussion of the collisional narrowing theory, the historical precedence in Raman spectroscopy, its development through several models, including 'inverse power law', Gordon rotational diffusion, etc., and its application to the spectra reported here are detailed in the following paragraphs.

Theoretical Considerations

Prior to the initiation of this contract, most diagnostic CARS experiments and associated modeling were performed at low pressures, one atmosphere typically, where it is a reasonable approximation to assume that the CARS signatures consist of a collection of independent, isolated transitions. Because CARS is a nonlinear process whose strength is proportional to the squared modulus of the third-order nonlinear electric susceptibility, it was known that interference effects arising from line overlap could make very important contributions to the CARS signature. If the transition line positions and Raman linewidths are known to a reasonable precision, however, these interference effects can be accurately accounted for. At higher pressures, it was recognized that the assumption of independently broadened transitions would no longer suffice, and that a reformulation of the expression for the resonant contribution to the nonlinear susceptibility would be necessary.

N₂ CARS SPECTRUM
EXPERIMENT AND THEORY
0.4 cm⁻¹ RESOLUTION



It has long been known in such diverse spectroscopies as infrared, Raman, microwave, atomic hyperfine, and ultrasonics, that the mathematical treatment of overlapping spectral lines is not adequately given in terms of isolated lines undergoing ordinary pressure broadening (Ref. 15). The mathematical formulation of the overall bandshape resulting from line overlap was first given by Baranger (Ref. 16) and Kolb and Griem (Ref. 17). The central result of these analyses is the need to specify a so-called relaxation or transition rate matrix whose diagonal elements are related to the width and shift of isolated lines, and whose off-diagonal elements control the rate of intensity transfer between adjacent lines. When the pressure has increased to the point where adjacent lines are substantially overlapped, these off-diagonal elements give rise to a collapse or coalescence of the collection of lines into an unresolved bandshape whose width can actually decrease with increasing pressure. This is the well-known phenomenon of collisional, or motional narrowing.

Under this contract, the existing analyses of the collisional narrowing effect were extended to describe the effect in spectroscopies derived from the third-order electric susceptibility. A generalized expression for the susceptibility was derived which remains valid for substantial line overlap. For the vibration-rotation transitions of main interest in combustion research, it is most likely a good assumption to ignore vibrational processes such as vibrational dephasing and vibrational relaxation, and furthermore to neglect any variation of the rates of inelastic rotational energy transfer with vibrational quantum number. Given these approximations, the important off-diagonal linewidth parameters are given simply by the first-order rate coefficients for rotationally inelastic energy transfer.

Certain relationships involving the off-diagonal relaxation rate parameters are known; for example, scattering matrix unitarity requires that the sum of off-diagonal elements in a given column equal the isolated linewidth in the column, and detailed balance relationships connect the values for forward and reverse processes. However, this is not generally enough information to specify the entire matrix. Unfortunately, it is not presently possible to calculate these off-diagonal elements on an ab initio basis with the same semi-classical theories that have been very successful in predicting the widths of isolated lines (Ref. 18). While this formidable problem is being resolved, it has been necessary to resort to parameterization of the off-diagonal elements. In Ref. 13, it was shown that good results could be obtained by assuming an "exponential gap" relationship between relaxation matrix element and the rotational energy defect for the associated inelastic energy transfer process.

Use of the generalized expression for the third-order electric susceptibility does involve some calculational difficulties, because at each frequency mesh point of interest a so-called "G-matrix" related to the aforementioned relaxation matrix must be inverted. This process can be quite cumbersome and costly in computer run time for those molecules whose CARS spectra consist of very large numbers of Q-branch

transitions. Example of the latter are CO_2 , H_2O , and even N_2 when the temperature is quite high. A search for a somewhat simpler approach to be applied to high pressure H_2O CARS spectra led to investigation of the Gordon "Rotational Diffusion" model (Ref. 19). This research was not directly supported under this contract, but since it represents just a special case of the more generalized susceptibility expression, and has been used in the analysis of spectra obtained under this contract, it forms an important part of any discussion of results. This model is based on a picture of molecular collisional processes in which strong collisions simply cause a thermal randomization of the rotational angular momentum. Based on this assumption, the relaxation rate off-diagonal parameters are specified, with no adjustable parameters required. Further, it is not necessary to invert the G-matrix for this particular case. The effect of narrowing is accounted for in the susceptibility algorithm by a simple summation and subsequent division. This makes possible a drastic simplification of the numerical task involved in narrowing calculations, and makes possible the modeling of CO_2 and H_2O CARS spectra that would otherwise be too expensive.

The rotational diffusion model gives very good agreement with N_2 CARS spectra at 300 K and 1630 K. It also agrees quite satisfactorily with the measured pressure dependence of the room temperature CARS bandwidth of CO_2 , as can be seen in Fig. 5. The slight disagreement at the higher pressures is most likely due to uncertainty in the Q-branch linewidths for CO_2 ; no data on these widths are presently available, and the assumption has been made that the Q-branch linewidths are equal to those of the pure rotational S-branch. Use of slightly smaller values for the Q-branch linewidths, which would be physically realistic, would resolve the disagreement at high pressure.

The one criticism that can be made about use of the rotational diffusion theory is that for N_2 it does not give quite enough narrowing at low pressure where the collisional narrowing effect is just beginning to become important. This is a small defect, but it can be remedied by parameterization of the relaxation rate parameters, and resort to the full G-matrix inversion. In the latter stages of this contract, further research was performed on the subject of rotational relaxation and particularly the semi-empirical models for rotational transfer rates. One model for rotationally inelastic rate coefficients that has had a great deal of success in correlating the vast amount of experimental data accumulating on this subject is based on an inverse power law relationship between energy defect and inelastic rate coefficient (Ref. 21). That is, the inelastic energy transfer rate is assumed to be proportional to the absolute value of the inelastic energy defect raised to a negative power which is an unknown parameter. In this way, the theory can be fitted to the experiment, and it has been found that a value of the power fit parameter equal to -0.5 results in very good agreement with the 300 K data of Ref. 13. Agreement at the highest pressures ($p \approx 100$ atm) is optimized by assuming a physically realistic contribution of vibrational processes to the line broadening of 4%. The same values of the fit parameters give good agreement with the hot, high pressure N_2

spectra, as shown in Fig. 6. Also shown in Fig. 6 is a calculation based upon isolated line theory; it is plain that any attempt to analyze spectra at these extremes of temperature and pressure with isolated line calculations would lead to highly inaccurate inferred temperatures. The fact that the first vibrational hot band appears in the N_2 spectrum even at 103 atmospheres augurs well for CARS thermometry of high pressure gases, and is a confirmation of the assumption that vibrational rate processes remain slow relative to rotational relaxation.

The inverse power law model has also given very good agreement with inverse Raman spectra of N_2 obtained by G. Rosasco and W. Lempert of NBS (Ref. 22). These spectra, obtained with extremely high resolution using cw laser sources at pressures between 1/2 and 2 atmospheres, are very revealing of departures from isolated line behavior caused by collisional narrowing.

Based on the investigations of this contract, it is fair to state that the modeling of high pressure CARS spectra has proved to be tractable; theoretical spectra are in good agreement with experiment for N_2 over a wide range of temperature and pressure. Satisfactory agreement can be obtained using a very simple model of the rotational relaxation processes, the Gordon "Rotational Diffusion" model. No adjustable parameters are involved, and the expression for the third-order susceptibility simplifies to one involving no more computational expense than an isolated line calculation. For N_2 , theory-experiment agreement in the low pressure regime can be improved by resort to a semi-empirical expression for the off-diagonal relaxation matrix parameters; the inverse power law relationship is probably the best available at present, and gives good agreement with the N_2 results. In CO_2 , the very large number of Q-branch transitions comprising the CARS signature requires that the rotational diffusion theory be employed for reasons of efficiency; fortunately, the model also explains the CO_2 symmetric stretch mode pressure dependence quite accurately.

PICOSECOND CARS INVESTIGATIONS

A perceived limitation of CARS has been that nonlinear mixing produces a background signal which interferes with measurements when the concentration of the target species is low. Polarization orientation techniques (Ref. 12) have been employed to suppress the nonresonant background but the resonant signal is decreased as well, a factor which can be critical in the detection of minority species. Kanga and Sceats (Ref. 23) introduced a technique which exploits the difference between the temporal responses of the target species and the background. They delayed a second pump beam to probe the coherent excitation produced by previous temporally synchronous pump and Stokes beams. A reduction in the background signal in a mixture containing 10 percent CS₂ dissolved in toluene in the liquid phase was shown. Dzhidzhoev, et al. (Ref. 24) demonstrated background suppression in gaseous NH₃ using a mode-locked Nd:YAG laser at 1.06 μ along with an optical parametric oscillator to generate a coherent excitation in the vibrational mode (3334 cm⁻¹). A portion of the Nd:YAG output was frequency-doubled and delayed to suppress the background.

The investigations reported here were undertaken to study background suppression in gaseous N₂ using delayed pump techniques. A broadband Stokes laser was selected to generate the entire CARS spectrum simultaneously, the approach typically employed for time-resolved diagnostics. The following section briefly reviews previous experiments using a delayed pump to suppress the nonresonant background in CARS measurements. Subsequently, the experimental apparatus and the measurements are described. The theory of transient coherent Raman spectroscopy is outlined and a simple model describing the measurements is presented and used to discuss the results. Finally, implications for diagnostics are assessed.

CARS Nonresonant Susceptibility Effects

The nonlinearity of CARS produces mixing which results in constructive and destructive interferences between nearby resonant transitions and between the resonant part of the susceptibility and the background. This can be seen by writing the resonant contribution as a sum of real and imaginary parts and expanding:

$$\begin{aligned} |X^{(3)}|^2 &= \left| \sum_j (\chi_j' + i\chi_j'') + \chi^{nr} \right|^2 \\ &= \left(\sum_j \chi_j' \right)^2 + \left(\sum_j \chi_j'' \right)^2 + 2\chi^{nr} \sum_j \chi_j' + \chi^{nr2} \end{aligned} \quad (1)$$

The real part of the susceptibility is an anti-symmetric function of the detuning frequency ($\Delta\omega = \omega_j - \omega_1 + \omega_2$) where ω_j is the Raman transition frequency. The imaginary part is symmetrical, and the nonresonant susceptibility is largely real (Ref. 25). For a minority resonant species, $\chi^{nr} \gg \sum_j \chi_j'$, and the spectrum consists

of a constant background with a dispersion shaped modulation at the resonance frequency. When the resonant species mole fraction is sufficiently low the modulation can be 'lost' in the background, thereby setting a maximum detection limit.

Several techniques have been devised to suppress the nonresonant background. The most widely employed, polarization orientation, makes use of the difference between the tensor properties of the electronic contribution to the third order susceptibility and that due to the resonant nuclear response. Bunkin, et al. (Ref. 26) showed that the nonresonant electronic contribution is suppressed for certain orientations of the polarization vectors of the laser fields and an analyzer in the CARS beam. It has also been shown however, that the suppression of the non-resonant signal is accompanied by a factor of sixteen loss in the resonant mode signal for isotropic Raman modes (Ref. 25). Eckbreth and Hall (Ref. 12) found in background suppression experiments with carbon monoxide that, under some circumstances, the CARS signal can be reduced by over two orders of magnitude.

There are other methods for background suppression (or resonant contribution enhancement). Lotem, et al. (Ref. 27) demonstrated a technique which enhanced the resonance spectra of cyclohexane with respect to a benzene background. Their technique uses a third input frequency ω_0 tuned so that the difference frequency $\omega_0 - \omega_2$ is resonant with another molecular resonance. This technique has not been demonstrated in the gas phase and does not offer complete background suppression. Electronic resonance CARS has also been used to enhance Raman resonances (Ref. 28). This technique uses lasers which, in addition to having a Raman resonance at $\omega_1 - \omega_2$, also are resonant with an electronic transition in the probed molecular species through a one photon absorption. This technique may prove useful for a select few molecular species, however most major molecules have electronic transitions in the relatively inaccessible spectral region below 2000 Å (Ref. 22).

Pulse-Sequenced CARS

Kamga and Sceats (Ref. 23) first suggested the pulse-sequenced technique for background suppression. This technique exploits the difference in the response times for electronic and resonant vibrational contributions to the third order susceptibility. Three beams are used. Two at frequencies ω_1 and ω_2 are applied simultaneously to the medium. A transient coherent excitation in the nuclear and electron distributions is excited by these. Collisions dephase the coherent excitation, but the dephasing is much more rapid for electronic excitation than for the vibrational excitation. The third beam therefore is delayed until the electronic excitation has dephased, the vibrational excitation remains, so the background is effectively suppressed. The dephasing time for electronic excitations is $\sim 10^{-1} - 10^{-2}$ picoseconds (Ref. 29), whereas the vibrational dephasing time for gases at atmospheric pressure is on the order of 10^2 picoseconds.

Kamga and Sceats demonstrated background suppression in the liquid phase using the 656 cm^{-1} vibrational Raman mode of CS_2 . Two dye lasers were synchronously-pumped by an actively mode-locked argon ion laser. The Stokes frequency was provided by a rhodamine 6G dye laser tuned to 17452 cm^{-1} . The pulse duration was set by etalons at about 30 psec. The second dye laser using sodium fluorescein provided a 3-5 psec pulse tuned to 18109 cm^{-1} that was used to provide both pump and probe pulses using a beamsplitter and optical delay. The three beams were crossed to satisfy phase matching (Ref. 5), and spatial filtering was used to select the CARS signal due to the delayed probe alone. Kamga and Sceats measured the CARS signal as a function of time delay for several detuning frequencies. These decay curves were used to synthesize CARS spectra at a fixed time delay. A substantial reduction of the background was observed at a delay of 20 psec with respect to the zero time delay spectrum.

Recently Dzhidzhoev, et al. (Ref. 24) used delay techniques to demonstrate nonresonant background cancellation in gaseous ammonia. Coherent excitation in the totally symmetric vibration mode at 3334 cm^{-1} was generated with the fundamental ($1.06\text{ }\mu$) of a passively mode-locked Nd:YAG laser mixed with the infrared output of an optical parametric oscillator. A portion of the Nd:YAG beam was doubled and delayed to probe the coherent excitation.

For a slightly different reason, Magnitskii and Tunkin recently used the same approach as Dzhidzhoev, et al. to measure transient CARS in H_2 from 1 to 10 atmospheres (Ref. 30). An optical parametric oscillator pumped by a mode-locked Nd:YAG laser was used to excite H_2 molecular vibrations (4155 cm^{-1}) by tuning the OPO to $1.9\text{ }\mu\text{m}$ wavelength. The OPO had a bandwidth of 100 cm^{-1} . The Q(1) transition was isolated with a monochromator and delay curves were measured for various pressures. Magnitskii and Tunkin determined linewidths from the exponential decay rates, and demonstrated that the measured linewidths agreed with previous measurements showing Dicke narrowing in H_2 (Ref. 31).

The goal of the investigation reported here was to demonstrate transient coherent Raman techniques in gaseous N_2 at one atmosphere and to evaluate the attendant resonant mode signal penalty. These experiments are reported in the following section.

N_2 Delayed CARS Experiments

The apparatus used to generate broadband CARS with a mode-locked train of pulses is shown in Fig. 7. The major components of this system are a mode-locked Nd:YAG laser and a synchronously-pumped dye laser. The Nd:YAG output is frequency-doubled and used to provide the pump frequency ω_1 , and to synchronously-pump a broadband dye laser, which provides the Stokes-shifted frequency ω_2 .

TRANSIENT COHERENT RAMAN SPECTROSCOPY APPARATUS



Mode-Locked Nd:YAG Laser

The Nd:YAG used in these experiments is a standard Quanta-Ray laser (DCR1-A), that was modified at UTRC for these experiments. The Q-switch and polarizer were removed and a contacted dye cell was incorporated with the back reflector. Eastman-Kodak dye #9860 dissolved in 1, 2 dichloroethane is used in this cell to passively mode-lock the oscillator. The dye solution is circulated in a laminar flow through the 1 mm thick dye cell. A Brewster polarizer is positioned between the back reflector and the oscillator rod.

The unstable resonator of the Quanta-Ray laser design (Ref. 32) was retained. Other experiments have reported the operation of mode-locked unstable resonator Nd:YAG lasers (Refs. 33-35). The resonator investigated by Liu and Yen (Ref. 34) was quite close to the Quanta-Ray design having comparable values for the equivalent Fresnel number, magnification and cavity length. Reali (Ref. 35) noted that the dye cell in contact with the back reflector forms a lens and its effect must be taken into account for proper operation of the laser. Accordingly, the original 4-m radius-of-curvature back reflector was replaced with a 10-m mirror.

The entire mode-locked train is amplified in the (unmodified) Quanta-Ray amplifier and doubled in the standard HGR-2 doubler. The design parameters and performance are summarized in Table 1. Figure 8 shows a photograph of a typical mode-locked train of pulses measured with the output of an HP 5082-4220 PIN Diode (Ref. 36) displayed on a Tektronix 7104 oscilloscope. The pulse duration of the Nd:YAG fundamental was measured using two photon fluorescence (Ref. 37) in rhodamine 6G. A pulse duration of 35 ps was indicated, similar to the duration measured by other investigators (Ref. 33-35).

The performance of the mode-locked Nd:YAG laser can be compared to the commercial mode-locked YAG lasers that have recently come onto the market. Two suppliers currently offer such lasers, Quantel and Quantronix. The Quantel laser has a polarization coupled stable resonator cavity and features a design that permits the laser to be readily changed from Q-switched (~ 15 ns) operation to passively mode-locked operation by inserting a TIR steering prism into the cavity. The Model 471 is comparable in energy to the Quanta-Ray (DCR-1A). The performance of this model: pulse duration = 35 ps, $E(1.06 \mu\text{m}) = 150$ mJ, $E(5230 \text{ \AA}) = \sim 16$ mJ, and 7-9 pulses per train at 10 Hz repetition rate is similar to the performance of the Quanta-Ray laser mode-locked in these experiments. The Quantronix laser is not passively mode-locked but rather uses an acousto-optic modulator to actively mode-lock the laser. The flashlamps of this laser are on continuously. The output consists of a train of pulses at 100 MHz repetition frequency with an individual pulse duration of ~ 100 ps. This type of operation would not be appropriate for these experiments because of the long duration of the pulses.

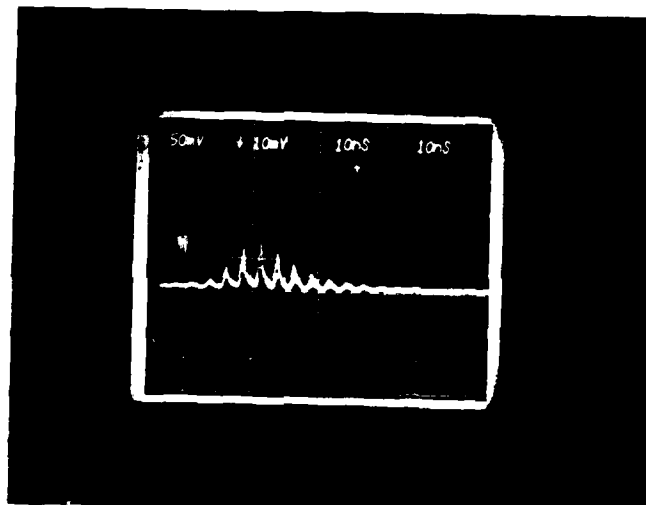
TABLE 1

MODE-LOCKED Nd:YAG OSCILLATOR/AMPLIFIER

Equivalent Fresnel No., $N_{eq} = 1.5$
Magnification, $M = 1.5$
Cavity Length, $L = 75$ cm
Pulse duration ($1.06 \mu\text{m}$) ≈ 35 ps
Bandwidth $\approx 0.5 \text{ cm}^{-1}$
 $t_p \Delta\nu = 18 \text{ ps-cm}^{-1}$
Number of pulses in train = 9-12
Beam divergence ≈ 1 milliradian (60/70J)
Energy per mode-locked train (mJ) (10 Hz)

E_L (osc/amp)	$E_{1.06\mu}$	$E_{0.532\mu}$
60/0	50	3.5
60/10	60	4
60/40	130	9
60/70	200	20

Nd: YAG MODE-LOCKED TRAIN



TIME, 10 ns/DIV →

100 SHOT AVERAGE

Synchronously-Pumped, Broadband Dye Laser

The synchronously-pumped dye laser is shown in Fig. 9. The resonator is stabilized with three quartz rods. The length is tuned by a micrometer adjustment at the back reflector end of the cavity. The dye is longitudinally pumped, slightly off axis with approximately 25 percent of the Nd:YAG output. Rhodamine 640 (Exciton) dye dissolved in methanol at a concentration of 7.1×10^{-5} moles/liter is circulated through the dye cell. The output of the dye oscillator is amplified in a longitudinally pumped dye cell which is series connected with the flow circulation through the oscillator. Approximately 38 percent of the total output of the Nd:YAG laser is used to pump the amplifier. A delay line is used to synchronize the amplifier pump pulse train to the synch-pumped oscillator output pulse train. The delay is adjusted to produce the maximum amplification. Figure 10 shows an oscilloscope photograph of the 2x Nd:YAG and dye laser mode-locked trains. The optical and cable delays in the two legs were adjusted and checked so that Fig. 10 is a true representation of the temporal development of the dye pulse train relative to the Nd:YAG laser train. The dye laser output builds up rapidly and matches fairly well the YAG output.

The synchronously-pumped dye laser energy was about 0.15 mJ for the entire mode-locked train for the oscillator/amplifier combination. The dye laser spectral width was about 130 cm^{-1} FWHM. The dye laser pulsewidth was not measured, but collinear CARS measurements in which the frequency doubled Nd:YAG laser output was delayed with respect to the dye pulse train indicate the dye pulse duration is comparable to the pump pulse.

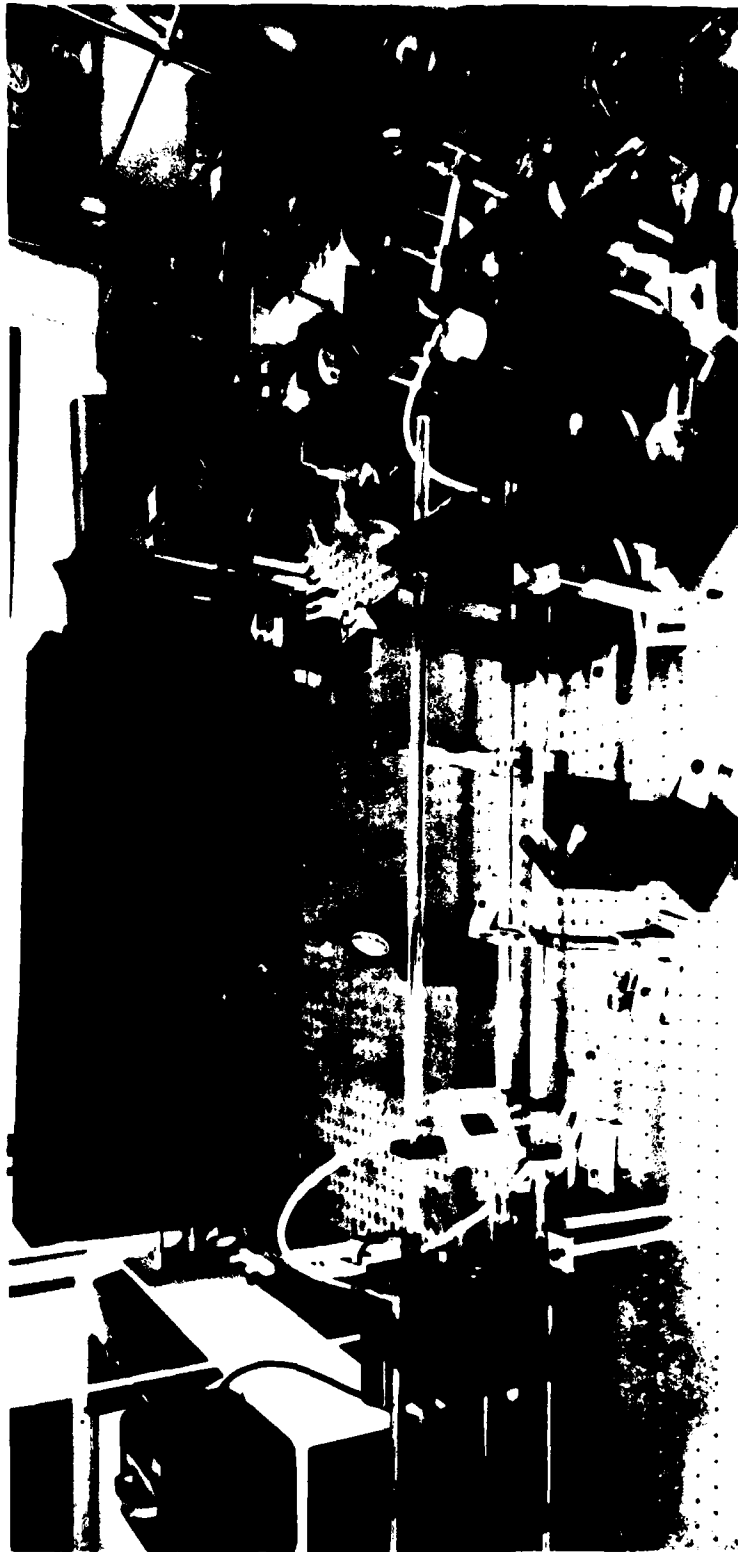
Flame N₂ Experiments

Spectrally-resolved picosecond CARS measurements were undertaken with a collinear beam configuration, and no pump delay. These tests were conducted at atmospheric pressure in room air and in a small laboratory burner. The burner used in the tests was a 7.5 cm diameter premixed tube bundle design burning a premixed stoichiometric flame. The measured flame temperature in this burner is around 1700 K. For these tests the collinearly generated CARS beam was separated with colored glass, and narrowband interference filters, dispersed in a 0.5 m monochromator (Spex 1870) and detected with a photomultiplier (RCA 31034A). The spectral resolution was $\sim 3 \text{ cm}^{-1}$.

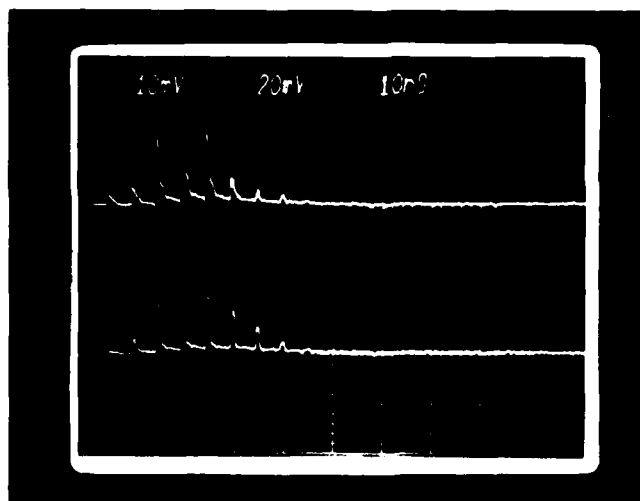
There may be differences between CARS spectra generated with conventional Q-switched multimode and mode-locked lasers. The reason for this is the difference in the phase distribution between these sources. The CARS spectrum results from a convolution of the pump laser and the Stokes laser. For a conventional multimode laser the modal phases are randomly distributed and in computing the spectrum the various modal contributions must be added up incoherently. That is

$$I_3(\omega_3) \propto \sum_{ijk} |P_3^{(ijk)}|^2 \quad (2)$$

SYNCHRONOUSLY-PUMPED DYE LASER RESONATOR



**COMPARISON OF 2x Nd: YAG AND SYNCHRONOUSLY PUMPED DYE LASER
MODE-LOCKED TRAINS**



SYNC PUMPED
DYE LASER

2x Nd: YAG

TIME, 10 ns/DIV →

On the other hand, if the pump and Stokes lasers are mode-locked, then the phases are determinate and can be set equal to zero. In this case, a coherent addition of the various polarization amplitudes must be performed, so that

$$I_3(\omega_3) \propto \sum_{ijk} \sum_{i'j'k'} |p_3^{(ijk)}| |p_3^{(i'j'k')}| \quad (3)$$

These different convolutions lead to differences in the calculated spectrum. This could not be confirmed in the spectra measured here, perhaps because of the limited spectral resolution.

Time Delay Measurements

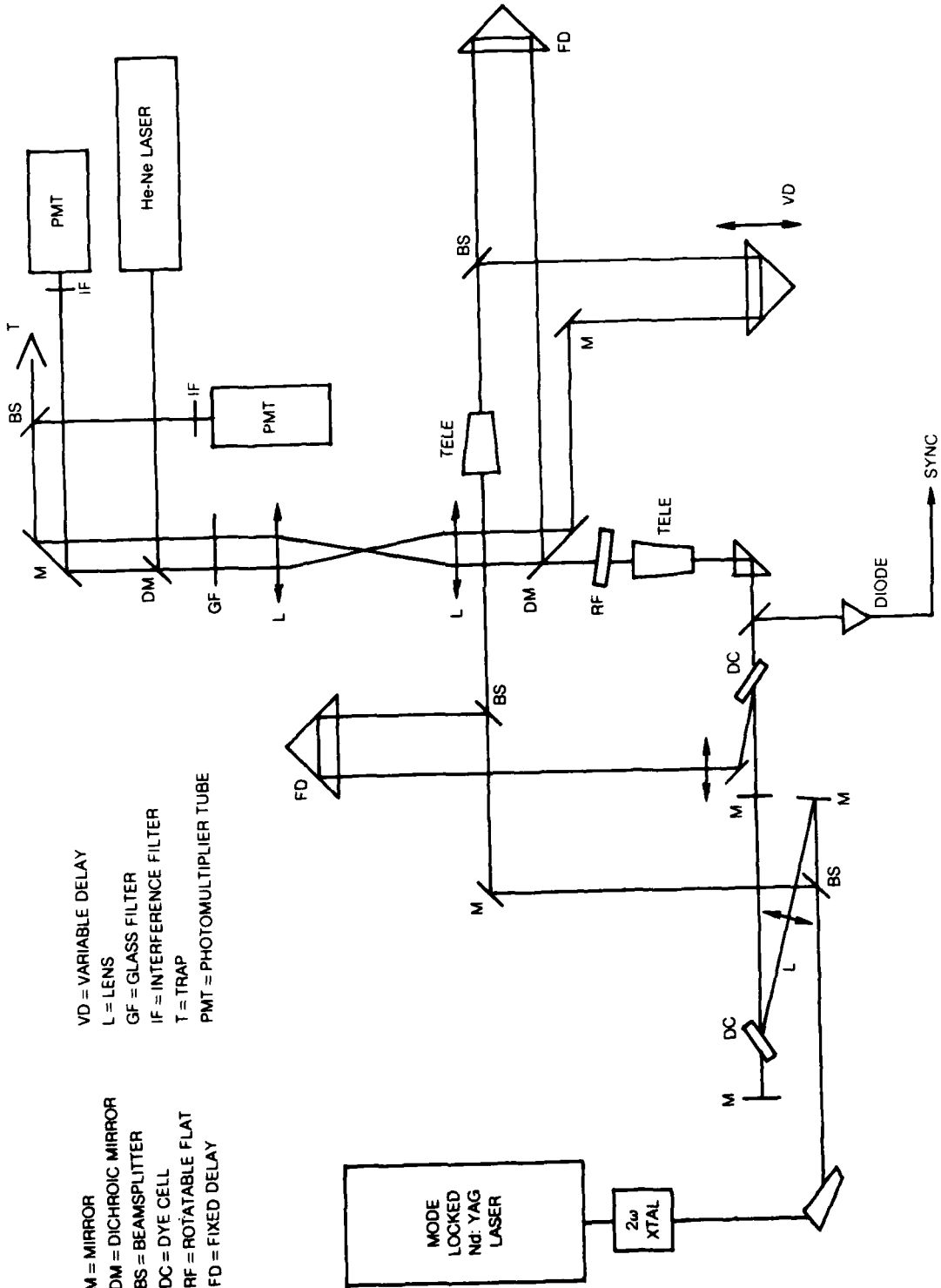
Measurements were made in which the difference frequency $\omega_1 - \omega_2$ was tuned to the N_2 vibrational Raman resonance at 2331 cm^{-1} . The apparatus used is shown in Fig. 11. The synchronously-pumped dye laser/amplifier output is beam expanded and sent through a dichroic mirror where it is combined with the undelayed pump beam ω_1 . A rotatable flat (RF) permits the phase matching to be optimized (Ref. 5). The pump, after portions of it have been split off to pump the dye oscillator and amplifier, is sent through a telescope to contract the beam somewhat and then is split into two equal beams. One beam is sent through an optical delay which remains fixed once the proper timing with respect to the dye laser pulse is determined. The other portion of the Nd:YAG beam (ω_1) is sent through a variable delay which permits delays up to 330 psec. The delayed pump beam also reflects from the dichroic mirror and is focused into the test region. The Stokes and pump beams are blocked with a glass filter and the remaining CARS beams are sent to photomultiplier tubes for detection. Interference filters and cutoff filters in front of the photomultiplier tubes provide additional isolation of the CARS signals. The PMT signals are processed by a dual-channel, digital boxcar averager which is triggered from a PIN diode viewing a portion of the dye laser output. The beams arising from collinear phase matching and BOXCARS (Ref. 5) phase matching are detected using spatial filtering to separate them. The collinear CARS is generated by the undelayed pump and the Stokes, while the BOXCARS signal was generated by the delayed pump. The BOXCARS signal vanishes when either of the three beams is blocked.

The measured CARS signals as a function of time delay are shown in Figs. 12 and 13 for pressures of 13 and 67 atm in N_2 . The delayed BOXCARS signal is normalized to the undelayed collinear CARS signal. The zero in the time delay is arbitrarily selected corresponding to a fixed micrometer setting, and has been maintained constant throughout the measurements. For these gas densities, the dephasing time is shorter than the pulse duration, and therefore there is little difference to be expected between the two responses. The two measured dependences indeed are identical within the limits of scatter in the data. Except for the absolute signal amplitude, a similar response is expected for the nonresonant electronic contributions to the third order susceptibility. Experiments with carbon dioxide confirmed this.

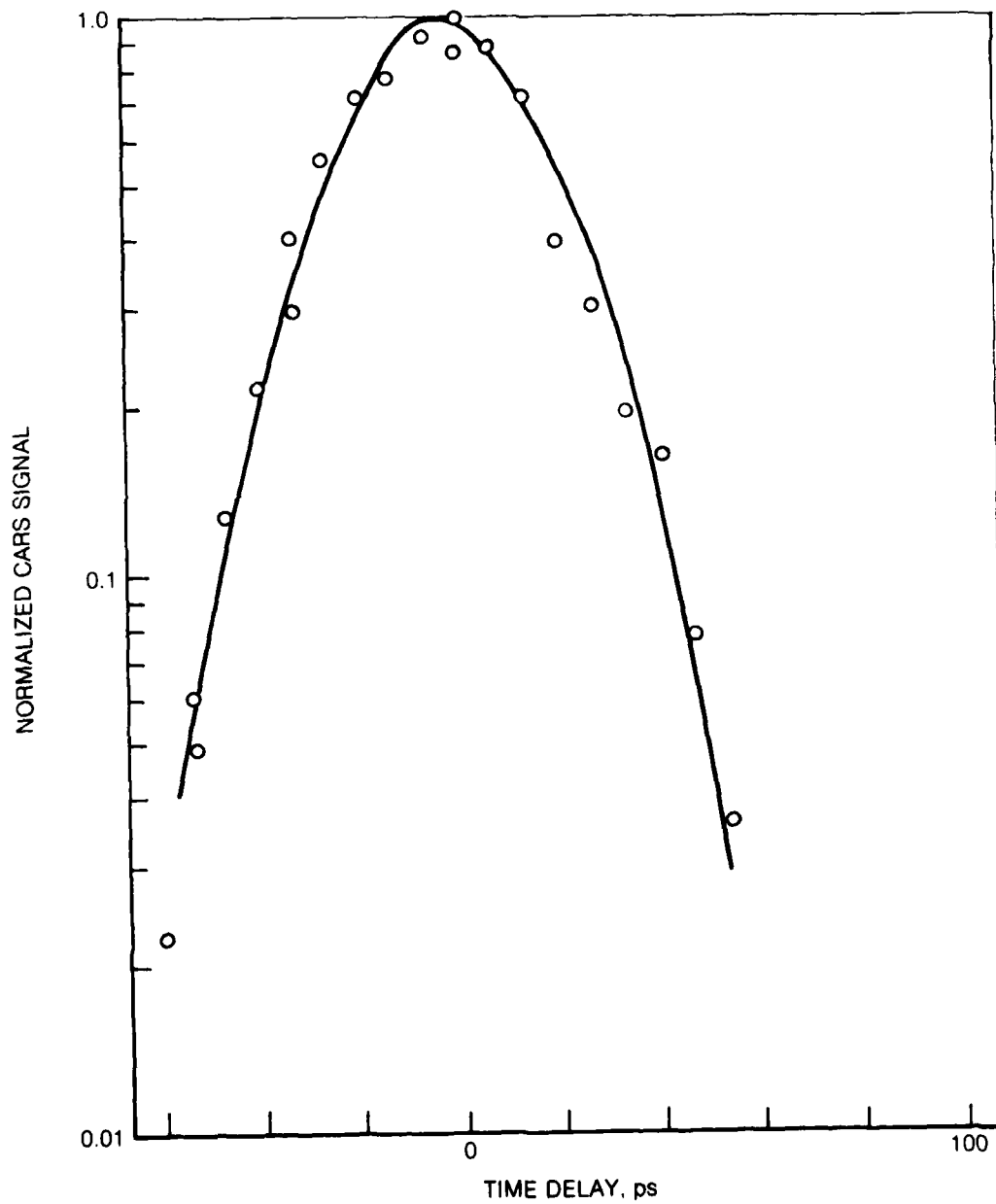
SCHEMATIC OF PULSE DELAY BOXCAR APPARATUS

M = MIRROR
 DM = DICHOIC MIRROR
 BS = BEAMSPLITTER
 DC = DYE CELL
 RF = ROTATABLE FLAT
 FD = FIXED DELAY

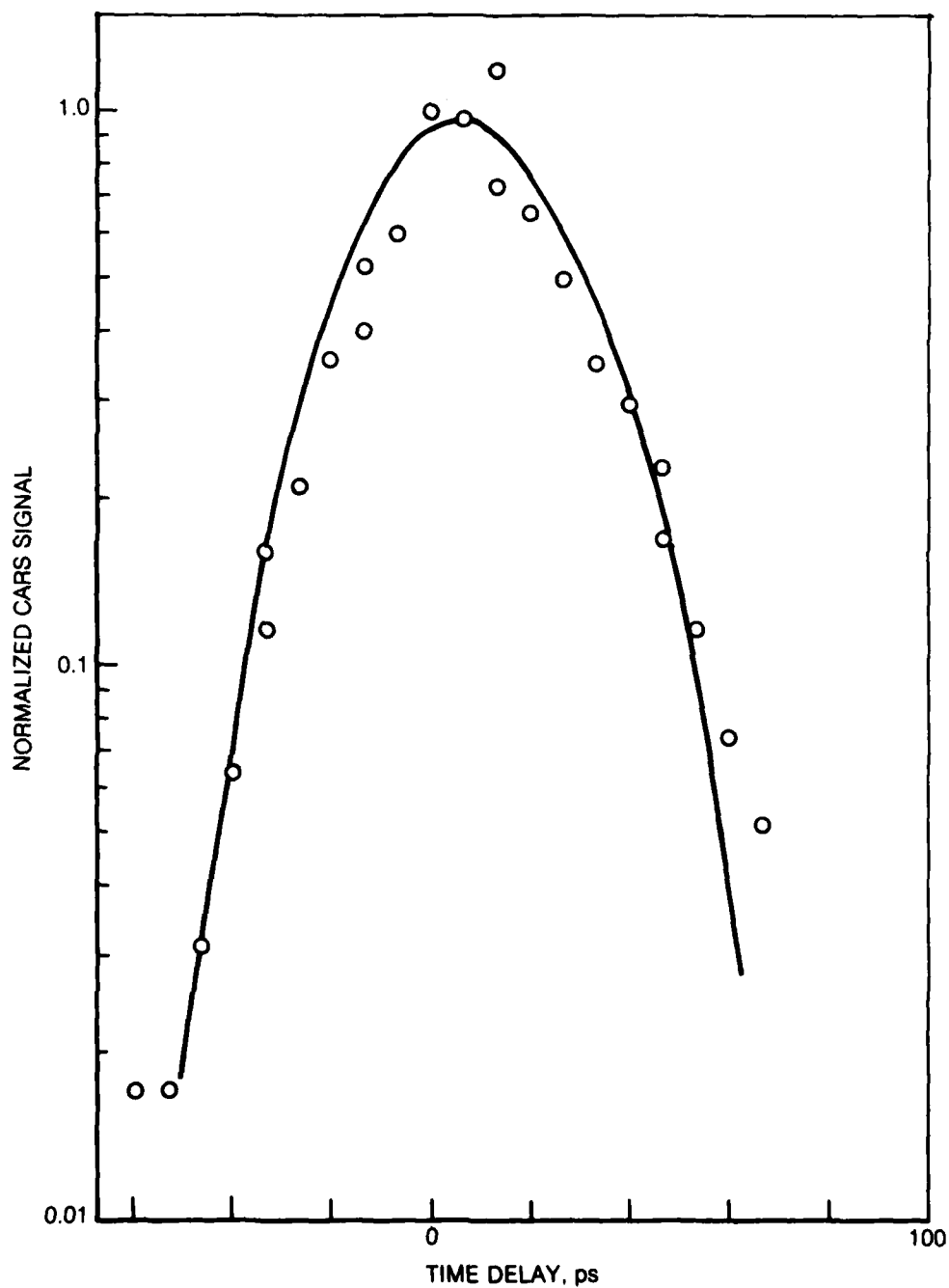
VD = VARIABLE DELAY
 L = LENS
 GF = GLASS FILTER
 IF = INTERFERENCE FILTER
 T = TRAP
 PMT = PHOTOMULTIPLIER TUBE



CARS DELAY MEASUREMENTS IN N₂ AT 13 ATM



CARS DELAY MEASUREMENTS IN N₂ AT 67 ATM



CARS delay measurements in N_2 at 1 atm are shown in Fig. 14. The data labeled w/o etalon represent the Raman signal measured as a function of time delay with the synchronously-pumped dye laser operated broadband. The decay rate is less rapid than the higher pressure data and is exponential for time delays between 20 and 80 picoseconds. This contrasts with the high pressure data which is Gaussian in shape as a function of time delay. The decay rate of the w/o etalon curve in Fig. 14 corresponds to a time constant of about 30 psec, much less than the rate expected from a dephasing time of 100 psec, i.e., $T_2/2 = 50$ psec, corresponding to the Raman linewidth (Ref. 38). In order to explain this apparent discrepancy, it is necessary to examine the theory of transient coherent Raman spectroscopy.

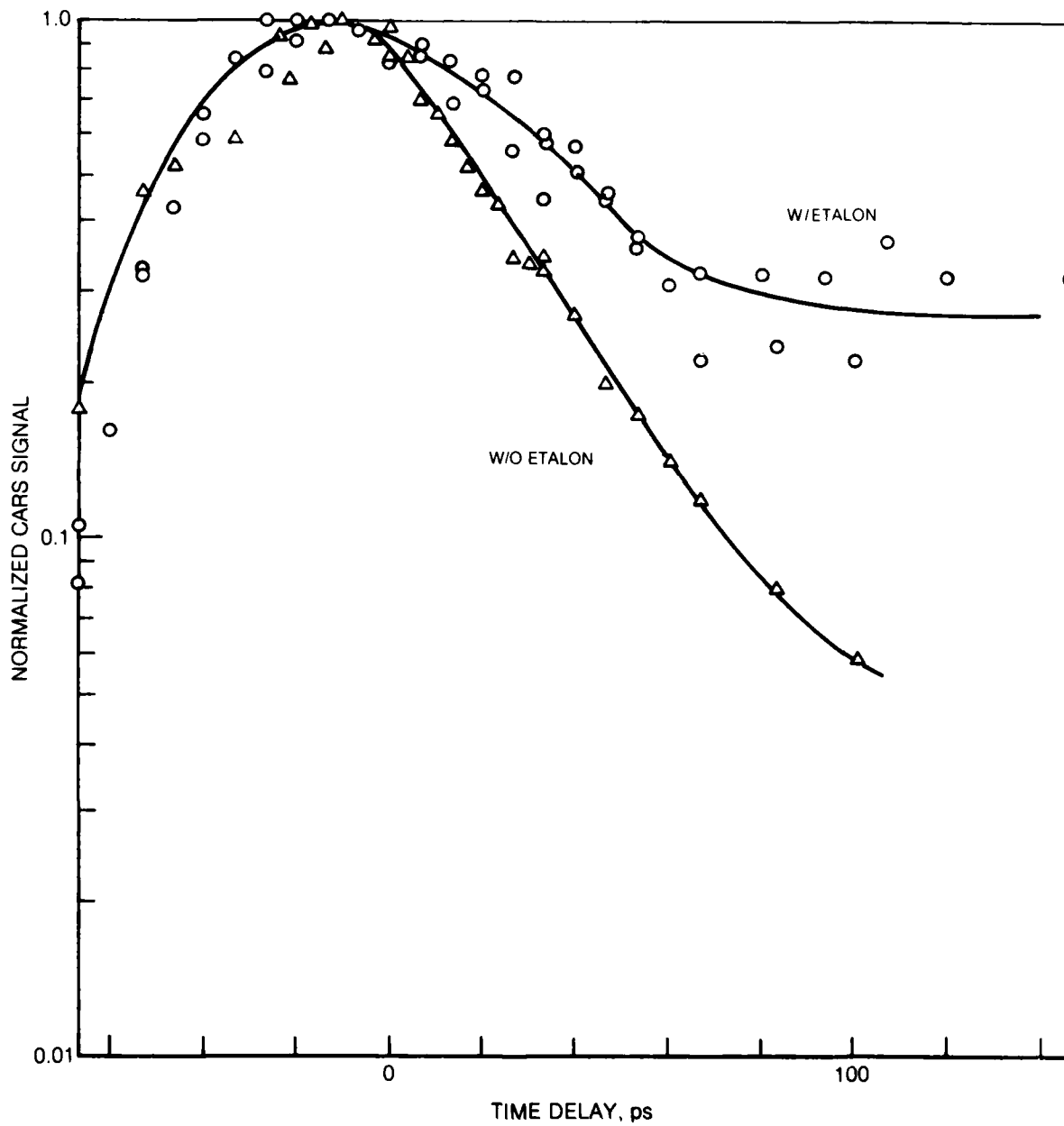
Theory of Transient Coherent Raman Spectroscopy

Transient Raman scattering has been the subject of considerable interest, particularly for the probing of the very rapid vibrational interactions occurring in condensed phases. Coherent pump and probe techniques for the transient probing of vibrational excitations in liquids were described in an excellent review by Laubereau and Kaiser in 1978 (Ref. 39). The methods developed by these authors employ an intense pump beam of short duration to excite a coherent vibrational excitation by stimulated Raman scattering. After the passage of the exciting optical pulses the remaining coherent vibrational excitation decays by collisions. The rate of decay is measured with a weak probe pulse which is delayed with respect to the stronger excitation. The measured decay rate then is related to molecular processes occurring in the sample. Laubereau and Kaiser described several methods of excitation, with the most generally applicable being stimulated Raman. This technique is similar to that described in this report, but differs in the important aspect of the method by which the Stokes frequency is generated. In this report, the Stokes wave is generated by the synchronously-pumped dye laser. In contrast, Laubereau and Kaiser use the Raman-shifted wave generated by stimulated Raman scattering to generate the Stokes frequency. The Stokes wave builds up from the spontaneous Raman scattering to relatively high levels due to the large gain coefficient for intense fields in concentrated molecular systems. Gains of 10^{10} - 10^{11} are not unusual for intensities of 10^9 - 10^{10} W/cm². For gases, however, the gain is not high enough for this approach to be practical, hence the synchronously-pumped dye laser.

Laubereau and Kaiser in their review derive the coupled differential equations governing the evolution of the Stokes amplitude E_S , the coherent vibrational amplitude Q , and the vibrational excitation (population) n , as follows:

$$\frac{\partial E_S}{\partial x'} = \kappa_1 E_L E_S^* \quad (4)$$

CARS DELAY MEASUREMENTS IN N₂ AT 1 ATM



$$\left(\frac{\partial}{\partial t'} + \frac{1}{T_2} \right) Q = \kappa_2 E_L E_S^* \quad (5)$$

$$\left(\frac{\partial}{\partial t'} + \frac{1}{T_1} \right) n = \frac{a}{8\hbar} (E_L E_S^* Q^* + E_L^* E_S Q). \quad (6)$$

here x' and t' are the coordinate and time in a frame moving at velocity v , the group velocity of the Stokes pulse. The coupling coefficients κ_1 and κ_2 are given by

$$\kappa_1 = \frac{\pi \omega_S^2 a N}{c^2 \kappa_S} \quad (7)$$

and

$$\kappa_2 = \frac{a(1-\bar{n})}{4m(\omega_L - \omega_S)} \quad (8)$$

E_L is the amplitude of the pump laser, and T_1 and T_2 represent the population lifetime (energy relaxation time) and the dephasing time, respectively. N is the total number density of the probed species, a is the isotropic part of the Raman polarizability, \bar{n} is the fractional population of the upper vibrational level at thermal equilibrium and ω and κ denote respectively the circular frequency and the wave-number of the waves, denoted by the subscripts L and S .

Carman, et al. (Ref. 40) gave a general closed form solution for these equations. This solution is also described in the Laubereau and Kaiser review (Ref. 39), in which the form of the initial Stokes field is also considered. Carman, et al. and Laubereau and Kaiser found the solutions for high gain to depend only weakly on the absolute magnitude of the initial Stokes fields. In the case considered here, the Stokes field is large, and will be taken to be invariant with x' . The solution of Eqs. (4-6) simplifies considerably in this case. This simplification is justified since the gain at the Stokes frequency is small. These calculations will be outlined, but it is instructive to consider first the physical picture of delayed CARS.

The model of the delayed pump probing of Raman anti-Stokes resonances can be described as follows. The pump and Stokes waves incident on the medium in the focal volume excite the resonant molecular vibrational level. Since the lasers are mode-locked, they possess a very narrow distribution of phases, and a coherent wave is generated in the material coordinate with a well-defined phase. The coherence of the material excitation decays by collisions as determined by the dephasing time T_2 .

The excited population decay on the other hand is determined by the vibrational relaxation rate, T_1 . The coherent wave then builds up, from an initially small value, at a rate determined by the pulse duration and intensity of the pulses, and proceeds to decay with a time constant proportional to T_2 . If $T_2 < T_p$, the coherent excitation decays essentially with the laser pulses.

The short time constant of molecular processes dictates the use of mode-locked lasers. The pulse duration of a mode-locked laser is determined by the bandwidth of the laser medium and the number of cavity modes under the gain curve. There is a fundamental relationship between the pulse duration and the gain bandwidth, since these variables are Fourier transform pairs. The product of the bandwidth, $\Delta\nu$, and the pulse duration, T_p , is given by $\Delta\nu T_p \geq K$ (Ref. 41). The constant K depends on the shape of the pulses (Ref. 41). For Gaussian pulses K is 0.441. Therefore for the gain bandwidth, Δk , in wavenumbers, $\Delta k T_p \geq 15 \text{ ps-cm}^{-1}$, for Gaussian pulses.

The finite linewidth laser means that several frequencies in the molecule are excited simultaneously. These frequencies can interfere, producing beating on a time scale of $(\nu_i - \nu_j)^{-1}$, where ν_i and ν_j are the frequencies corresponding to the i -th and j -th Raman resonances. Laubereau, Wochner and Kaiser (Ref. 42) observed this beating in the coherent excitation and probing of the tetrahedral A_{1g} vibration of CCl_4 around 459 cm^{-1} . Isotope shifts in the two chlorine isotopes split the Raman line into four main frequency components separated by approximately 3 cm^{-1} . Beating was observed in the coherent probe signal as a function of delay time on a time scale of $\sim 11 \text{ psec}$ in good agreement with the frequency splitting observed in the spontaneous Raman spectrum.

In the practice of CARS spectroscopy, there are two approaches to generating the spectrum of a molecule. One utilizes a relatively narrow bandwidth Stokes laser that is scanned in frequency to generate successively the molecular spectrum. The advantage of this technique is that very high spectral resolutions can be obtained. The other approach is to use a broadband Stokes laser to generate the entire molecular spectrum during each laser pulse. The latter approach is desirable for practical diagnostic applications, where rapid measurements are sometimes required. The broadband approach was selected here in order to compare directly picosecond CARS diagnostics to conventional CARS measurements with 0 (10^{-8} sec) pulses. The effect of beating on the picosecond CARS spectrum of nitrogen must also be considered because of the broad Stokes bandwidth. The fundamental vibrational Q-branch band ($\Delta J = 0$, $\nu = 0 \rightarrow 1$) is split by centrifugal distortion and the vibrational frequencies are given by (Ref. 43)

$$\omega_{01}(J) \sim \omega_0 - \alpha_e J(J+1) \quad (9)$$

The effect of the distribution of frequencies can be included by calculating the sum of the various vibrational components. This sum is calculated according to the following equations.

$$\frac{dQ_j}{dt} + \frac{Q_j}{T_2} = \kappa_2 E_L(t) E_S(t) \quad (10)$$

$$\langle q_j \rangle = Q_j \cos(\omega_j t + \phi_j) \quad (11)$$

$$|Q_{\text{tot}}|^2 = \left| \sum_j f_j \langle q_j \rangle \right|^2 \quad (12)$$

where E_L and E_S are the time dependent amplitudes of the pump and the Stokes lasers, respectively, and Q_j is the vibrational excitation of the j -th rotational level. $\langle q_j \rangle$ is the instantaneous coordinate of the j -th wave produced by E_L and E_S , with anti-Stokes frequency ω_j and phase ϕ_j . The phase constant can be arbitrarily set to zero without loss of generality. The total amplitude of the coherent wave including all rotational components j is given by the sum in Eq. (12) where f_j is the fractional population of the j -th rotational level.

The total amplitude $|Q_{\text{tot}}|^2$ is not directly measured in pulse delay techniques. The ultrashort laser pulses are too short for direct observation with standard electronic detectors. Instead the time-integrated scattering signal is observed. This is given in Ref. (39) as a function of the time delay, t_D , between the pump laser pulse and the delayed probing pump pulse (L_2)

$$S_{\text{coh}}(t_D) = \frac{CN_{\text{AS}}}{2\pi} f(\Delta k_{\text{AS}}) \int dt' E_{L_2}(t' - t_D)^2 \times \left| \sum_j f_j |Q_j(t')| \exp[i\Delta\omega_j t' + i\phi_j(t')] \right|^2, \quad (13)$$

where n_{AS} is the index of refraction at the anti-Stokes frequency, $f(\Delta k_{\text{AS}})$ is a function of the wavevector mismatch (Ref. 39), and E_{L_2} is the amplitude of the delayed pump signal. The convolution in this integral has relatively little effect in the calculations reported, therefore, the coherent excitation description is retained in the results shown later.

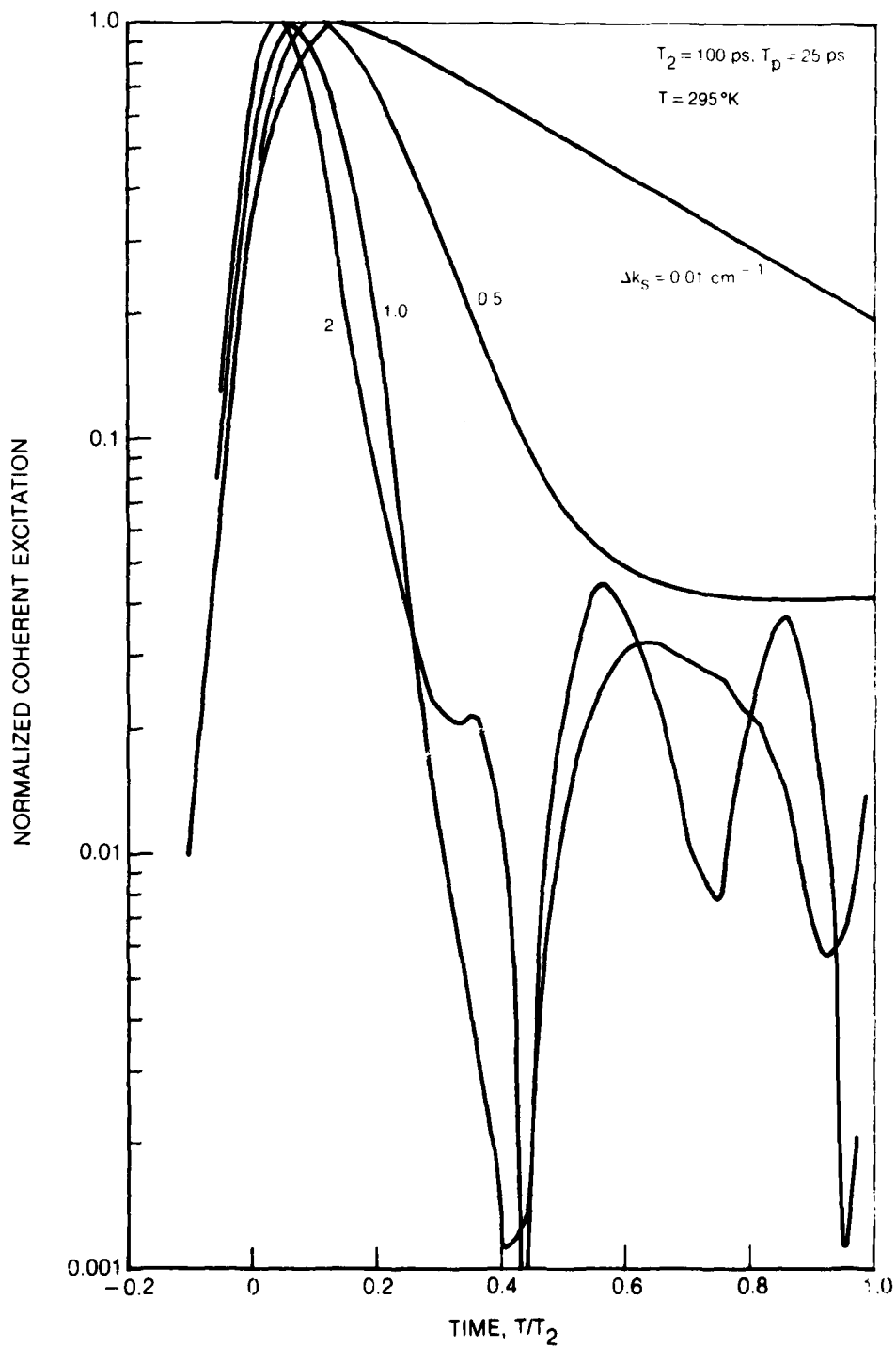
The time dependence of Q_j has been calculated by Runge-Kutta integration of Eq. (10) assuming Gaussian pulses for the pump and Stokes fields. The initial value of Q_j was assumed to be zero. The summation in Eq. (12) was formed using Eq. (11) to calculate the time dependent waves. The frequencies ω_j contained in Eq. (11) are much higher than the time step Δt used in the calculations, as a time step $\Delta t < \omega_j^{-1}$ would not be practical. Note however, that the large number of frequencies in the summation smooth the envelope of the resultant function. The result then is a function which has high frequencies which the calculation samples at the rate of Δt^{-1} . A number of calculations were performed where the time step was varied, effectively changing the sampling frequency, and it was found that the substructure varied considerably but the envelope shape did not. Accordingly, the

envelope of the resulting waves was determined, and it is that that is shown in the calculations. Figure 15 shows the normalized coherent excitation as a function of T/T_2 , the time after the pulse divided by the dephasing time, with the spectral width of the dye laser as a parameter. The curve for $\Delta\kappa_S = 0.01 \text{ cm}^{-1}$ is shown because it represents the temporal behavior of the individual rotational components. It is valid to give this curve this interpretation only because the $.01 \text{ cm}^{-1}$ dye laser bandwidth is less than that for a transform limited pulse of 25 psec as assumed in this calculation. The ratio T_2/T_p equals 4.0 indicative of a dephasing time of 100 psec. This dephasing time corresponds to the spontaneous Raman line-width of 0.1 cm^{-1} at 300 K and 1 atm (Ref. 38).

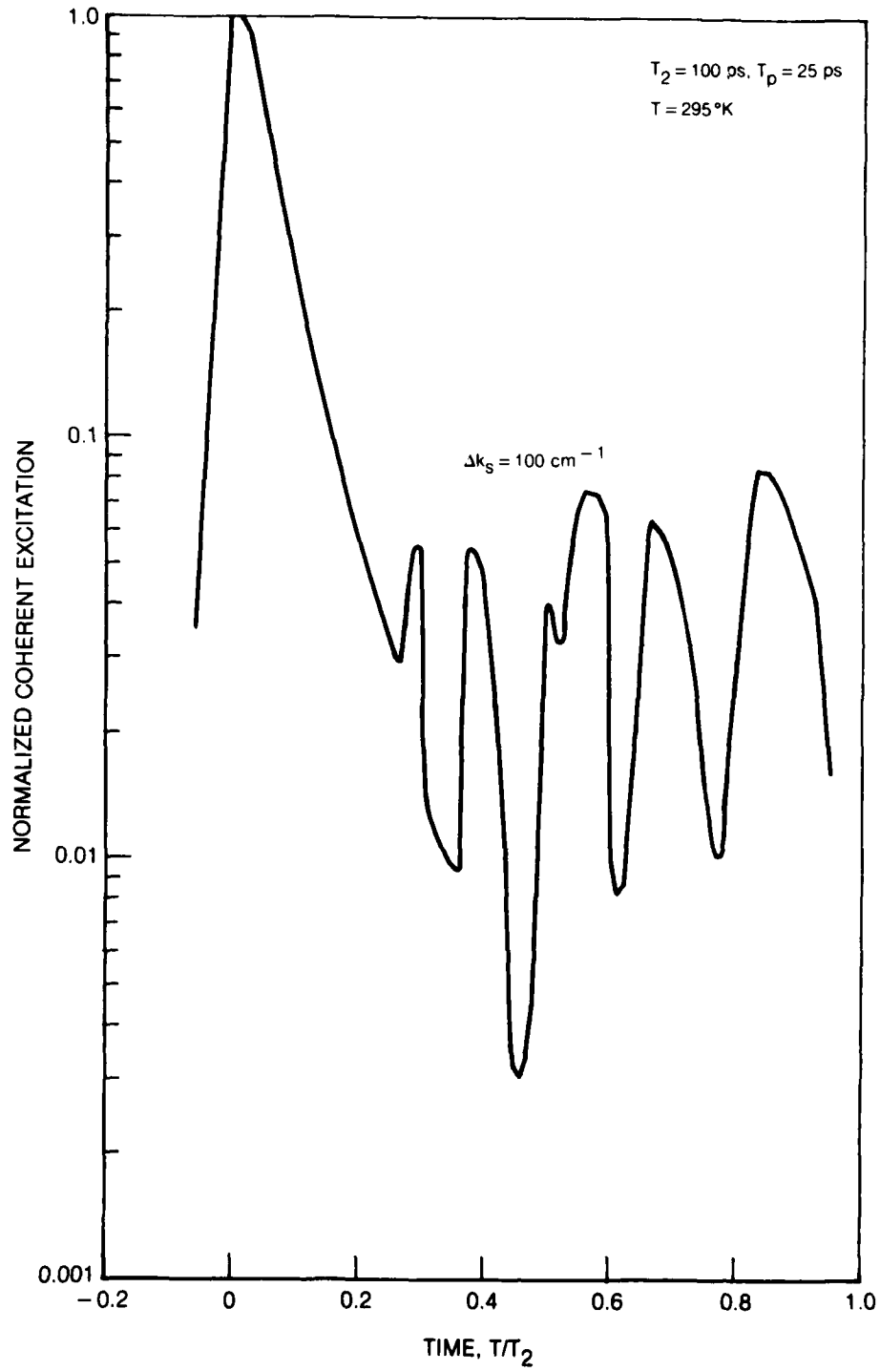
The dye laser width is taken to be Gaussian characterized by $\Delta\kappa_S$ (FWHM). The effect of larger dye laser spectral widths is to excite more ro-vibrational frequencies which interfere causing the total coherent excitation to decay very rapidly at first. At longer times, since the individual amplitudes remain relatively large, constructive and destructive interferences cause beating. The beating period is irregular because of the nonlinear dependence of the frequencies on j . The initial decay for $\Delta\kappa_S \geq 1 \text{ cm}^{-1}$ very nearly follows the input pulsewidth. The initial decay and interference are even more dramatic for the case where $\Delta\kappa_S = 100 \text{ cm}^{-1}$ as shown in Fig. 16. This width is more nearly typical of the broadband dye laser used in these experiments. The initial decay is quite rapid and interference produces irregular beating for $T/T_2 > 0.2$.

The temporal dependence of the coherent excitation shown in Fig. 16 is representative of the broadband Stokes laser case shown, in Fig. 14, by the curve labeled w/o etalon. Both curves show a rapid decrease in the signal as a function of time following the application of the excitation pulses. To check the calculated effect of restricting the number of excited Raman transitions, the Stokes bandwidth was narrowed by inserting an etalon into the synchronously pumped laser cavity. The etalon had a free spectral range of 11.4 cm^{-1} so the dye laser output spectrum consisted of a series of spikes with this frequency spacing. An analyzing etalon with a FSR of 0.67 cm^{-1} indicated that the frequency spread of an individual spectral peak was less than this value. Since the N_2 Raman spectrum is less than 10 cm^{-1} at $T = 295 \text{ K}$, only a narrowband of Raman frequencies is resonant with the 5320 \AA pump. The decay curve for this case is shown in Fig. 14 as the data labeled w/etalon. The decay is clearly slower in this case and is not exponential, as predicted by the calculations. For a time delay greater than 50 psec, the 1 atm signal decays slowly. This curve should be compared with the high pressure data, which is expected to be similar to the decay of a nonresonant signal, since $T_2 < T_p$ in both cases. Suppose that N_2 is present as a minority species in a mixture such that at zero time delay, the nonresonant signal contribution is equal to the resonant contribution. Then at a delay of 100 psec these data would indicate that the nonresonant signal should be two or three orders of magnitude smaller than the resonant signal which is also decaying but at a slower rate. For this time delay the resonant signal would decrease by a factor of about 5. The low power of the Stokes laser precludes this from being demonstrated, because the CARS signal is near the limit of detection in our experiments.

CALCULATED COHERENT EXCITATION IN N₂ GAS WITH DYE BANDWIDTH PARAMETER



CALCULATED COHERENT EXCITATION IN N₂ GAS WITH BROADBAND STOKES



Discussion of Results

The simple theory developed for N_2 illustrates the importance of interference effects in gaseous nitrogen transient coherent Raman spectroscopy. This simple theory has several shortcomings, however. The theory does not consider spatial variations in the anti-Stokes wave, nor does it include what properly should be a convolution between the Stokes laser and pump bandwidths. Furthermore, the Raman transitions are treated as isolated, a fact that certainly is not valid for the lowest rotational transitions even at one atmosphere. At higher pressure collisional narrowing effects become more important (Refs. 13 and 19) throughout the spectrum, but then the dephasing time will be less as well, and the technique would not be applicable.

Although the simple theory cannot be expected to accurately predict the shape, width and magnitude of the interferences in the delay curve, it should give a reliable prediction of their position. The Raman transition frequencies used in these calculations were taken from Gilson, et al. (Ref. 44). No attempt has been made to identify particular extremes with frequency differences in the Raman spectrum.

It is instructive to reexamine the previously cited references, i.e., Kamga and Sceats (Ref. 23), Dzhidzhoev, et al. (Ref. 24), and Magnitskii and Tunkin (Ref. 30) in the light of the present observations.

Kamga and Sceats measured delay curves for a liquid sample: CS_2 in toluene. The Raman spectrum in the liquid phase consists of a single sharp resonance. Interference effects are not expected for liquid samples unless discrete frequencies remain as in the case of the CCl_4 isotopes as studied by Laubereau, Wochner and Kaiser (Ref. 42).

Transient coherent Raman spectroscopy of gaseous ammonia was examined by Dzhidzhoev, et al. (Ref. 24). The rotational structure of the NH_3 vibrational Raman band is expected to consist of small number of closely spaced transitions. Therefore, interference effects would not be expected to be strong in ammonia even though a relatively broadband Stokes source (30 cm^{-1}) was used.

Magnitskii and Tunkin (Ref. 30) observed delayed ω_1 probe signals in H_2 using as a Stokes source, an optical parametric oscillator, having a bandwidth of 100 cm^{-1} . The Raman Q-branch spectrum of H_2 consists of several lines of alternating intensity (Ref. 43) which would be excited by the spectrally broad Stokes beam, so that beating is expected to be important. This point though brings out something that is important to understand. The coherent excitation of each individual transition is the result of a rapid buildup along with the excitation pulses followed by an exponential decay at a rate determined by the dephasing time. Beating arises when a detector is used to observe simultaneously all the Raman frequencies. The completely isolated transition will not show beating. Magnitskii and Tunkin observed no beating because they isolated a single transition (Q(1)). This, as a practical matter, is more difficult in N_2 .

Conclusions

If a stronger narrowband Stokes laser had been available, the measurements show it should be possible to suppress the nonresonant background by approximately two orders of magnitude relative to the resonant mode signal near one atmosphere pressure. At the same time, the loss in the resonant signal would be less than an order of magnitude. The short dephasing time at higher pressures however, would limit the utility of the transient Raman pump and probe technique in high pressure media for nitrogen-like molecules, due to the fundamental limitation of the pulse duration-frequency bandwidth product.

For optimum background cancellation the pump and Stokes lasers should both be operated with a narrow bandwidth and a short pulse duration to minimize the number of Raman frequencies excited. This means the CARS sources should be transform-limited. In this regard, the approach using an optical parametric oscillator may give a higher energy conversion to the Stokes frequency, but the pulses are not generally transform-limited, and therefore may not be appropriate for N₂-like molecules.

The transient Raman pump and probe technique promises to produce excellent results for liquid materials as has been demonstrated by Laubereau and Kaiser and their co-workers. The technique may also be useful for selected gases at atmospheric pressure. At high pressure the technique is not generally applicable. On the other hand, the signal loss associated with polarization orientation suppression would be more than compensated by the signal increase at elevated pressures.

REFERENCES

1. J. W. Nibler, W. M. Shaub, J. R. McDonald and A. B. Harvey: Coherent Anti-Stokes Raman Spectroscopy. In Vol. 6, Vibrational Spectra and Structure. J. R. Durig, Ed., Elsevier, Amsterdam, 1977.
2. A. C. Eckbreth, P. A. Bonczyk and J. F. Verdieck, Prog. Energy Combust. Sci. 5, 253, 1979.
3. S. Druet and J-P. E. Taran: Coherent Anti-Stokes Raman Spectroscopy. In Chemical and Biological Applications of Lasers. C. B. Moore, Ed., Academic Press, New York, 1979.
4. A. C. Eckbreth, R. J. Hall, J. A. Shirley and J. F. Verdieck: Spectroscopic Investigations of CARS for Combustion Applications. In Advances in Laser Spectroscopy, B. A. Garetz and J. R. Lombardi, Ed., Heyden and Son, Inc., 1981.
5. A. C. Eckbreth, Appl. Phys. Letters 32, 421, 1978.
6. G. L. Switzer, W. M. Roquemore, R. P. Bradley, P. W. Schreiber and W. B. Roh, Appl. Opt. 18, 2343, 1979.
7. A. C. Eckbreth, Combust. Flame 39, 133, 1980.
8. I. A. Stenhouse, D. R. Williams, J. B. Cole and M. D. Swords, Appl. Opt. 18, 3819, 1979.
9. M. E. McIlwain and L. E. Harris, 17th JANNAF Combustion Meeting, CPIA Publication 329, 1980, II-379.
10. K. Knapp and F. J. Hindelang: Measurements of Temperatures in a Shock Tube by Coherent Anti-Stokes Raman Spectroscopy (CARS). To be published in Proceedings of 13th International Symposium on Shock Tubes and Waves, July 6-9, 1981. The Niagara Frontier, New York.
11. A. C. Eckbreth and R. J. Hall, Combust. Flame 36, 87, 1979.
12. A. C. Eckbreth and R. J. Hall, Comb. Sci. and Tech. 25, 175, 1981.
13. R. J. Hall, J. F. Verdieck and A. C. Eckbreth, Opt. Comm. 35, 69, 1980.
14. K. A. Marko and L. Rimai, Opt. Lett. 4, 211, 1979,
15. R. G. Gordon, J. Chem. Phys. 46, 448, 1967.

REFERENCES (Cont'd)

16. M. Baranger, Phys. Rev., 111, 434 1958; 112, 855, 1958.
17. A. C. Kolb and H. Griem, Phys. Rev., 111, 514, 1958.
18. J. Bonamy, L. Bonamy, and D. Robert, J. Chem. Phys. 67, 4441, 1977.
19. R. J. Hall and D. A. Greenhalgh, Opt. Comm. 40, 417, 1982.
20. R. J. Hall and J. F. Verdick: Rotational Diffusion Theory Calculations of High Pressure N₂ and CO₂ CARS Bandshapes. Presented at VIII International Conference on Raman Spectroscopy, Bordeaux, France, September 1980.
21. D. E. Prichard, N. Smith, R. D. Driver, and T. A. Brunner, J. Chem. Phys. 70, 2115, 1979.
22. G. Rosasco and W. Lempert. To be published.
23. F. M. Kanga and M. G. Sceats, Opt. Letters 5, 126, 1980.
24. M. S. Dzhidzhoev, S. A. Magnitskii, S. M. Saltiel, A. P. Tarasevich, V. G. Tunkin and A. I. Kholodnykh, Sov. J. Quantum Elec. 11, 681, 1981.
25. R. J. Hall and A. C. Eckbreth, Coherent Anti-Stokes Raman Spectroscopy (CARS): Application to Combustion Diagnostics. To appear in Laser Applications (Vol. V), R. K. Erf, ed., Academic Press.
26. A. F. Bunkin, S. G. Ivanov, and N. I. Koroteev, Sov. Tech. Phys. Letts. 3, 182, 1977.
27. H. Lotem, R. T. Lynch, Jr., and N. Bloembergen, Phys. Rev. A14, 1748, 1976.
28. B. Attal, O. O. Schnepp, and J-P. E. Taran, Opt. Comm. 24, 77, 1978.
29. W. Zinth, Opt. Commun. 34, 479, 1980.
30. S. A. Magnitskii and V. G. Tunkin, Sov. J. Quantum Electron. 11, 1218, 1981.
31. J. R. Murray and A. Javan, J. Mol. Spectrosc. 29, 502, 1969.
32. R. L. Byer and R. L. Herbst, The Unstable-Resonator YAG, Laser Focus, 48, July 1978.
33. R. J. Dewhurst and J. Jacoby, Opt. Commun. 28, 107, 1979.

REFERENCES (Cont'd)

34. P. Liu and R. Yen, *Appl. Optics* 18, 600, 1979.
35. G. C. Reali, *Opt. Commun.* 35, 264, 1980.
36. G. H. McCall, *R. Sci. Instrum.* 43, 865, 1972.
37. M. A. Duguay, J. W. Hansen and S. L. Shapiro, *IEEE J. Quant. Elec.* QE-6, 725, 1970.
38. A. Owyong and L. A. Rahn, *IEEE J. Quantum Elec.* QE-15, 25D, 1979.
39. A. Laubereau and W. Kaiser, *Rev. Mod. Phys.* 50, 607, 1978.
40. R. L. Carman, F. Shimizu, C. S. Wang and N. Bloembergen, *Phys. Rev.* A2, 60, 1970.
41. W. H. Lowdermilk, *Technology of Bandwidth-Limited Ultrashort Pulse Generation in Laser Handbook*. Vol. 3, M. L. Stitch, ed., North-Holland, Amsterdam, 1979.
42. A. Laubereau, G. Wochner and W. Kaiser, *Phys. Rev.* A13, 2212, 1976.
43. G. Herzberg, *Molecular Spectra and Molecular Structure I. Spectra of Diatomic Molecules*, D. Van Nostrand, Princeton, 1950.
44. T. R. Gilson, I. R. Beattie, J. D. Black, D. A. Greenhalgh and S. N. Jenny, *J. Raman Spectrosc.* 9, 361, 1980.

APPENDIX A

PUBLICATIONS/PRESENTATIONS UNDER ARO CONTRACT DAAG29-79-C-0008
CARS DIAGNOSTICS OF HIGH PRESSURE COMBUSTION

1. R. J. Hall, J. F. Verdieck and A. C. Eckbreth: CARS Diagnostics for High Pressure Combustion. Presented at the 35th Symposium on Molecular Spectroscopy. Ohio State University, June 1980.
2. J. A. Shirley, R. J. Hall, J. F. Verdieck and A. C. Eckbreth: New Directions in CARS Diagnostics for Combustion. AIAA Paper 80-1542. Snowmass, Colorado, July 1980.
3. R. J. Hall and J. F. Verdieck: Collisional Narrowing of the High Pressure CARS Spectrum of N_2 . Presented at the VII International Conference on Raman Spectroscopy, Ottawa, Canada, August 1980, p. 700.
4. R. J. Hall, J. F. Verdieck and A. C. Eckbreth: Pressure-Induced Narrowing of the CARS Spectrum of N_2 . Opt. Comm., Vol. 35, pp. 69-75, 1980.
5. A. C. Eckbreth, R. J. Hall, J. A. Shirley and J. F. Verdieck: Investigations of Coherent Anti-Stokes Raman Spectroscopy (CARS) for Practical Combustion Diagnostics. Paper Presented at the Fifth International Symposium on Air-Breathing Engines. Bangalore, India, 1981.
6. R. J. Hall and A. C. Eckbreth: Combustion Diagnosis by Coherent Anti-Stokes Raman Spectroscopy (CARS). Opt. Eng., Vol. 20, pp. 494-500, July-August 1981.
7. A. C. Eckbreth, R. J. Hall, J. A. Shirley and J. F. Verdieck: Spectroscopic Investigations of CARS for Combustion Applications. In Vol. 1, Advances in Laser Spectroscopy. B. A. Garetz and J. R. Lombardi, Ed., Heyden and Sons, London, 1982, p. 101.
8. J. F. Verdieck, J. A. Shirley, R. J. Hall and A. C. Eckbreth: CARS Thermometry in Reacting Systems. In Vol. 5, Temperature, Its Measurement and Control in Science and Industry. J. F. Schooley, ed., AIP, New York, 1982, p. 595.
9. R. J. Hall and D. A. Greenhalgh: Application of the Rotational Diffusion Model to Gaseous N_2 CARS Spectra. Opt. Comm., Vol. 40, pp. 417-420, 1982.
10. J. F. Verdieck, R. J. Hall, J. A. Shirley and A. C. Eckbreth: Some Applications of Gas Phase CARS Spectroscopy. J. Chem. Ed., Vol. 59, pp. 495-503, 1982.
11. R. J. Hall and J. F. Verdieck: Rotational Diffusion Theory Calculations of High Pressure N_2 and CO_2 CARS Bandshapes. Presented at the VIII International Conference on Raman Spectroscopy, Bordeaux, France, September 1982.
12. J. H. Stufflebeam, J. F. Verdieck, and R. J. Hall: CARS Diagnostics of High Pressure and Temperature Gases. Abstract Submitted for the AIAA 18th Thermophysics Conference, Montreal, Canada, June 1983.

R82-954566-F

APPENDIX B

PARTICIPATING SCIENTIFIC PERSONNEL AND DEGREES AWARDED DURING THIS CONTRACT

A. C. Eckbreth
R. J. Hall
J. A. Shirley
J. H. Stufflebeam
J. F. Verdieck

R82-954566-F

APPENDIX C

COLLISIONAL NARROWING OF THE HIGH PRESSURE CARS SPECTRUM OF N₂

COLLISIONAL NARROWING OF THE HIGH PRESSURE CARS SPECTRUM OF N₂*

Robert J. Hall and J. F. Verdick

United Technologies Research Center
East Hartford, Connecticut, USA 06108

ABSTRACT - The CARS spectrum of N₂ has been investigated experimentally over the pressure range of one to approximately 100 atmospheres. The spectra show evidence of collisional narrowing, and are in good agreement with theory.

RESUME - Le spectre CARS de N₂ a été recherché par expérience pour des pressions entre une et cent atmosphères. Les spectres demont rétrécissement à cause des collisions et sont bien d'accord avec la théorie.

By solving the equation of change for the density operator with the interaction energy $-\frac{1}{2}\alpha E^2$, and with a collision integral representing line-width effects¹, the third-order, nonlinear electric susceptibility governing resonant CARS generation from vibrational Q-branch transitions is shown to be given by

$$\chi_3 = \frac{iN}{\hbar} \sum_r \alpha_r \sum_s \alpha_s \Delta\rho_s^{(0)} \left[\mathbf{G} \right]_{rs}^{-1} \quad (1)$$

where α is isotropic polarizability; E is electric field strength; N is active molecule number density, and $\Delta\rho_s^{(0)}$ is the normalized population difference for vibration-rotation Q-branch $Q(s)$. The elements of the G -matrix are given by

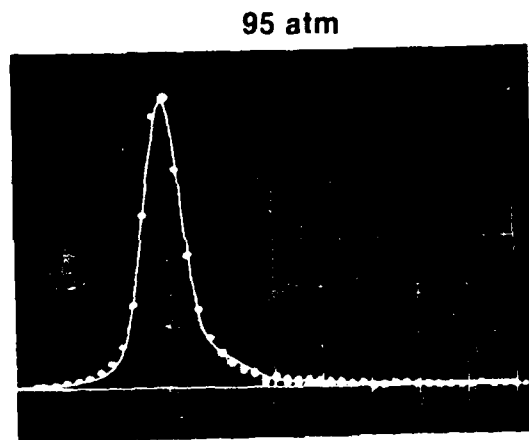
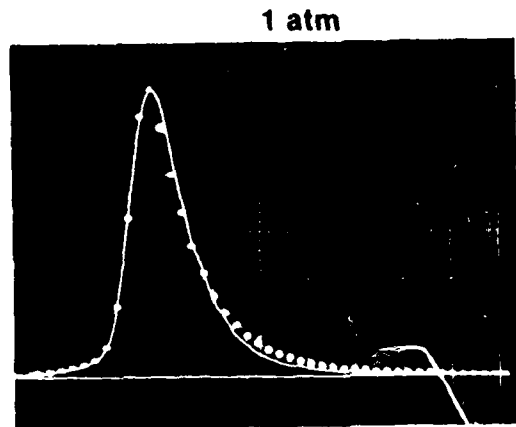
$$G_{rs} = i(\omega_1 - \omega_2 - \omega_r) \delta_{rs} + \frac{\Gamma_r}{2} - i\Delta_r \delta_{rs} + \gamma_{rs}(1 - \delta_{rs}) \quad (2)$$

where ω_1 and ω_2 are the frequencies of the pump and Stokes sources, respectively; ω_r , Γ_r , and Δ_r are the vacuum frequency, isolated linewidth, and shift, respectively, of transition $Q(r)$, and the off-diagonal linewidth elements γ_{rs} govern the rates of collisional energy transfer between lines. The presence of the γ_{rs} causes a change in the broadening of the CARS signatures at pressures where individual N₂ Q-branches have begun to overlap. Further increases in pressure are expected to result in a continuous narrowing of the overall CARS signature, a manifestation of the phenomenon of collisional, or pressure-induced narrowing.^{1,2}

Experimentally, a high pressure vessel with coaxial optical access has been employed to study the 300°K CARS spectrum of N₂ over the pressure range one to 95 atmospheres. The pump source was generated by frequency-doubling the output of a pulsed Nd:YAG laser; the broadband Stokes source was provided by a dye oscillator-amplifier driven by a portion of the pump output. The pump laser and dye laser beams were combined by means of a

dichroic mirror and focussed in the high pressure test cell, generating coaxial CARS. The pump beam was attenuated with neutral density filters in order to eliminate stimulated Raman scattering, which can be a problem at high pressures with unattenuated, high intensity beams. At the higher pressures, the CARS signature was readily visible as a bright blue spot. Detection of the CARS signal was carried out using a one meter Jobin-Yvon monochromator fitted with an optical multichannel analyzer, providing an instrumental resolution of about 1.5 cm⁻¹.

As a function of increasing pressure, the width of the N₂ CARS signature was found to decrease continuously from one to about 50 atmospheres, with little variation in the range 50-95 atmospheres. Calculations based on Equation (1) were found to be in good agreement with these results over the entire pressure range. Figure 1 displays theory-experiment comparisons at one and 95 atmospheres. The significant role that collisional narrowing plays at 95 atmospheres can be appreciated by considering the fact that the isolated linewidths for N₂ Q-branches are 0(10 cm⁻¹) at this pressure³, and the overall width of the CARS spectrum would be at least 10 cm⁻¹ if the narrowing mechanism were not present. As seen, the width at 95 atmospheres is about 75% of the one atmosphere value. In the theoretical calculations of Figure 1, the isolated Q-branch linewidths of Ref. 3 were scaled linearly with pressure. The selection rule $\Delta J = \pm 2$ was assumed in calculating the γ_{rs} ; together with detailed balance and S-matrix unitarity relationships, this results in a determinate set of γ_{rs} containing no adjustable parameters.



Frequency ($.5 \text{ cm}^{-1}$ per dot)

Figure 1. Comparison of experimental and theoretical N_2 CARS signatures at one and 95 atmospheres. The white dots are experimental points, and the theoretical predictions are given by the solid white lines. The pump laser bandwidth is $.4 \text{ cm}^{-1}$, and the instrumental resolution is 1.5 cm^{-1} .

ACKNOWLEDGEMENT

The authors wish to thank Dr. A. C. Eckbreth for many helpful discussions, and Mr. Normand Gantick for his very capable assistance with the experiments.

* Work carried out under Army Research Office Contract DAAG29-79-C-0008.

REFERENCES

1. V. Alekseyev, et.al., IEEE JOE, QE-4, 654 (1968)
2. A. D. May, J. C. Stryland, and G. Varchese, Can. J. Phys., 48, 2331 (1970).
3. A. Owyong and L. A. Rahn, High Resolution Inverse Raman Spectroscopy in a Methane Air Flame, IEEE/OSA Conference on Laser Engineering and Application, Digest of CLEA papers, IEEE JOE, QE-15, 250-260 (1979).

R82-954566-F

APPENDIX D

PRESSURE-INDUCED NARROWING OF THE CARS SPECTRUM OF N₂

PRESSURE-INDUCED NARROWING OF THE CARS SPECTRUM OF N₂*

Robert J. HALL, James F. VERDIECK and Alan C. ECKBRETH
United Technologies Research Center, East Hartford, Connecticut, USA

Received 28 April 1980
Revised manuscript received 10 June 1980

The coherent anti-Stokes Raman spectroscopy (CARS) spectrum of N₂ has been recorded experimentally over the pressure range from one to 100 atmospheres. The pressure dependence of the 300 K vibrational Q-branch signature is strongly affected by collisional narrowing. A theoretical model of CARS generation for overlapping spectral lines gives good agreement with the experimental results over the entire pressure range.

1. Introduction

Coherent anti-Stokes Raman spectroscopy (CARS) is a nonlinear, three-wave, optical mixing technique that is being successfully applied as a diagnostic tool in a number of different fields [1-4]. Of particular promise is the application of CARS for combustion diagnostics, where its coherence and high conversion efficiency make it well suited for spatially and temporally precise probing of the high interference environments characteristic of practical devices. The usefulness of CARS has been demonstrated by temperature measurements in a highly sooting diffusion flame [5], an internal combustion engine [6], and in liquid-fuelled combustors [7-9]. Single pulse spectra have also been obtained in turbulent combustion media [8,9], offering the potential for determination of the spectrum of turbulent temperature fluctuations. Because N₂ is the dominant constituent of air-fed combustion, it has therefore received the most attention in the foregoing experiments.

While most of these experiments have been carried out at one atmosphere pressure, there are strong practical motivations for extending CARS diagnostic capabilities to higher pressures because high pressure combustion is very important in such contexts as air-breathing and rocket propulsion, and ballistic com-

pression. As an example, better efficiency is obtained from gas turbines if they are operated at higher pressure. In addition, studies of the pressure dependence of overlapping spectral lines can reveal information about intermolecular collisional energy transfer processes, as will be seen.

2. Collisional narrowing

In N₂ CARS thermometry, the signature is dominated by vibrational Q-branch transitions. At low pressure, where the homogeneous Raman linewidths in N₂ are small ($\sim 0.1 \text{ cm}^{-1} \text{ atm}^{-1}$) [10], the CARS intensity distribution will be determined by frequency splitting between lines due to vibration-rotation interaction. The isolated linewidths can be expected to broaden linearly with pressure, but at pressures where significant line overlap occurs the character of the broadening changes, and the phenomenon of collisional narrowing [11-19] will thereafter govern the CARS intensity distribution. Because the interaction of vibration and rotation is so small in N₂, the vibrational Q-branches are very closely spaced, and substantial line overlap will occur even at moderate pressures.

Collisional narrowing was first observed experimentally by Bloembergen et al. [11] in studies of nuclear magnetic resonance. Alekseyev and Sobelman [12] showed theoretically that collisional energy transfer between overlapping Raman lines would give rise to a

* Research supported in part by the Army Research Office, Durham, N.C. under Contract #DAAG29-79-C-0008.

narrowing of the Raman signature with increasing pressure. The pressure dependence of the spontaneous Raman spectrum of N_2 was investigated by Mikhailov [13] and by May et al. [14]. The latter high resolution experiments showed that the fundamental vibrational band of N_2 undergoes a continuous contraction in width as the pressure increases from about 30 to roughly 350 atmospheres. This result was confirmed by Wang and Wright [15]. Collisional narrowing is also an explanation for the fact that the Raman spectrum of liquid N_2 is even sharper than it is in the gaseous state [16].

In the gas phase, the broadening of isolated N_2 Q -branches arises mainly from lifetime limiting, rotationally inelastic collisions, and as the pressure is increased, this collisional energy transfer becomes increasingly frequent. Eventually molecules will undergo so many changes of rotational quantum number during a scattering process that they will tend to radiate at an average frequency rather than that of individual lines. The intensity distribution will then collapse toward a center of gravity determined by the frequency of the transition associated with the largest Boltzmann population. The narrowing effect can also be thought to arise from a reduced rotationally inelastic collision frequency that is caused by the coalescence of lines [20].

3. Theory of collisional narrowing in CARS

In CARS, incident laser beams at frequencies ω_1 and ω_2 (termed the pump and Stokes sources, respectively) interact through the third-order, nonlinear electric susceptibility, χ_3 , to produce polarization at $\omega_3 = 2\omega_1 - \omega_2$. If the frequency difference $\omega_1 - \omega_2$ coincides with the frequency of a Raman-active vibrational mode, a coherent oscillation is excited in the molecule, and the CARS polarization appears resonantly enhanced as the upper side band of a polarizability modulated at this difference frequency.

The interaction energy governing the nuclear response may be expressed as $-\frac{1}{2}\alpha E^2$ where α is molecular polarizability and E is electric field strength. For two monochromatic sources

$$\begin{aligned} E_1(t) &= \frac{1}{2}(A_1 e^{-i\omega_1 t} + \text{c.c.}), \\ E_2(t) &= \frac{1}{2}(A_2 e^{-i\omega_2 t} + \text{c.c.}), \end{aligned} \quad (1)$$

E^2 will contain the terms

$$\frac{1}{2} A_1 A_2^* e^{-i(\omega_1 - \omega_2)t} + \text{c.c.}, \quad (2)$$

which will be responsible for the resonant nuclear contribution to the polarization. In terms of the molecular density operator, $\rho(t)$, the third-order polarization $P_3(t)$ may be expressed as:

$$P_3(t) = N \text{Tr}(\rho \alpha) E_1(t), \quad (3)$$

where N is the number density of Raman-active molecules. Fourier-transforming (3) gives:

$$\tilde{P}_3(\omega) = N \int \text{Tr}[\tilde{\rho}(\omega - \omega') \alpha] \tilde{E}_1(\omega') d\omega'. \quad (4)$$

where the \sim denotes Fourier transform. The equation of motion for the density matrix is now solved with the interaction energy $h(t) = -\frac{1}{2}\alpha E^2$, and with a collision integral representing linewidth effects [12]. This equation is:

$$\dot{\rho} = -\frac{i}{\hbar} [H_0, \rho] - \frac{i}{\hbar} [h(t), \rho] + \int (S^+ \rho S - \rho) F(g) dg, \quad (5)$$

where H_0 is the unperturbed molecular hamiltonian, S is the collisional scattering matrix, and $F(g)$ is the rate of g -type collisions. The collision integral assumes the validity of the impact approximation and thus this analysis is limited to the binary collision regime. Eq. (5) is now solved in the usual manner [21] by a perturbation expansion in powers of the interaction energy $h(t)$. If the resulting equation of change for the first order correction to (5) is Fourier-transformed, and the operations of eq. (4) carried out, then χ_3 is the coefficient of $\frac{1}{8} A_1^2 A_2^*$ in the expression for the Fourier components of the polarization. The resulting expression for χ_3 is:

$$\chi_3 = \sum_t \frac{iN\alpha_t}{\hbar} \sum_s \alpha_s \Delta\rho_s^{(0)} [G]_{ts}^{-1}, \quad (6)$$

where the t and s indices denote the collection of quantum numbers (vibrational-rotational) belonging to particular Q -branch transitions, $\Delta\rho_s^{(0)}$ is the unperturbed fractional population difference for transition s , and G_{ts} is the "G matrix" that is given by:

$$\begin{aligned} G_{ts} &= i(\omega_1 - \omega_2 - \omega_t) \delta_{ts} \\ &+ (\Gamma_t/2 - i\Delta_t) \delta_{ts} + \gamma_{ts} (1 - \delta_{ts}). \end{aligned} \quad (7)$$

Here ω_r , Γ_r , and Δ_r are the vacuum frequency, isolated linewidth, and shift, respectively, of transition r ; δ_{rs} is the Dirac delta function; and γ_{rs} is an off-diagonal linewidth parameter. Γ_r , Δ_r and γ_{rs} are in turn related to the scattering matrix S by the relationships:

$$\begin{aligned} \frac{1}{2} \Gamma_r - i\Delta_r &= \int (1 - S_{r_1 r_1}^* S_{r_2 r_2}) F(g) dg, \\ \gamma_{rs} &= -\int S_{r_1 s_1}^* S_{s_2 r_2} F(g) dg, \end{aligned} \quad (8)$$

where the subscripts 1 and 2 refer to the initial and final quantum states, respectively, of the transitions r and s . Vibrationally inelastic collisions ($\Delta v \neq 0$) can be ignored in N_2 at room temperature, so that to a good approximation

$$S_{v_j, v_j'} = S_{v_j, v_j'} \delta_{vv'} \quad (9)$$

If the influence of vibration-rotation interaction and vibrational dephasing collisions are also neglected, so that

$$S_{v_j, v_j'} = S_{j j'} \delta_{vv'} \quad (10)$$

one gets the result that for Q-branches

$$\begin{aligned} \frac{1}{2} \Gamma_r &= \int (1 - |S_{rr}|^2) F(g) dg, \\ \gamma_{rs} &= -\int |S_{sr}|^2 F(g) dg, \quad \Delta_r = 0, \end{aligned} \quad (11)$$

where the r and s now refer to the rotational quantum number of the transition, i.e., $Q(r)$. Thus, in the absence of vibrational effects, the shifts vanish and the γ_{rs} are real. In addition to the known inefficiency of N_2 vibrational relaxation, the fact that the shifts in N_2 are relatively small [14,15] and that the isolated linewidths display essentially no vibrational dependence nor evidence of vibrational dephasing [10] lend support to these approximations. Thus, our calculations have been made neglecting vibrational dependences of linewidth parameters. One consequence of eq. (10) is that the γ_{rs} will only couple Q-branches belonging to the same vibrational band.

The unitarity principle of the S -matrix

$$\sum_s |S_{rs}|^2 = 1, \quad (12)$$

leads to the following relationship between Γ_r and the γ_{rs}

$$\sum_{s \neq r} \gamma_{sr} = -\Gamma_r/2. \quad (13)$$

Further, the γ_{rs} will obey detailed balance relationships:

$$\rho_s^{(0)} \gamma_{rs} = \rho_r^{(0)} \gamma_{sr}, \quad (14)$$

where $\rho^{(0)}$ denotes the normalized rotational Boltzmann population.

If the γ_{rs} are ignored in the G -matrix equation (7), then

$$[G]_{rs}^{-1} = \frac{\delta_{rs}}{i(\omega_1 - \omega_2 - \omega_r) + \Gamma_r/2} \quad (15)$$

and eq. (6) becomes

$$\chi_3 = \frac{2N}{\hbar} \sum_r \frac{\alpha_r^2 \Delta \rho_r^{(0)}}{2(\Delta\omega_{12} - \omega_r) - i\Gamma_r}. \quad (16)$$

This conventional sum representation is therefore strictly valid only for isolated lines.

For moderate pressures where the line overlap is small, one can expand G_{rs}^{-1} as follows:

$$[G]_{rs}^{-1} \approx [G_{rr}^{(0)}]^{-1} \delta_{rs} - (G_{rr}^{(0)})^{-1} \gamma_{rs} (G_{ss}^{(0)})^{-1} (1 - \delta_{rs}), \quad (17)$$

where

$$G_{rr}^{(0)} = i(\omega_1 - \omega_2 - \omega_r) + \Gamma_r/2.$$

Substituting into eq. (6) gives

$$\begin{aligned} \chi_3 &= \frac{2N}{\hbar} \sum_r \frac{\alpha_r^2 \Delta \rho_r^{(0)}}{2\Delta\omega_r - i\Gamma_r} \\ &\quad - \frac{iN}{\hbar} \sum_r \frac{\alpha_r}{i\Delta\omega_r + \Gamma_r/2} \sum_s \frac{\gamma_{rs} \alpha_s \Delta \rho_s^{(0)}}{i\Delta\omega_s + \Gamma_s/2}. \end{aligned} \quad (18)$$

This expression is valid in the limit of small overlapping. In general, however, the complex G -matrix has to be numerically inverted.

Eq. (11) shows that the off-diagonal linewidth parameters γ_{rs} govern the rates of collisional energy transfer between lines $Q(r)$ and $Q(s)$. While the Γ_r and Δ_r determine the width and shift of isolated lines, the off-diagonal linewidth parameters control the collapse or coalescence of overlapping lines which occurs in collisional narrowing. If vibrationally inelastic and dephasing collisions are slow, then the γ_{rs} are equivalent to minus the first-order rate constants for rota-

tional cross-relaxation. For N_2 , which consists of ortho- and para-modifications, the selection rule on rotational quantum number for these processes will be $\pm 2, \pm 4, \dots$. Unless the selection rule ± 2 is assumed, however, the number of unknown linewidth parameters exceeds the number of relationships between these (eqs. (13), (14), and adjustable parameters will have to be introduced if the γ_{rs} cannot be calculated on an a priori basis.

In the calculations to follow, a provisional model for the γ_{rs} has been employed in which the rate constant for the transition $J \rightarrow J'$ is assumed to be proportional to the exponential of the rotational energy defect [22,23]. That is, for downward transitions ($J' < J$) $\gamma_{J',J}$ is given by:

$$\gamma_{J',J} = d_{J'} A_J \exp(-C_J |\Delta E_{JJ'}|/kT), \quad (19)$$

where $d_{J'}$ is the rotational degeneracy of J' , A_J and C_J are parameters, and $\Delta E_{JJ'}$ is the rotational energy defect. For upward ($J' > J$) transitions, detailed balance gives

$$\gamma_{JJ'} = d_J A_{J'} \times \exp(-\Delta E_{JJ'}/kT) \exp(-C_J |\Delta E_{JJ'}|/kT). \quad (20)$$

This general functional form for the rotational relaxation rate matrix describes the relaxation patterns of hydrogen halides fairly well [22], and has an information theoretic foundation [23]. If a set of C_J is assumed, then the values of the A_J parameters follow from eqs. (13) and (14).

Values of $C_J \gg 1$ correspond to a diagonally dominant rate matrix; that is, one in which values of γ_{rs} close to the diagonal dominate ($\Delta J = \pm 2$). The other limit, $C_J \ll 1$, corresponds to a situation in which all rotational levels are strongly coupled by collisions, and all values of ΔJ (even) occur with comparable probability. In the calculations to follow, the isolated linewidths reported in [10] were scaled linearly with pressure, and shifts were not included.

4. Experimental

CARS spectra of gaseous nitrogen were obtained by means of broadband collinear CARS generation in a high pressure vessel. Bandwidths (fwhm) were measured with a high resolution monochromator as a func-

tion of pressure from one to one hundred atmosphere for comparison with the theoretical predictions. For these investigations, the 532 nm output from a Q-switched, frequency-doubled neodymium: YAG pulsed laser (Quanta-Ray Model DCR) was combined with the broadband output of a circulating-dye laser, end-pumped with a portion of the doubled Nd:YAG output. The 532 nm radiation was narrowed to a bandwidth of $\sim 0.4 \text{ cm}^{-1}$ (as measured by a double monochromator) with an intracavity etalon. The Stokes beam from the dye laser was wavelength centered at 607 nm by adjusting the dye concentration; the bandwidth was about 200 cm^{-1} . The dye laser energy was approximately 10 mJ, in a $\sim 8 \text{ ns}$ pulse. More detailed descriptions of the experimental aspects of CARS are given in [5] and [8].

Collinear CARS was achieved by combining the 532 nm pump beam and the Stokes dye laser beam with a dichroic mirror and focussing into the cylindrical high pressure cell. The emerging beams, including the nascent CARS beam, were collimated and spectrally dispersed with an extra dense flint prism. The pump and Stokes beams were trapped and the CARS beam directed to the double monochromator for scans of the bandwidth. At the higher pressures, $p > 20 \text{ atm}$, the pump laser beam was attenuated by a factor of 100 with neutral density filters. This attenuation prevented breakdown and stimulated Raman scattering (SRS) from taking place. The CARS signals were averaged with a PAR boxcar averager in the A/B mode; the B channel normalizing signal was obtained by splitting off a portion of the CARS beam before entering the spectrometer. The CARS spectra were scanned at the slowest available rate, $1 \text{ cm}^{-1}/\text{min}$. The resolution of the double monochromator was measured by scanning a low-pressure Pen-Ray xenon lamp and found to be 0.38 cm^{-1} .

5. Discussion

The overall instrumental resolution was sufficiently good to give an N_2 signature at one atmosphere in which individual even- J vibrational Q-branch transitions could be observed (fig. 1). At higher pressures, it was no longer possible to observe these Q-branches, and the experimental spectrum tended to assume a more symmetrical shape, with an overall width slightly

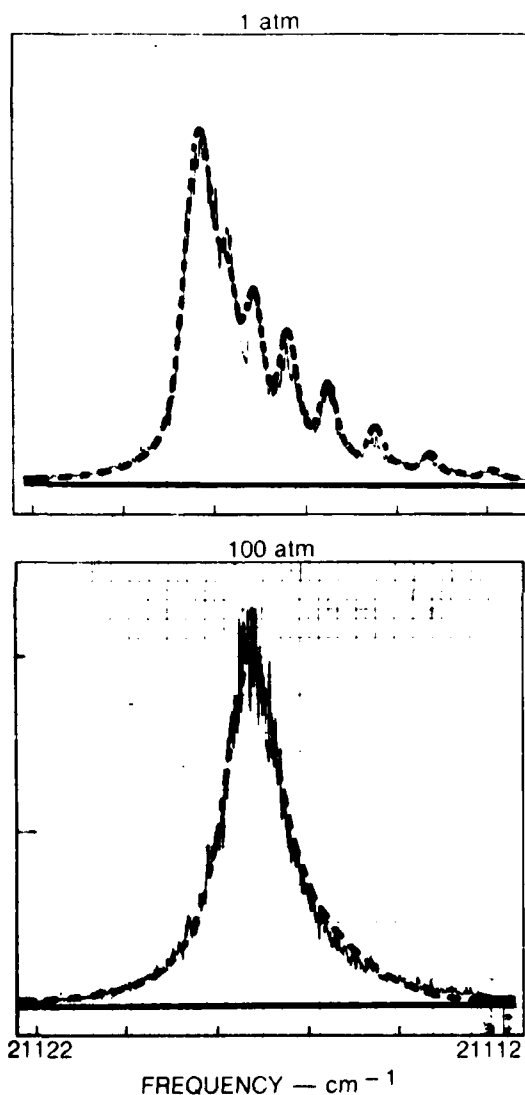


Fig. 1. CARS signatures of 300 K N_2 at one and 100 atm, — experiment, - - - theory. The isolated linewidths reported in [10] were scaled linearly with pressure in the calculations.

less than the one atmosphere value. Fig. 1 also shows a typical 100 atm spectrum with a width of about 1.5 cm^{-1} . Also shown in fig. 1 are theoretical predictions based on eqs. (6), and (19), (20).

In generating the theoretical curves shown in fig. 1,

it was found that calculations based on the selection rule $|\Delta J| = 2$ resulted in a predicted width of about 1 cm^{-1} at 100 atm, a value about 33% lower than that observed. The good agreement exhibited at 100 atm resulted from assuming that the C_J parameters (eqs. (19), (20)) all had a value of 1.75. In fact, collisional narrowing was found to play a role in obtaining the good agreement shown at one atmosphere. In the isolated line approximation, the Q-branches at one atmosphere stood out too strongly, and better agreement was obtained by taking narrowing into account. It is apparent from fig. 1 that the spectrum maximum undergoes a shift of slightly more than 1 cm^{-1} over this pressure range. The theoretical curve, which does not include line shifts, was translated on the frequency axis until the peaks coincided.

The very significant role that collisional narrowing plays in the high pressure experimental signatures can be appreciated by considering fig. 2, where theoretical predictions based on the isolated line approximation (dotted line) and overlapping line theory (solid line) are compared. The width of an isolated line signature will be determined by the homogeneous linewidths if these quantities are larger than a spectral bandwidth determined by the rotational population distribution and the spacing between Q-branch transitions. At 100 atm the homogeneous linewidths will have values of about 10 cm^{-1} , and the predicted isolated line signature has an overall bandwidth of about this value.

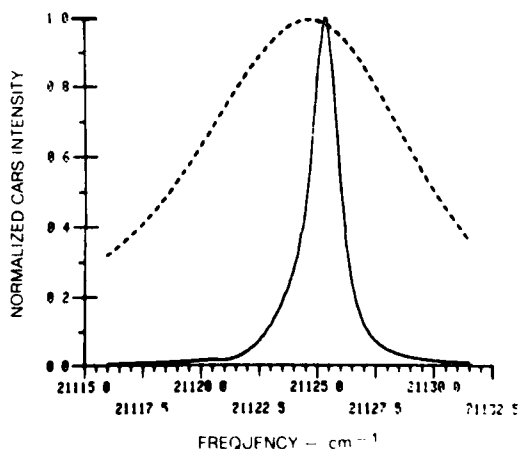


Fig. 2. Comparison of calculated 100 atm signature with and without collisional narrowing, — with narrowing, - - - without narrowing.

Collisional narrowing caused by line overlap thus results in a contraction of the 100 atm N_2 CARS signature of about 85%.

The pressure dependence of the CARS signature bandwidth (fwhm) is shown in fig. 3. The experimental points represent data which were collected over a period of two weeks; a particular symbol denotes data from one day's runs. The scatter in the data most likely result from the extreme alignment sensitivity which arises from working at the resolution limit of the double monochromator, coupled with the very long optical lever arms which direct the CARS beam to the monochromator. Additionally, the assignment of bandwidth to each spectrum is prone to subjective error in reading of peak height and full width at half-height. This subjective error is random, and is estimated to be at least $\pm 0.1 \text{ cm}^{-1}$. This seems reasonable in view of the fact that the spectrometer resolution is $\sim 0.4 \text{ cm}^{-1}$. With these remarks in mind, the experimental data suggest that the bandwidth is essentially constant, after the narrowing of the Q-branch structure which occurs from one to about 10 atm.

Theoretical calculations for two values of the C parameter (suppressing the J subscript) are shown in

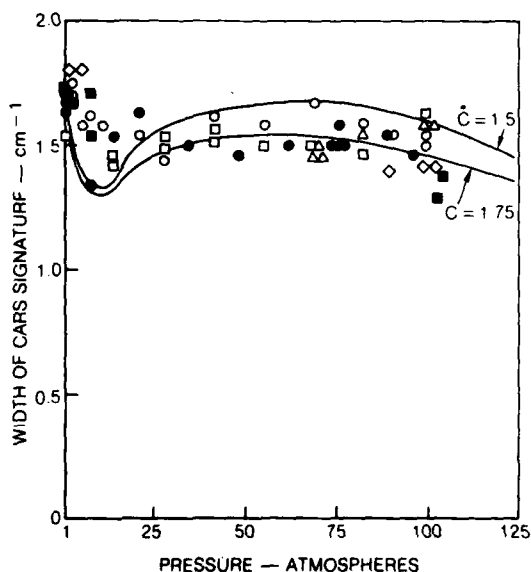


Fig. 3. Pressure dependence of the CARS signature width (fwhm). The solid lines give the theoretical predictions, and the various \circ , Δ , and \square symbols denote the results of different series of experimental scans taken over a period of several weeks.

fig. 3, with the $C = 1.75$ curve giving slightly better overall agreement. There appears to be a slight discrepancy between experiment and theory for low pressures up to approximately 10 atm, where the theory exhibits a pronounced local minimum. Otherwise, the agreement is quite good. The calculated profiles have a complicated dependence on C . As has been stated, use of a diagonally dominant ($\Delta J = \pm 2$) rotational relaxation rate matrix leads to predicted profiles that are narrower than those observed. As C is reduced in magnitude, the predicted widths increase; for $C = 1$, the 100 atm value is 1.75 cm^{-1} . Further reductions in the value of C , however, result in a contraction of the bandwidths. For $C = 0.75$, good agreement with experiment is achieved at 10 and 100 atm, but the intermediate widths are much too large. In the limit of strongly coupled rotational states ($C \rightarrow 0$), the predicted bandwidths are again much narrower than those observed experimentally. Thus, these experimental results are most consistent with a relaxation rate matrix that lies between the limits of diagonal dominance and strong coupling. In the best fit calculation $\Delta J = \pm 2$ steps are predominant, but small contributions from $\Delta J = \pm 4, \pm 6, \dots$ are important as well.

In fig. 3, the theoretical width reaches a shallow maximum between 50 and 75 atm, and then resumes a continuous narrowing with increasing pressure. Calculations for pressures higher than those shown in fig. 3 show that the bandwidth should undergo narrowing out to about 300 atm. This pressure dependence is somewhat different than that reported for the spontaneous Raman spectrum of N_2 [14,15], where a maximum at about 30 atm is followed by a continuous narrowing out to about 350 atm. This difference is not surprising due to the nonlinear nature of CARS.

CARS could be employed for species concentration measurements by making integrated intensity measurements. At low pressures, where line overlap is small, the integrated intensity for a majority species is predicted to vary linearly with pressure. This assumes, of course, that the pressure is not so low that Dicke narrowing or Doppler broadening effects are important. For higher pressures, the integrated CARS signal is predicted to vary much more rapidly with pressure. As the pressure increases from 50 to 300 atm, the predicted dependence goes from quadratic to nearly cubic, and then reverts at the higher range to approximately a quadratic dependence. These are the depen-

dences expected for a single transition with a width that either is independent of pressure (quadratic), or varies inversely with pressure (cubic). This is consistent with the picture of collisional narrowing causing a coalescence of lines into a single effective transition radiating at an average frequency. While this predicted quadratic-cubic pressure dependence has favorable implications for CARS species concentration measurements, interference from the background nonlinear susceptibility will make this variation considerably less dramatic for a minority species.

Although the particular model for the off-diagonal linewidth elements employed here is physically plausible and is commonly employed in studies of rotational relaxation, it is possible that other semi-empirical functional forms [24,25] for the rotational relaxation rates will also give good results. It would be most desirable not to have to rely on the use of adjustable parameters. Ultimately, it should be possible to calculate all the linewidth elements for N_2 in terms of intermolecular potential parameters in much the same way that the isolated linewidths and shifts are calculated [20,26]. Also, the role of line shifts will have to be accounted for, particularly if higher density regimes are investigated.

6. Summary and conclusions

Investigations of the 300 K N_2 CARS spectrum over the range from one to 100 atm have shown that collisional narrowing plays an important role in determining the shape of the profile over the entire pressure range. The pressure dependence of the N_2 CARS spectrum is somewhat different from that reported for the spontaneous Raman spectrum. An expression for the third-order, nonlinear electric susceptibility has been derived which is valid for overlapping spectral lines, and calculations based on this generalized susceptibility expression are in good agreement with the experimental results.

The authors wish to acknowledge helpful discussions about CARS theory with Dr. R.L. St. Peters, and the very capable assistance of Mr. Normand Gantick with the experiments.

References

- [1] J.W. Nibler, W.M. Shaub, J.R. McDonald and A.B. Harvey, *Vibrational spectra and structure*, Vol. 6, ed. J.R. Durig (Elsevier, Amsterdam, 1977).
- [2] S. Druet and J.P. Taran, *Chemical and biological applications of lasers*, ed. C.B. Moore (Academic Press, New York, 1979).
- [3] J.W. Nibler and G.V. Knighten, *Topics in current physics*, Vol. II, ed. A. Weber (Springer-Verlag, Heidelberg, 1979) Ch. 7.
- [4] A.C. Eckbreth, P.A. Bonczyk and J.F. Verdick, *Prog. Energy Combust. Sci.* 5 (1979) 253.
- [5] A.C. Eckbreth and R.J. Hall, *Combustion and Flame* 36 (1979) 87.
- [6] I.A. Stenhouse, D.R. Williams, J.B. Cole and M.D. Swords, *Appl. Optics* 18 (1979) 3819.
- [7] B. Attal, M. Pealat and J.P. Taran, *AIAA-80-0282*, 18th Aerospace Sciences Meeting, Pasadena, CA, January, 1980.
- [8] A.C. Eckbreth, to be published in *Combustion and Flame*, (1980); also Annual Meeting of the American Chemical Society, Washington, D.C. (1979).
- [9] G.L. Switzer, L.P. Goss, W.M. Roquemore, R.P. Bradley, P.W. Schreiber and W.B. Roh, *AIAA-80-0353*, AIAA 18th Aerospace Sciences Meeting, Pasadena, CA (1980).
- [10] A. Owyong and L.A. Rahn, *IEEE/OSA Conf. on Laser engineering and applications*, Digest of CLEA papers, *IEEE JOE*, QE-15 (1979) 25D-26D.
- [11] N. Bloembergen, E.M. Purcell and R.V. Pound, *Physical Review* 73 (1948) 679.
- [12] V. Alekseyev, A. Grasiuk, V. Ragulsky, I. Sobelman and F. Faizulov, *IEEE J. Quantum Electronics*, QE-4 (1968) 654; V. Alekseyev and I. Sobelman, *The broadening of overlapping spectral lines*, Lebedev Physical Institute (Moscow), preprint N58 (1968).
- [13] H. Mikhailov, *Proc. Lebedev Phys. Inst. (Moscow)* 28 (1964) 150.
- [14] A.D. May, J.C. Stryland and G. Varghese, *Canadian Journal of Physics* 48 (1970) 2331.
- [15] C.H. Wang and R.B. Wright, *J. Chem. Phys.* 59 (1973) 1706.
- [16] M.F. Crawford, H.L. Welsh and J.H. Harrold, *Can. J. Phys.* 30 (1952) 81.
- [17] P. Dion and A.D. May, *Can. J. Phys.* 51 (1973) 36.
- [18] T. Witkowitz and A.D. May, *Can. J. Phys.* 54 (1976) 575.
- [19] R.G. Gordon, *J. Chem. Phys.* 45 (1966) 1649.
- [20] J. Bonamy, L. Bonamy and D. Robert, *J. Chem. Phys.* 67 (1977) 441.
- [21] N. Bloembergen, *Nonlinear optics* (W.A. Benjamin, New York, 1965) p. 26.
- [22] J.C. Polanyi and K.B. Woodall, *J. Chem. Phys.* 56 (1972) 1563.
- [23] R.B. Bernstein, *J. Chem. Phys.* 62 (1975) 4570.
- [24] D.E. Pritchard, N. Smith, R.D. Driver and T.A. Brunner, *J. Chem. Phys.* 70 (1979) 2115.
- [25] R.K. Lengel and D.R. Crosley, *J. Chem. Phys.* 67 (1977) 2085.
- [26] D. Robert and J. Bonamy, *Journal de Physique* 10 (1979) 923.

[1] J.W. Nibler, W.M. Shaub, J.R. McDonald and A.B.

R82-954566-F

APPENDIX E

COMBUSTION DIAGNOSIS BY COHERENT ANTI-STOKES RAMAN SPECTROSCOPY (CARS)

Combustion diagnosis by coherent anti-Stokes Raman spectroscopy (CARS)

Robert J. Hall
Alan C. Eckbreth
United Technologies Research Center
East Hartford, Connecticut 06108

Abstract. Coherent anti-Stokes Raman spectroscopy (CARS) appears very promising for the remote, spatially and temporally precise probing of hostile combustion environments due to its large signal conversion efficiency and coherent signal nature. CARS is a wave mixing process in which incident laser beams at frequencies ω_1 and ω_2 , with a frequency difference tuned to a Raman resonance in the molecular species being probed, interact to generate a coherent signal at frequency $\omega_3 = 2\omega_1 - \omega_2$. By analyzing the spectral distribution of the CARS signal, temperature measurements can be performed. Species concentration measurements derive from the intensity of the CARS radiation or, in certain cases, from its spectral shape. CARS spectra have been recorded in a variety of flames from the major flame constituents and generally show very good agreement with computer synthesized spectra. Significantly, CARS has been successfully demonstrated with both liquid and gaseous fuels in the primary zone and exhaust of practical combustors. Both thermometry and species concentration measurements have been performed. High pressure effects on CARS spectra have also been examined.

Keywords: combustion and analysis; nonlinear optics; Raman spectroscopy.

Optical Engineering 20(4), 494-500 (July/August 1981).

CONTENTS

1. Introduction
2. CARS
3. Thermometry
 - 3.1. Nitrogen
 - 3.2. Hydrogen
 - 3.3. Water vapor
 - 3.4. Carbon dioxide
4. Concentration measurements
5. Summary
6. Acknowledgments
7. References

1. INTRODUCTION

Laser spectroscopy is playing an increasing role in the diagnostic probing of the hostile, but easily perturbed, environments characteristic of combustion processes. Physical probes can seriously perturb the flame properties they seek to measure, are often limited in their spatial resolution and temporal response, and may not survive at high temperatures and pressures. Spatially precise laser spectroscopy, on the other hand, has the potential for the remote, nonperturbing, *in situ* measurement of temperature and species concentrations in combustion processes. Laser techniques are also capable of high temporal resolution. Three approaches which are spatially and temporally precise have received much attention in the last several years: spontaneous Raman scattering, coherent anti-Stokes Raman spectroscopy (CARS), and laser-induced fluorescence.¹⁻³ Raman scattering and CARS are best suited to thermometry and major species concentration measurements, while laser-induced fluorescence is applicable to measurement of flame radicals at trace levels. Raman scattering and laser-induced fluorescence are incoherent scattering processes in which the generated signal is dispersed into 4π sr. CARS is a coherent wave-mixing process in which the signal emerges as a laser-like beam in a precise direction.

Spontaneous Raman scattering has been widely investigated and is well understood.^{4,5} It has been utilized in a number of practical situations, but its application is often restricted to certain fuels, stoichiometries, cycles, and locations. Due to its inherent weakness, it is generally limited to application in relatively "clean" flames. With increases in fuel droplet fragment and soot concentrations, laser-induced interferences such as fluorescence and incandescence can exceed and mask detection of the Raman signals.¹ With greater emphasis being directed toward less clean, alternate fuels, stronger diagnostic techniques are required which can operate over a broad range of fuel specifications, stoichiometries, and combustion approaches. Both CARS and laser-induced fluorescence appear to possess this capability,¹ but only CARS has been demonstrated to date in practical combustion environments.⁶⁻⁹ The two techniques have complementary capabilities and have been under development in our and other laboratories for several years. In this paper, attention will be restricted to CARS. The next section of the paper summarizes the theory and application of CARS for combustion diagnostics. Succeeding sections survey the use of CARS for temperature and species concentration measurements in a variety of flame and combustion systems.

2. CARS

The theory and application of CARS are well explained in several reviews which have appeared recently.^{1, 10-12} As illustrated in Fig. 1, incident laser beams at frequencies ω_1 and ω_2 (termed the pump and Stokes respectively) interact through the third order nonlinear susceptibility of the medium, $\chi_{ijkl}^{(3)}(-\omega_3, \omega_1, \omega_1, -\omega_2)$, to generate polarization and coherent radiation at frequency $\omega_3 = 2\omega_1 - \omega_2$. When the frequency difference ($\omega_1 - \omega_2$) is close to the frequency ω_R , of a Raman resonance of a certain species, the magnitude of the radiation at ω_3 is resonantly enhanced and results in a signature uniquely characteristic of that species. In isotropic media such as gases, the third order susceptibility is actually the lowest order nonlinearity exhibited, i.e., due to symmetry considerations, second order effects are nonexistent. The third order nonlinear susceptibility tensor is of fourth rank. The subscripts denote the polarization orientations of the four fields in the order listed parenthetically. In

Invited Paper (P-10) received March 2, 1981; accepted for publication March 12, 1981; received by Managing Editor March 19, 1981.
© 1981 Society of Photo-Optical Instrumentation Engineers.

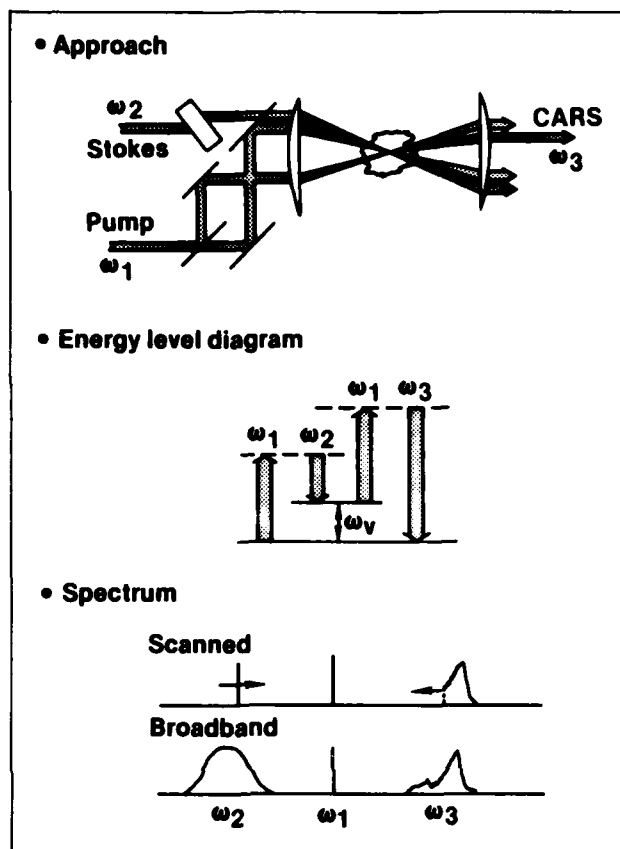


Fig. 1. Coherent anti-Stokes Raman spectroscopy (CARS).

isotropic media, the tensor must be invariant to all spatial symmetry transformations and the 81 tensor elements reduce to just three independent components. In CARS, which is frequency degenerate, there are only two independent elements.

In all of the experiments to be described in this paper, vibrational Raman resonances are probed, and, because the vibrational modes of the molecules are mainly symmetric (small depolarization), only Q-branch transitions with no change in rotational quantum number are important. The CARS spectrum is governed by the squared modulus of the third-order electric susceptibility, which in the isolated line approximation (small overlap between neighboring transitions) may be expressed as:

$$\chi^{(3)} = \frac{2N}{\hbar} \sum_j \frac{\alpha_j^2 \Delta \rho_j^{(0)}}{2(\omega_1 - \omega_2 - \omega_j) - i\Gamma_j} + \chi^{NR} \quad (1)$$

where the j summation is over all Q-branch transitions; N is the number density of Raman-active molecules; α_j , $\Delta \rho_j^{(0)}$, ω_j , and Γ_j are the polarizability matrix element, Boltzman population difference, frequency, and isolated linewidth, respectively, of transition Q(j); and the χ^{NR} term is an essentially dispersionless, background contribution arising from distortion of electron orbits, and, in some cases, from remote vibrational resonances. The tensor subscripts denoting polarization orientation of the electric field have been dropped.

The susceptibility thus consists of resonant components from Raman-active transitions in the species of interest and a nonresonant, mainly electronic, contribution from all of the molecular constituents present. The resonant contribution to the CARS signal is proportional to the square of the active molecule number density and contains information about the gas temperature through the Boltzmann population factors. For very low concentrations, the desired

resonant signal merges into a baseline level due to the nonresonant background susceptibility. When the modulation of this dispersionless background becomes undetectable, the trace species is nominally no longer measurable. At one time, this was perceived to be a major limitation to CARS diagnostics. However, the resonant and nonresonant terms have different tensor properties. By proper orientation of the laser field and CARS detection polarizations, the nonresonant electronic contributions can be cancelled, permitting measurements of lower concentrations if the signal level is adequate. In certain concentration ranges, the presence of the nonresonant susceptibility can actually be used to advantage. As long as the background modulation is detectable, concentration measurements can actually be made from the *shape* of the CARS spectrum, a unique feature of CARS spectroscopy. Both of these aspects will be subsequently demonstrated.

Measurements of medium properties are performed from the shape of the spectral signature and/or intensity of the CARS radiation. The CARS spectrum can be generated in either of two ways, as seen in Fig. 1. The conventional approach is to employ a narrowband Stokes source which is scanned to generate the CARS spectrum sequentially. For nonstationary and turbulent combustion diagnostics, this approach is not appropriate due to the nonlinear dependence of CARS on temperature and density. Generating the spectrum piecewise in the presence of large density and temperature fluctuations leads to signatures weighted toward the high density, low temperature excursions, and true medium averages cannot be obtained. The alternate approach¹³ is to employ a broadband Stokes source. This leads to weaker signals, but the entire CARS spectrum is generated with each pulse, permitting instantaneous measurements of medium properties. For efficient signal generation, the incident beams must be so aligned that the three-wave mixing process is properly phased. In gases, phase matching occurs when the input laser beams are essentially aligned parallel to or collinear with each other. In many diagnostic circumstances, however, this collinear phase matching leads to poor spatial resolution because the CARS radiation undergoes an integrative growth process. This difficulty can be circumvented by employing crossed beam phase matching, such as BOXCARS,¹⁴ or a variation thereof.¹⁵⁻¹⁷ In these approaches, Fig. 1, the pump beam and Stokes beam are crossed at a point to generate the CARS signal. CARS generation occurs only where the beams intersect and very high spatial precision is possible. The intersecting laser beams need not be coplanar¹⁸ and experimental simplifications can be gained using three-dimensional phase matching.

CARS spectra are more complicated than spontaneous Raman spectra, which are simply an incoherent addition of transitions. CARS spectra can exhibit constructive and destructive interference effects. For most molecules of combustion interest, these effects can be readily handled numerically since the theory of CARS generation is well understood. At United Technologies Research Center (UTRC), CARS computer codes have been developed and validated experimentally for the diatomic molecules N_2 , H_2 , CO , and O_2 ¹⁹ and the triatomics H_2O ²⁰ and CO_2 . Computer codes are extremely useful for studying the parametric behavior of CARS spectra and for data reduction.

Although CARS has no threshold per se and can be generated with cw laser sources, high intensity pulsed laser sources are required for most gas phase and flame diagnostics to generate acceptable signal-to-interference ratios, particularly with broadband generation and detection.¹ In the CARS work to be reported here, a frequency-doubled neodymium laser at 5320 Å provides the pump beam and also drives the broadband Stokes dye laser. Crossed-beam phase matching (BOXCARS), either planar or three dimensional, is used to ensure good spatial precision. The CARS signatures are detected with an optical multichannel analyzer (OMA) which permits capture of the entire CARS spectrum in a single pulse. In laminar flames and situations where fluctuation magnitudes are small, the CARS spectrum can be averaged on the OMA or scanned with a monochromator using a BOXCAR averager. Greater detail about the apparatus and experimental procedures may be found in Refs. 2, 9, and 18.

3. THERMOMETRY

Temperature measurements derive from the spectral shape of the CARS signature. Thermometry is therefore more easily performed than concentration measurements, which generally, but not always, require determination of absolute signal intensity levels. Temperature information can be extracted from any of a number of molecular constituents. In this section, CARS thermometry utilizing several molecules in a variety of measurement situations will be illustrated.

3.1. Nitrogen

Nitrogen is the dominant constituent in air-fueled combustion processes and is everywhere present in large concentrations. Performing temperature measurements from N_2 provides information on the location of the combustion heat release and, to some degree, the extent of chemical reaction. In Fig. 2 is displayed the calculated temperature dependence of the N_2 CARS spectrum for parameters corresponding to the experimental approach employed here. A de-

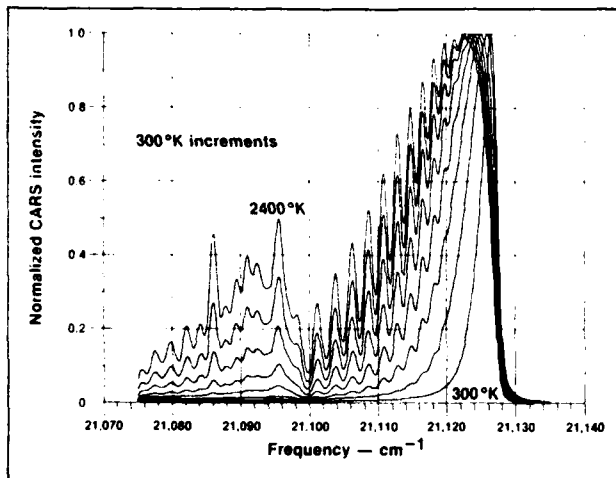


Fig. 2. Temperature variation of the CARS spectrum of N_2 for a pump linewidth of 0.8 cm^{-1} , a Stokes bandwidth of 150 cm^{-1} and a 1 cm^{-1} slit width.

scription of the computer code is summarized in Refs. 19 and 21. In the code, the dependence of the Raman linewidth on temperature and rotational quantum number is taken into account.²² At low temperatures, one sees the $v = 0 - 1$ band containing low J value Q branch transitions, i.e., $\Delta J = 0$ where J is the rotational quantum number. As is apparent, the low J Q branches are unresolved. As the temperature increases, the band broadens as the rotational population distribution shifts to higher J values. At very high temperatures, individual even J Q branches ranging from $Q(20)$ to $Q(40)$ can be resolved. The odd Q branches, which have a nuclear spin weighting equal to half of the even number branches, are reduced in intensity by about a factor of four and do not stand out. At intermediate temperatures, fewer Q branch transitions are resolvable. For Q branches beyond $Q(40)$, overlap with the $v = 1 - 2$ band transitions occurs, giving rise to two prominent peaks in the "hot" band. At lower spectral resolution, e.g., $\sim 3 \text{ cm}^{-1}$, the fine structure shown in Fig. 2 is lost, but the spectra still exhibit good temperature sensitivity.

The accuracy of CARS N_2 thermometry has been examined in premixed flat flames by comparison with radiation-corrected, coated, fine wire thermocouples.²¹ The radiation corrections were experimentally calibrated at different flame temperatures by sodium line reversal. In Fig. 3, the CARS spectrum scanned at a resolution of 1 cm^{-1} in a 2110 K flame is displayed. The dotted curve is a theoretical least square fit to the experimental signature. The best fit temperature is 2104 K, with a standard deviation of 9 K. Similar agreement was obtained at lower flame temperatures.

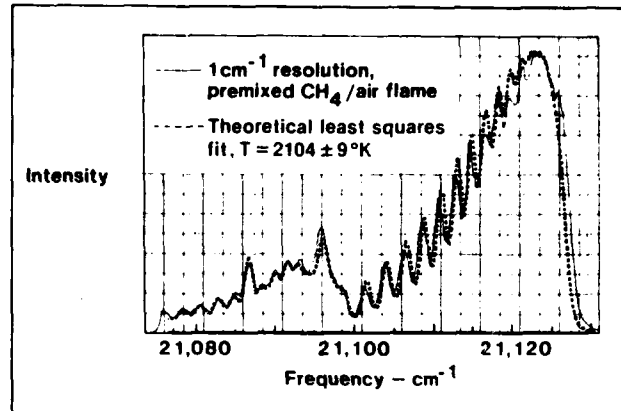


Fig. 3. Comparison of experimental (solid line) and theoretical least square fit (dashed) N_2 CARS spectra at a measured temperature of 2110K.

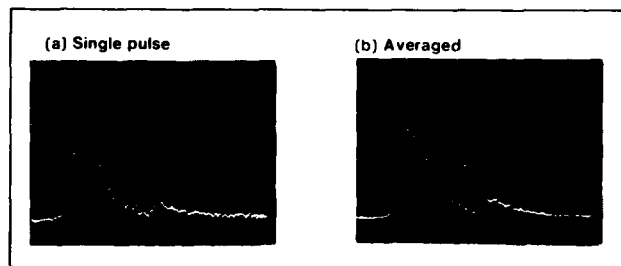


Fig. 4. Comparison of single-pulse and averaged CARS spectra from flame N_2 in a sooting propane diffusion flame.

The capability of CARS for use in highly sooting flames has been demonstrated.^{22,23} Although incoherent and coherent interferences from C_2 can be encountered in the N_2 CARS bands from a 5320 \AA pump laser, they are for the most part suppressible by appropriate Stokes laser bandwidth selection and use of a polarization filter. The C_2 is produced by the laser vaporization of soot which occurs even for $0 (10^{-8} \text{ sec})$ duration laser pulses. In Fig. 4 both a single pulse (10^{-8} sec) and an averaged N_2 CARS spectrum from a highly sooting, laminar propane diffusion flame are displayed for a spatial resolution of $0.3 \times 1 \text{ mm}$. The spectra are interference free and of high quality. The single pulse CARS spectrum is possible at laser energies an order of magnitude lower than those typically employed for single pulse spontaneous Raman scattering. Furthermore, in this sooting flame, laser modulated particulate incandescence¹ would exceed the Raman signal by several orders of magnitude, precluding successful measurements. In a turbulent flame, these single pulse temperature measurements would lead to determination of the temperature probability distribution function (PDF). Data such as those displayed in Fig. 4 have been employed to perform detailed axial and radial temperature surveys in laminar propane diffusion flames.²³ Figure 5 displays the radial variation of temperature in the sooting flame with height above the burner.

Recently, the feasibility of CARS for measurement in practical combustion systems has been demonstrated. In tests at our laboratory,⁹ BOXCARS thermometry was performed in two different, liquid-fueled combustors housed in a 50 cm dia combustion tunnel. Delicate instrumentation was housed in a control room adjacent to the burner test cell and the CARS signals were piped out employing 20 m long, 60μ dia fiber optic guides. In Fig. 6 are shown CARS signatures of N_2 averaged for 10 sec at two different axial locations in the primary zone of a Jet A fueled swirl burner. At the upstream, $x = 6 \text{ cm}$, location, CARS measurements were made through the fuel spray and the temperature was found to be about 900 K at an overall

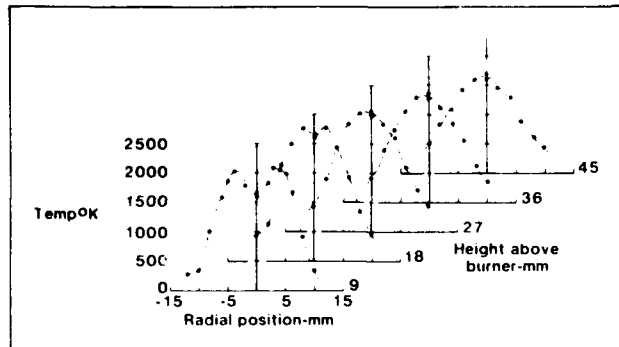


Fig. 5 Radial temperature profiles determined by CARS in a laminar propane diffusion flame.

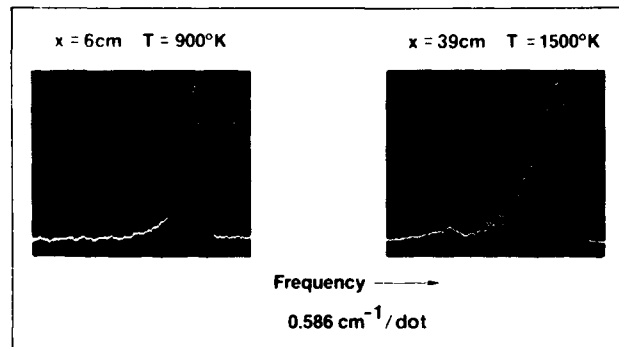


Fig. 6. Spatial variation of temperature from averaged CARS spectra of N_2 in swirl burner with Jet A fuel.

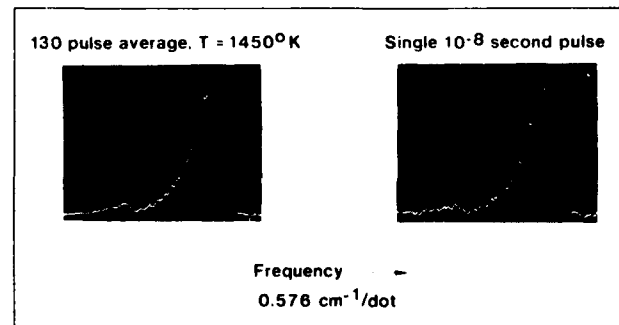


Fig. 7. Comparison of averaged and single pulse N_2 CARS spectra in swirl burner with refractory back wall fueled with Jet A at an overall equivalence ratio of 0.8.

equivalence ratio of 0.8. At the downstream location, where the flame was very luminous, the temperature increased to 1500 K. In Fig. 7 is shown a comparison of a single pulse (10^{-8} sec) and an averaged CARS spectrum (10 sec) in the Jet A fueled swirl burner fitted with a refractory back wall to simulate a furnace more closely. The single pulse, although of slightly lower quality, is fairly good and would permit credible measurements. Measurements were also successfully performed in the exhaust of a JT-12 combustor burning Jet A.⁹ Single pulse spectra were virtually indiscernible from the averaged data. CARS measurements downstream in the exhaust were in very good agreement, i.e., 10 to 50 K, with temperatures determined by aspirating thermocouple probes.

Most practical combustor devices, of course, operate at pressures considerably in excess of atmospheric. It is known from spontaneous Raman studies, however, that remarkable changes in spectra can

occur when the collision-induced Raman line broadening becomes comparable to the separation between the individual vibration-rotation transitions. At this point, the isolated Raman linewidths continue to broaden linearly with pressure, but collisional energy transfer between adjacent J-states causes adjacent transitions to coalesce or collapse toward a frequency center of gravity. The simple representation of $\chi^{(3)}$ (Eq. (1)) as a sum of independently broadened transitions is no longer valid in regions of strong line overlap. This is referred to as collisional narrowing and its effect must be included in the diagnostic interpretation of high pressure CARS spectra. In most diatomic molecules, collisional narrowing becomes important above a few atmospheres of pressure, with the effect becoming less pronounced as temperature is increased.

For N_2 , recently developed theories account for the phenomenon quite well at 300 K,²⁴ and the agreement with data at higher temperatures also appears to be good. As an illustration, Fig. 8 displays theory-experiment comparisons of N_2 CARS spectra at ~ 1600 K and pressures of 7.8 and 28.2 atmospheres. At 7.8 atmospheres fine

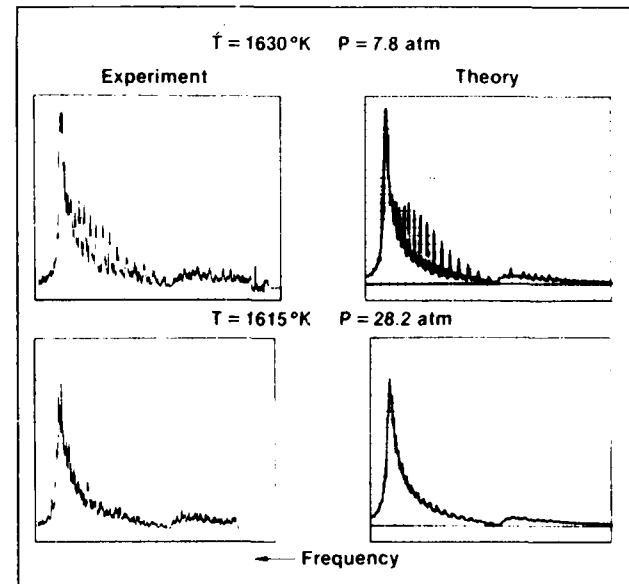


Fig. 8. Comparison of observed and predicted pressure dependence of N_2 CARS spectra at 1630 K.

structure is still apparent, and collisional narrowing plays a very small role. At 28.2 atmospheres, the isolated Q-branch linewidths have increased to the point where individual Q-branches can no longer be resolved, and collisional narrowing is playing a significant role. In the isolated line approximation, the width of the fundamental band and the hot band peak height are both about 30 percent larger at 28.2 atm than the values observed in the experimental signature. With narrowing included in the calculation, the theory is in very good agreement with experiments, as can be seen in Fig. 8.

3.2. Hydrogen

H_2 , when sufficiently abundant, is ideal for combustion thermometry because of the simplicity of its spectrum, as seen in Fig. 9.²⁵ The line spectra are components of the vibrational Q branch, $v = 0 - 1$, $\Delta J = 0$. The adjacent rotational components are well separated due to the large H_2 vibration-rotation interaction, making the spectrum particularly simple to interpret. The intensity alteration between even and odd J lines again is due to nuclear spin statistics in which the odd lines have three times the statistical weight of the even-numbered transitions. H_2 BOX-CARS signatures such as those shown in Fig. 9 have been used to measure temperatures at various locations in a flat H_2 -air diffusion flame.²⁵ Approximate temperatures were deduced

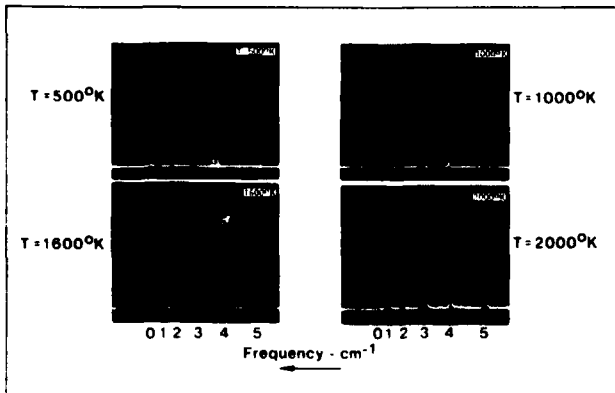


Fig. 9. CARS spectra of H₂ in H₂-air diffusion flame at temperatures determined from relative strengths of indicated Q-branch transitions. Frequency scale corresponds to 0.60 cm⁻¹ per dot.

from the ratios of the CARS intensities of the Q(1), Q(3), and Q(5) transitions. Agreement among the temperatures deduced from the three intensity ratios was good, i.e., the standard deviation varied from 2 to 8 percent over the range of 900 K to 2100 K. Better accuracy would probably result from using ratios of integrated line strengths instead of the peak intensities. The results of temperature profiling the flat diffusion flame are shown in Fig. 10, where temperatures deduced from H₂ and O₂ CARS spectra are compared to measure-

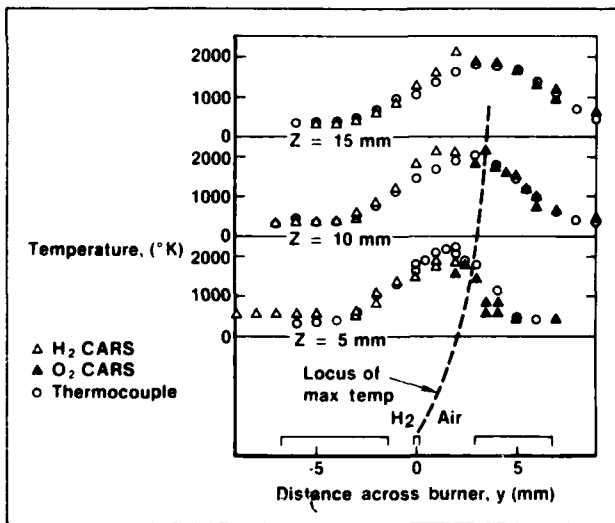


Fig. 10. Temperature measurements in a flat H₂-air diffusion flame. Symbols: circles, radiation-corrected thermocouple; open triangles, H₂ CARS; and solid triangles, O₂ CARS. Dotted curve is locus of maximum temperature.

ments with a radiation corrected thermocouple. The CARS spectrum of O₂, omitting spectroscopic details, is qualitatively quite similar to that of N₂. The temperatures agree quite well in cooler regions of the flame. Larger discrepancies occur at the higher temperatures where the concentrations are low and signal-to-noise ratio is poorer. By spectrally integrating the H₂ spectra and comparing the integrated intensity to that generated simultaneously from a high pressure gas cell in a parallel reference leg, density measurements have been made in the flat diffusion flame. These were in fair comparison, i.e., ~50 percent, with H₂ concentrations measured by spontaneous Raman scattering.

3.3. Water vapor

Water vapor is the major product of air-fueled hydrogen combustion and often the dominant product species of hydrocarbon-fueled combustion. Its measurement is an important gauge of the extent of chemical reaction and of overall combustion efficiency. Figure 11 displays an H₂O CARS spectrum at 1 cm⁻¹ resolution in the post-flame region of an atmospheric pressure, premixed CH₄-air flame at 1700 K.²⁰ Also shown in Fig. 11 is the CARS computer code predic-

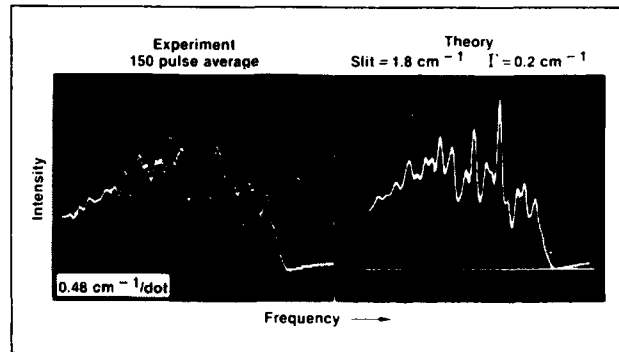


Fig. 11. Comparison of experimental and theoretical CARS spectra of water vapor in a flame at 1700 K. A pressure-broadened linewidth $\Gamma = 0.2$ cm⁻¹ was assumed for all transitions in the calculation.

tion for the experimental conditions. While only the ν_1 symmetrical mode of H₂O is Raman active, the involved rotational energy level structure of this asymmetric rotor gives rise to a complex CARS signature. In the calculations, nearly one thousand vibrational-rotational Q branch transitions are included at flame temperatures. The peaks seen in the spectrum arise from spectral overlapping of the various transitions.

Good agreement between experiment and theory has also been achieved in test cells of pure H₂O for temperatures in the range 300 K to 800 K.²⁰ The predicted and observed spectra exhibit a pronounced sensitivity to temperature, making the H₂O molecule potentially attractive for CARS thermometry. However, theory-experiment agreement is obtained only for relatively large Raman linewidths,²⁰ and H₂O CARS will be a reliable diagnostic tool when more information about the temperature-, concentration-, and Q-branch dependences of these linewidths is obtained. Work is currently underway at our laboratory to resolve these questions.

3.4. Carbon dioxide

The other major product of hydrocarbon combustion besides water vapor is, of course, carbon dioxide. In Fig. 12 is shown the CARS spectrum of CO₂ in the postflame zone of a CO-air flame at 1520 K. The experimental signature displays a fundamental band at a Raman shift of about 1388 cm⁻¹, corresponding nominally to the transition between the ground vibrational state and the first symmetric stretch state. A number of "hot bands," corresponding to vibrationally excited initial states, also appear at larger shifts. Studies of CO₂ CARS spectra in different flames at varying temperatures show that the strength of the hot bands is strongly dependent on temperature, making these features useful for thermometry. Unlike the other spectra presented earlier, there is little rotational smearing of the vibrational bands, a consequence of the extremely small vibration-rotation interaction in CO₂. Each vibrational band represents the contributions of approximately 100 Q-branch transitions. Not shown in Fig. 12 is a slightly weaker sequence of vibrational bands whose fundamental occurs at a Raman shift of 1285 cm⁻¹, and whose hot bands occur at smaller shifts. The fact that two distinct vibrational sequences occur is a consequence of "Fermi resonance": because the symmetric stretch frequency nearly coincides with twice that of the bending mode, anharmonic terms in the intramolecular potential can cause a large perturbation of the corresponding eigen-

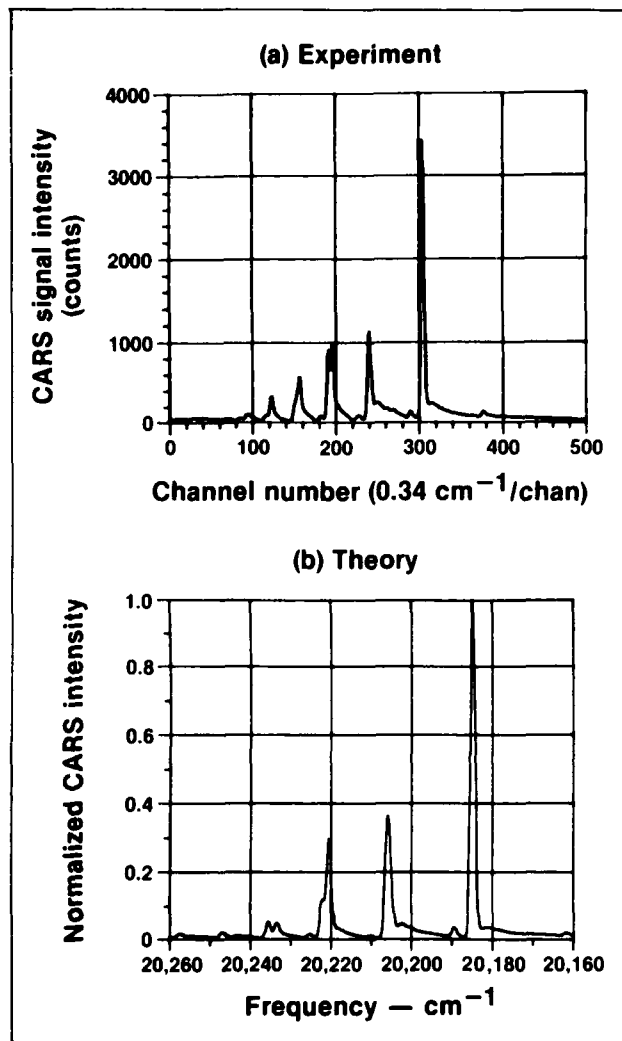


Fig. 12. Comparison of experimental and theoretical CARS signatures of CO_2 in a flame at 1520 K.

states, and a mixing of the symmetric stretch and bending modes occurs.

Also shown in Fig. 12 is a theoretical calculation for $T = 1520$ K. As can be seen, the agreement with experiment is fairly good, with a few minor discrepancies. Similar agreement is obtained in other flames at different temperatures. The calculation of vibrational energy levels, rotational constants, and spontaneous Raman cross sections basically follows the treatment of Courtoy.²⁶ It has been found, however, that better agreement is obtained if tabulated values²⁷ for the rotational constants are employed. Further investigations relating to spectral constants, linewidths, and possibly collisional narrowing will likely result in even better agreement between experiment and theory.

4. CONCENTRATION MEASUREMENTS

In general, concentration information derives from the intensity of the spectrally integrated CARS signal,²⁸ assuming that the nonresonant susceptibility contribution is negligible or has been suppressed in a manner to be detailed shortly. As alluded to earlier, species detection sensitivity is limited for conventional CARS approaches with aligned polarizations due to the presence of the background nonresonant

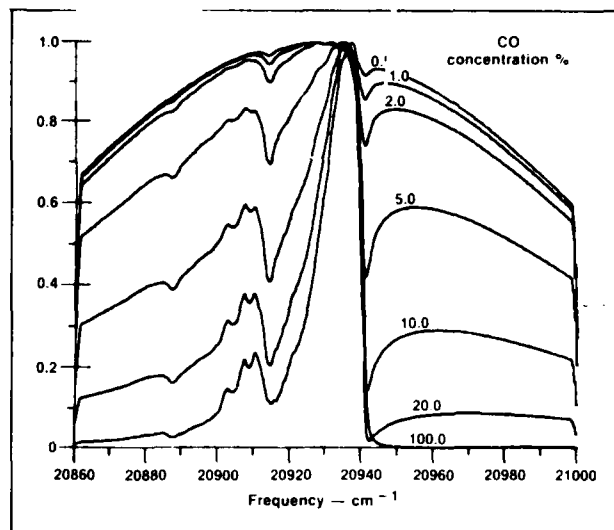


Fig. 13. Computer CARS spectra of CO at various concentrations at 1800 K.

susceptibility. This situation is quite evident in the computer calculations for CO at 1800 K shown in Fig. 13. A similar situation exists with O_2 .²⁵ As seen, the CARS resonant spectrum at 20 percent concentration rises well out of the nonresonant background, which is only slightly evident, and the hot band, $v = 1 - 2$, is quite prominent. As the concentration decreases, the modulation and the nonresonant background become more significant; at still lower concentrations, the degree of modulation decreases until the signal, i.e., the modulation, is lost in the nonresonant background and the species is no longer detectable. To the extent that the nonresonant susceptibility is known or can be approximated, the concentration of a particular species can be obtained from the shape of the CARS spectrum, obviating the requirement for absolute intensity measurements. The concentration range appropriate to spectral curve fitting for concentration measurements will vary from molecule to molecule and with gas composition and temperature. For molecules with closely spaced vibrational-rotational transitions such as CO, O_2 , and N_2 at flame temperatures, the range is approximately 0.1 to 20 percent. This approach has been quantitatively verified in the case of CO, as seen in Fig. 14. There, an experimental CARS signature of CO in the postflame region of a premixed CO-O_2 flat flame is displayed. The thin solid line is the theoretical CARS overlay at a CO concentration of 3.6 percent corresponding to the level experimentally measured with a quartz microprobe sampling system and a nondispersive infrared analyzer. As can be seen, the agreement between the CARS and probe measurements is quite good. This approach was also verified by CARS measurements

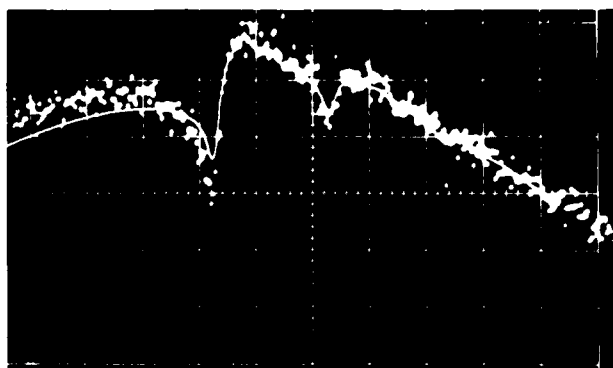


Fig. 14. Comparison of experimental and computed (solid line) CARS spectra in a flame at a concentration of 3.6%. $T = 2100$ K.

in cold, calibrated gas mixtures. The spectral fitting approach has been employed to perform O_2 measurements as well²⁵ and to map O_2 decay through the flat H_2 -air diffusion flame previously mentioned.

For concentration measurements at lower levels than permitted by spectral fitting, the background nonresonant susceptibility can be suppressed by appropriately orienting the laser field and CARS-detection polarizations.^{29,30} Number densities are then obtained from the strength of the spectrally integrated signal after appropriate calibration, e.g., using an external reference cell. In Fig. 15, background susceptibility suppression is demonstrated for CO in a flat CO-air diffusion flame. Folded, nonplanar BOXCARS,¹⁸ was employed together with broadband Stokes generation and optical multichannel spectral detection. With aligned polarizations, the characteristic modulated CARS spectrum (Fig. 13) is obtained. By orienting the ω_1 pump field polarizations and CARS analyzer relative to the horizontally polarized ω_2 Stokes field, as shown, the nonresonant susceptibility was reduced by over two orders of magnitude and the background free CARS spectrum of CO was obtained.

Unfortunately, the polarization approach leads to a considerable loss in signal intensity. The resonant mode signal reduction is at least a factor of sixteen. In addition, there is the signal loss associated with the suppression of the nonresonant susceptibility itself. In a recent experimental study,³¹ the CO detectivity of broadband CARS with and without background suppression was compared. With crossed-beam phase matching, better concentration sensitivity, by about a factor of five, was found by not suppressing the background. With the background suppressed, the CARS signal level, i.e., number of photons, limited the detection sensitivity. With the background present, detectivity was limited by the loss of modulation in the nonresonant susceptibility profile. In those circumstances where detectivity is not photon but background limited, e.g., low spatial resolution, high pressure, concentration sensitivity will be enhanced by employing nonresonant susceptibility suppression.

With the background suppressed, density measurements are based on the strength of the spectrally integrated CARS signature. This usually requires the use of a reference cell to normalize pulse-to-pulse laser power fluctuations, to serve as a calibrating standard, and to account for small optical misalignments. Reference cells may not be practical when probing turbulent, soot- and droplet-laden gases because they cannot account for effects such as beam steering, defocusing, and attenuation. It seems desirable, then, to perform concentration measurements from spectral shapes whenever possible. In essence one utilizes the nonresonant susceptibility at the measurement location as an *in situ* reference. For unmodulated spectra, i.e., when the nonresonant susceptibility is suppressed or unimportant, there are other approaches to *in situ* referencing. These approaches are receiving considerable attention for turbulent combustion diagnostics because of their potential for circumventing the foregoing problems and are reviewed in Refs. 31 and 32.

Hydrocarbon fuels are Raman active, often with large Raman sections, and CARS could in principle be used to monitor fuel mixing and pyrolysis processes. Other than observing CARS spectra of hydrocarbons in flames or cells, little work of a quantitative nature has been reported, although this should be a fruitful area for future investigations.

5. SUMMARY

CARS is a laser spectroscopic technique appropriate to spatially and temporally resolved measurement of temperature and major species concentrations in combustion. It has been generated from all of the dominant constituents in air-fed, hydrogen-, and hydrocarbon-fueled combustion. Quite importantly, CARS has been demonstrated to be applicable to practical combustion systems.

6. ACKNOWLEDGMENTS

The authors would like to acknowledge many valuable technical discussions with Dr. Casper J. Ultee, the contributions of Dr. John A. Shirley and Dr. James F. Verdieck to the experiments, and the very capable technical assistance of Messrs. Edward Dzwonkowski

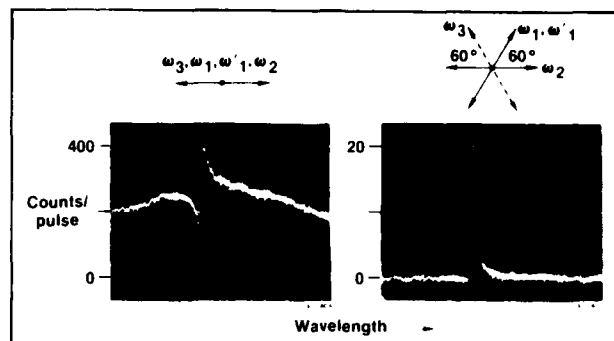


Fig. 15. Background nonresonant susceptibility suppression by polarization rotation. Folded BOXCARS in a flat CO-air diffusion flame.

and Normand Gantick. Separate portions of the research described herein were supported in part by the EPA, Project SQUID, NASA Langley, and the Army Research Office.

7. REFERENCES

1. A. C. Eckbreth, P. A. Bonczyk, and J. F. Verdieck, *Prog. Energy Combust. Sci.*, **5**, 253-322 (1979).
2. D. R. Crosley (Ed.), *Laser Probes for Combustion Chemistry*, ACS Symposium Series 134, (1980).
3. A. C. Eckbreth, Recent Advances in Laser Diagnostics for Temperature and Species Concentration in Combustion, Proc. of the 18th Symposium (International) on Combustion, The Combustion Institute (1981).
4. M. Lapp and C. Penney, *Laser Raman Gas Diagnostics*, Plenum Press, New York (1974).
5. S. Lederman, *Prog. Energy Combust. Sci.*, **3**, 1-34 (1977).
6. B. Attal, M. Pealat, and J. P. E. Taran, CARS Diagnostics of Combustion, AIAA Paper No. 80-0282 (1980).
7. I. A. Stenhouse, D. R. Williams, J. B. Cole and M. D. Swords, *Appl. Opt.* **18**, 3819-3825 (1979).
8. G. L. Switzer, L. P. Goss, W. M. Roquemore, R. P. Bradley and P. W. Schreiber, The Application of CARS to Simulated Practical Combustion Systems, AIAA Paper No. 80-0353 (1980).
9. A. C. Eckbreth, *Combust. Flame* **39**, 133-147 (1980).
10. J. W. Nibler, W. M. Shaub, J. R. McDonald and A. B. Harvey, Coherent Anti-Stokes Raman Spectroscopy, in J. R. Durig, Ed., *Vibrational Spectra and Structure*, Vol. 6, Elsevier, Amsterdam (1977).
11. S. Druet and J. P. Taran, Coherent Anti-Stokes Raman Spectroscopy, in C. B. Moore, Ed., *Chemical and Biological Applications of Lasers*, Academic Press, New York (1979).
12. J. W. Nibler and G. V. Knighten, Coherent Anti-Stokes Raman Spectroscopy, in A. Webber, Ed., *Raman Spectroscopy of Gases and Liquids*, Springer-Verlag, Berlin (1979).
13. W. B. Roh, P. W. Schreiber and J. P. E. Taran, *Appl. Phys. Lett.* **29**, 174-176 (1976).
14. A. C. Eckbreth, *Appl. Phys. Lett.* **32**, 421-423 (1978).
15. G. Laufer and R. B. Miles, *Opt. Comm.* **28**, 250-254 (1979).
16. A. Compaan and S. Chandra, *Opt. Lett.* **4**, 170-172 (1979).
17. K. A. Marko and L. Rimai, *Opt. Lett.* **4**, 211-213 (1979).
18. J. A. Shirley, R. J. Hall and A. C. Eckbreth, *Opt. Lett.* **5**, 380-382 (1980).
19. R. J. Hall, *Combust. Flame* **35**, 47-60 (1979).
20. J. A. Shirley, R. J. Hall and A. C. Eckbreth, Investigation of the CARS Spectrum of Water Vapor, Proc. of the Lasers '80 International Conference, New Orleans, La., December 16, 1980.
21. R. J. Hall, *Appl. Spect.* **34**, 700-701 (1980).
22. I. R. Beattie, J. D. Black and T. R. Gilson, *Combust. Flame* **33**, 101-102 (1978).
23. A. C. Eckbreth and R. J. Hall, *Combust. Flame* **36**, 87-98 (1979).
24. R. J. Hall, J. F. Verdieck and A. C. Eckbreth, *Opt. Comm.* **35**, 69-75 (1980).
25. J. A. Shirley, A. C. Eckbreth and R. J. Hall, Investigation of the Feasibility of CARS Measurements in Scramjet Combustion, Proc. of the 16th JANNAF Combustion Meeting, CPIA Publication 308, 487-509 (1979).
26. C. P. Courtney, *Can. J. Phys.* **35**, 608-648 (1957).
27. L. S. Rothman and W. S. Benedict, *Appl. Opt.* **17**, 2605-2611 (1978).
28. W. B. Roh and P. W. Schreiber, *Appl. Opt.* **17**, 1418-1424 (1978).
29. A. F. Bunkin, S. G. Ivanov and N. I. Koroteev, *Sov. Tech. Phys. Lett.* **3**, 182-184 (1977).
30. L. A. Rahn, L. J. Zych and P. L. Mattern, *Opt. Comm.* **39**, 249-253 (1979).
31. A. C. Eckbreth and R. J. Hall, CARS Concentration Sensitivity With and Without Nonresonant Background Suppression, *Combust. Sci. Tech.*, in press.
32. J. A. Shirley, R. J. Hall, J. F. Verdieck and A. C. Eckbreth, New Directions in CARS Diagnostics for Combustion, AIAA-800 1542 (1980).

R82-954566-F

APPENDIX F

CARS THERMOMETRY IN REACTING SYSTEMS

Reprinted from

TEMPERATURE

ITS MEASUREMENT AND CONTROL
IN SCIENCE AND INDUSTRY

VOLUME FIVE

James F. Schooley
Editor-in-Chief

1982

Published by

American Institute of Physics
335 East 45th Street
New York NY 10017

CARS thermometry in reacting systems*

J. F. Verdick, J. A. Shirley, R. J. Hall, and A. C. Eckbreth

United Technologies Research Center, East Hartford, Connecticut 06108

CARS (Coherent anti-Stokes Raman Spectroscopy) diagnostic techniques provide accurate temperature measurements in environments ranging from controlled laboratory flames to hostile systems such as gas turbine combustors and internal combustion engines. CARS is an optical wave mixing process wherein incident laser beams at frequencies ω_1 and ω_2 , with a frequency difference appropriate to the molecular species being probed, interact to generate the CARS signal at $\omega_s = 2\omega_1 - \omega_2$. Through analysis of the frequency distribution of the CARS spectrum, temperature measurements can be obtained. Concentration measurements derive from the intensity of the CARS radiation or, in certain cases, from its spectral shape. CARS is a remote, nonperturbing technique which determines temperature in a matter of seconds with good spatial resolution (of the order of millimeters). Under some circumstances, CARS signal levels are intense enough to permit "instantaneous," single pulse temperature measurements, i.e., $\sim 10^{-8}$ seconds. Because CARS is a coherent, nonlinear optical technique, it offers decided advantages over conventional incoherent spectroscopic methods. These advantages derive both from the strong CARS signal and its laser-like beam character which furnish excellent discrimination against interferences such as combustor luminosity and laser-induced interferences, which are often quite severe. In this paper, the fundamentals of CARS thermometry from both theoretical and experimental points of view, with emphasis on the nitrogen molecule, will be discussed in detail. Areas covered will include the accuracy of CARS thermometry, computer-generated CARS spectra, linewidth considerations and high pressure effects. Additionally, the use of other molecular thermometric probes for CARS diagnostics, H_2 , O_2 , H_2O , CO , and CO_2 , will be shown. Two important experimental techniques, BOXCARS, a particular laser beam configuration which achieves good spatial resolution, and single-shot thermometry, wherein the CARS spectrum from a single pulse is recorded, will be treated. The utilization of CARS thermometry will be illustrated by its application in several different flame systems and in practical combustor devices.

INTRODUCTION

Temperature measurements utilizing spectroscopic techniques such as absorption and emission spectroscopy are well established methods which have served well over many decades. More recently, Raman scattering and fluorescence, using laser sources, have been applied with considerable success. These spectroscopic techniques offer several advantages over probe thermometry such as remote operation, non-perturbation of the sample, and extremely high temperature capability. The major disadvantage of spectroscopic thermometry is that the system under investigation must be "seen", i.e., be visible through some type of optical ports.

This paper describes a more recent thermometric method based upon a coherent, nonlinear optical technique named CARS (for coherent anti-Stokes Raman spectroscopy). In addition to the advantages listed above, the CARS method offers several others; good accuracy (better than 1% demonstrated with nitrogen CARS thermometry), rapid measurement and processing (typically less than ten seconds), and most importantly, the capability for a high degree of spatial resolution (better than one millimeter). Additionally, the exciting potential for performing virtually instantaneous (in 10^{-8} seconds) temperature measurements is available with single pulse CARS. In this paper the term reacting system shall be loosely interpreted to mean combustion systems. The extension of CARS measurement to other types of chemically reacting systems is easily made. It should be emphasized, that in combustion, the single most important parameter to measure is the temperature. Given the initial conditions, and the temperature at a point in a combusting system, the products, heat release, and other parameters can be estimated quite well. For this reason, highly accurate, spatially precise measurements of temperature are a necessity in understanding and controlling combustion processes.

CARS thermometry has been applied to many diverse systems ranging from carefully controlled laboratory flames to such difficult cases as burning propellant strands. Internal combustion engines, gas turbine combustor cans, furnaces, shock tubes, and plasmas are among the several devices which have been probed by the CARS method. Some of these applications will be covered in detail, following a discussion of the theoretical and experimental aspects of CARS measurements. A comparison of the CARS spectra of several molecular species, of particular interest in combustion, which have been used for thermometry is also presented. The effect of high pressure on the CARS nitrogen spectrum is discussed to emphasize the dramatic spectral changes which occur with pressure increase.

CARS FUNDAMENTALS: THEORETICAL CONSIDERATIONS

Temperature measurements derived from spectroscopic techniques ultimately depend upon the Boltzmann equation, which, of course, determines the energy level population distribution with temperature. This fundamental dependence is also true of CARS temperature measurements; however, because of the nonlinear nature of the CARS effect, the derivation of temperature is somewhat more complicated. This complication makes the fitting of computer-modelled CARS spectra with experimental CARS spectra mandatory. For this reason an analytical modelling capability is of equal importance to the experimental program in any CARS installation.

CARS is a coherent, nonlinear process which involves the mixing of four optical fields in a material medium (liquid, gas, or solid). In the usual CARS experiment, two of the fields are derived from the same laser beam, called the pump beam, of frequency ω_1 . The other beam, the Stokes beam, has frequency ω_2 , which is less than ω_1 . The top portion of Fig. 1 sketches one experimental means of mixing

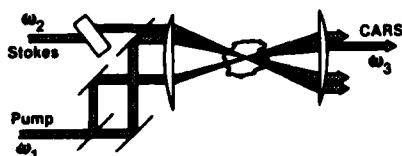
ω_1 and ω_2 to generate ω_3 , the CARS frequency. The middle section of Fig. 1 demonstrates the photon energy conservation requirement for CARS; namely, that

$$\omega_3 = 2\omega_1 - \omega_2 \quad (1)$$

Note also that $\omega_1 - \omega_2 = \omega_v$. When ω_v corresponds to a Raman-active vibrational-rotational transition in the molecule of interest, the CARS effect is strong, because of a quantum-mechanical resonance which will not be discussed here. Because of this resonance, the CARS effect is usually much stronger than the conventional spontaneous Raman effect. Equally important is the fact that the CARS radiation is generated in a laser-like beam nearly identical to the input beams. This means that, unlike Raman scattering, the entire CARS beam can be collected. Furthermore, this provides good discrimination against background, if aperturing is employed. Obviously, this provides a tremendous advantage when making measurements in highly luminous combustion devices. This point will be illustrated in more detail in the section on CARS applications.

The bottom portion of Fig. 1 depicts two different ways to generate an entire CARS spectrum. In the first of these, the pump frequency ω_1 is combined with a narrowband Stokes frequency, ω_2 , which is tuned, generating the CARS spectrum stepwise. The second method shown employs a broadband Stokes laser, ω_2 , which in combination with ω_1 , generates the entire CARS spectrum, ω_3 , from each laser pulse. This latter method offers the potential for making temperature measurements from a single, 10^{-8} second, laser pulse, as will be shown later.

• Approach



• Energy level diagram



• Spectrum

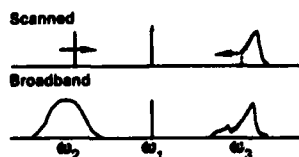


Fig. 1. Coherent anti-Stokes Raman spectroscopy (CARS).

The theoretical basis for CARS will be briefly sketched; for a more detailed, yet readable, account, the reader may refer to Ref. 1, and to the references contained therein. The physical origin of the CARS effect arises from the nonlinear response of molecules (both the electronic and nuclear portions) to the incident electric fields. This response is a macroscopic polarization (a charge distortion) that is proportional to the product of the three electric field amplitudes. This time dependent polarization then acts as an oscillating dipole source to generate the CARS radiation. The material parameter which relates the macroscopic polarization to the product of the electric fields is named the third order nonlinear susceptibility, $\chi^{(3)}$. It is a complex quantity and depends upon all molecules present in the sample. The electronic portion of $\chi^{(3)}$ is nearly frequency independent (unless an electronic transition is present) and is termed the nonresonant susceptibility, χ^{nr} . In contrast, the nuclear response of $\chi^{(3)}$ is strongly frequency dependent and complex, and is called the resonant susceptibility. The total susceptibility is written as

$$\chi^{(3)} = \sum_j (\chi' + i\chi'')_j + \chi^{nr} \quad (2)$$

where the bracketed term, the resonant portion, is summed over all transitions, j . In terms of $\chi^{(3)}$ and the incident laser intensities, the CARS intensity is given by (for the case of plane wave excitation, which is sufficient for our use here)

$$I_3 = K \left(\frac{\omega_3}{n_3} \right)^2 I_1^2 I_2 \left| \chi^{(3)} \right|^2 L^2 \quad (3)$$

where n_3 is the refractive index at frequency ω_3 ; I_1 and I_2 are the laser intensities at frequencies ω_1 and ω_2 respectively. L is an interaction length over which the input laser beams are strongly focused, and phase matching is achieved. Phase matching is achieved when the vector equation

$$\vec{k}_3 = 2\vec{k}_1 - \vec{k}_2 \quad (4)$$

is satisfied. The wave vector k is defined by $|k_1| = n_1\omega_1/c$, n_1 is the refractive index at frequency ω_1 . Equation (3) assumes the form shown when phase matching is satisfied. Phase matching is mainly a problem of directing the laser beams appropriately and will be discussed in detail in the experimental section.

The third-order susceptibility can be derived quantum-mechanically and expressed in spectroscopic terms as

$$\chi^{(3)} = \frac{2N}{h} \sum_j \frac{(\alpha_j)^2 \Delta_j}{2(\omega_1 - \omega_2 - \omega_j) - i\Gamma_j} + \chi^{nr} \quad (5)$$

where χ^{nr} has been separated from the resonant susceptibility, the summed term. The sum is often restricted to so-called Q-branch transitions, with $\Delta J = 0$ (no change in rotational quantum number) because the Q-branch transitions often dominate the CARS spectrum. In equation (5), N is the number density of the molecular species of interest; α_j , ω_j , and Γ_j are the polarizability matrix element

(related to the Raman cross section), the transition frequency, and the isolated Raman linewidth respectively, of transition $Q(j)$. The term Δ_j is the Boltzmann population difference and is responsible for the temperature dependence of $\chi^{(3)}$. Extracting the temperature from a CARS signal, which depends upon the squared modulus of $\chi^{(3)}$, is not a simple task and the assistance of computer model spectra is a necessity, as previously stated. Several examples of computer-model, predicted CARS spectra which demonstrate considerable sensitivity to temperature will be shown in a later section. In simple terms, the temperature is derived from the spectral distribution, i.e., the "shape" of the CARS signal. What factors determine the shape requires closer examination. Based upon consideration of equation (2), there are two limiting cases which determine the shape of a CARS spectrum as shown in Fig. 2. For the "strong signal" case, it is assumed that the resonant susceptibility is large compared to χ^{nr} . This leads to the resonance type of line shape indicated. An example of the strong case would be that of a majority species such as nitrogen in an air-fed combustion system. CARS spectra of the strong line case provide a basis for accurate temperature measurement. The other extreme, the "weak line" case, occurs when χ^{nr} is large compared to the resonant susceptibility. The desired resonant CARS signal then appears as a modulation or dispersion-type spectrum on the χ^{nr} background. This type of signal can be extremely useful for determining the concentration of a species by fitting the shape of the spectrum, without making an absolute signal intensity measurement. This topic will be treated briefly in a later section of this paper. A more complete, detailed description of the modelling of CARS spectra can be found in Refs. 2, 3. Those papers present the calculation of $\chi^{(3)}$ from spectroscopic constants and the Boltzmann distribution of energy levels. Instrumental factors such as laser linewidths and spectrometer resolution are taken into consideration.

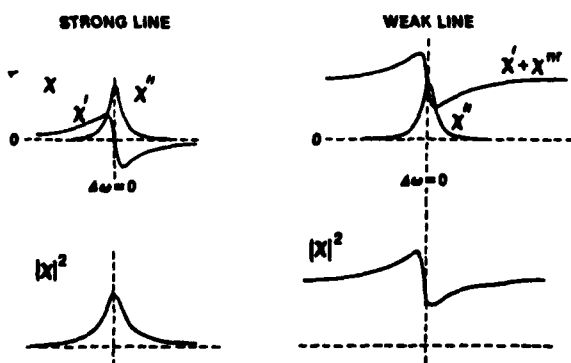


Fig. 2. Illustration of strong and weak line CARS intensity profiles.

CARS FUNDAMENTALS; EXPERIMENTAL CONSIDERATIONS

CARS is a coherent, nonlinear optical process, as stated previously. Laser sources are required in order to achieve signal coherence (obtain phase matching), and nonlinearity of response (requires

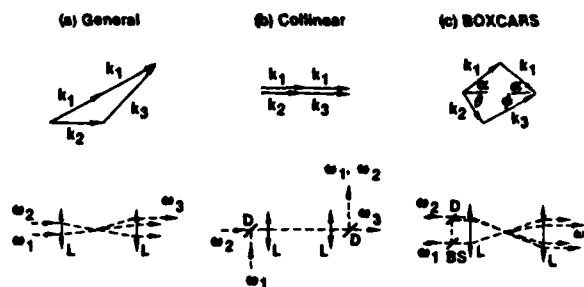


Fig. 3. Illustration of CARS phase-matching approaches. Subscripts denote beams: 1, pump; 2, Stokes; 3, anti-Stokes.

high intensities). Although CARS has been observed with continuous lasers (Ref. 4), high peak power, pulsed lasers are almost universally employed for the generation of CARS, particularly for gas phase diagnostics. This is the type of system which will be described in this section after a short description of phase matching.

In order to obtain the maximum CARS signal, the incident laser beams must be so aligned that the wave mixing process is properly phased. The CARS signal generated at a certain point will be in phase with CARS generated at other points in space leading to a constructive buildup of signal (rather than destructive interference, if out of phase). In Fig. 3a is shown the pictorial representation of equation (4), the general condition for phase matching. Underneath the vector diagrams are shown the experimental arrangement of the beams. In a gas, the refractive index changes little with wavelength, and the collinear arrangement of Fig. 3b satisfies the phase-matching condition. Although very easy to implement, the collinear configuration has very poor spatial resolution, as demonstrated by Eckbreth (Ref. 5). The length of sample interrogated by the CARS effect depends upon the focal length of field lens and can be quite large. For example, a 10 cm lens yields a sample length of only ~ 0.07 cm, but a 100 cm lens (which may be required in some instances) generates a sample length of ~ 7 cm. Clearly, using a long focal length lens, a collinear CARS measurement over a small scale burner would sample both hot and cold regions and, hence, would be considerably misleading. Recognizing this, Eckbreth (Ref. 5) devised a crossed-beam phase-matching scheme illustrated in Fig. 3c, called BOXCARS because of the shape of the diagram. In this case, CARS is generated only at the point where the three beams cross, which can have a dimension along the lens axis of ~ 1 mm, and less in the transverse direction. A further advantage of BOXCARS is that the CARS beam is almost completely spatially (hence spectrally) separated from the input laser beams, and is easier to isolate than the collinear case. Complete separation of the CARS beam is achieved if the BOXCARS diagram is folded (hence, folded BOXCARS) about the axis as shown in Fig. 4b. The arrangement of the incident and exiting beams, also shown, clearly demonstrates how the ω_3 beam is completely separated from the ω_1 and ω_2 beams. This spatial, and consequent spectral, separation is particularly advantageous for rotational CARS experiments (Ref. 6), where the spectral separation

filter. This signal is averaged on a BOXCAR averager and used to monitor and "tweak" the alignment of the CARS system. It is relatively immune to angular and translational motions of the CARS beam which occur during peaking up the alignment. The alignment of a CARS system should never be monitored through a narrow angular and spatial acceptance, such as a slit, where signal loss due to slight steering can be misinterpreted for alignment detuning. The spatial resolution of a given configuration is readily checked by generating CARS from within a translatable, thin microscope slide cover with the laser beams suitably attenuated to prevent optical damage to the glass. Microscope slide covers are generally less than 200 μm thick and allow the pointwise CARS signal contribution to be ascertained. Upon integration of the pointwise contributions, the spatial resolution can be found. In general, it is far better practice to measure the spatial resolution than to calculate it.

One advantage of broadband CARS is the simplicity of the Stokes dye laser which requires no elements for tuning and spectral condensation. A flowing dye cell, oriented at Brewster's angle, resides within a planar Fabry-Perot oscillator cavity. Because the dyes amenable to 532 μm pumping typically exhibit high gain, slightly off-axis pumping works quite well and leads to very good beam quality, i.e., low angular beam divergence, in contrast to that often obtained with transverse pumping. The dye spectrum is centered at the desired wavelength by selecting the dye appropriately and by adjusting its concentration. Solvent tuning can also be employed.

With the planar Fabry-Perot dye oscillator arrangement, bandwidths vary from 100 to 200 cm^{-1} , depending on the pump energy and dye employed. Binary dye mixtures are often used to improve dye conversion efficiency in the desired wavelength region. For single pulse CARS diagnostics or for spectral scanning of laminar flames, it is important that the dye spectrum be smooth and reproducible from pulse to pulse. The dye cavity is purposely designed to have a high Fresnel number and to accommodate as many modes as possible to "fill in" the spectrum. The pulse to pulse spectral stability of the dye laser has been examined on the OMD and found to be fairly good. Single pulse dye spectra display an irregular fine structure with an amplitude variation of $\pm 5\%$, presumably due to spatial "hole burning" in the dye laser. This fine structure averages out in time to produce spectrally-smooth profiles. High quality, averaged CARS spectra are readily achieved, but single pulse CARS spectra may exhibit some spurious structure, particularly at moderate spectral resolution, $< 1 \text{ cm}^{-1}$. At lower resolutions, $\geq 1 \text{ cm}^{-1}$, this fine structure is spectrally smeared and is not a problem. In broadband CARS, either the linewidth of the pump laser or the resolution of the monochromator/spectrograph determines the ultimate resolution of the spectrum. 1-m monochromators typically have a limiting resolution of about 0.5 cm^{-1} in the visible. 2xNd lasers with intracavity etalons have linewidths in the 0.1 to 0.4 cm^{-1} range, and 0.8 cm^{-1} without. CARS spectra so obtained thus have a limiting resolution between 0.5 and 1 cm^{-1} . This moderate resolution is generally more than sufficient for diagnostics. Furthermore, it is important to note that the large pump laser linewidth is not detrimental in regard to the strength of the CARS radiation. For broadband CARS generation, it is

easy to show that the spectrally integrated intensity of a CARS transition is independent of the pump laser linewidth.

Narrowband CARS systems for combustion diagnostics (Ref. 9) are conceptually similar to that described above with the obvious exception of the tunable Stokes source. For narrowband Stokes work, a variety of dye laser configurations exist, are commercially available or readily assembled. The oscillator sections are generally transversely-pumped to obtain gains high enough to overcome the insertion losses engendered by the spectral condensation scheme employed. The Hansch design (Ref. 10) of a circular telescope, large two dimensional grating has generally given way to one dimensional expansion schemes employing a grazing incidence grating (Ref. 11) or multiple-prism beam expanders (Ref. 12). The one-dimensional expanders require a grating large in one dimension only and greatly reduce cost.

The output from the monochromator can be detected by a photomultiplier tube or with an optical multi-channel analyzer OMA (Ref. 13). Photomultiplier signals are usually averaged with a boxcar integrator. Detection with an OMA is a better method, because the entire spectrum from each CARS pulse, is captured and many spectra may be summed over a desired number of pulses. Given sufficient signal strength, a single CARS pulse (typically 10 nanoseconds) can provide enough information to extract the temperature, as stated previously. Moreover, if the OMD signal is processed with an on-line laboratory minicomputer which can store model predicted CARS spectra, then temperature measurements can be made in a matter of seconds (10 seconds corresponds to 100 laser pulses). This capability is presently available at UTRC.

CARS THERMOMETRY

Temperature can be derived from a CARS spectrum because the vibrational - rotational quantum state populations depend upon temperature. Statistical mechanics tells us that the probability, $P(v, J)$ that a state with vibrational and rotational quantum numbers, v and J , is populated is given by (to first order of approximation)

$$P(v, J) = \frac{g_J(2J+1) e^{-E_v/RT} e^{-B_v J(J+1)/RT}}{Q_v Q_R(v)} \quad (6)$$

where g_J is the nuclear spin degeneracy; Q_v and $Q_R(v)$ are respectively the vibrational and rotational partition functions for level v ; E_v is vibrational energy and B_v is the rotational constant in state v ; k is the Boltzmann constant and T the equilibrium temperature. For most molecules of interest in combustion the vibrational CARS spectrum is dominated by Q-branch transitions, whose frequencies are given by (for a diatomic molecule)

$$\omega_{vJ} = \omega_e - 2 \omega_e x_e (v+1) - a_e J(J+1) \quad (7)$$

Thus, the two equations (6) and (7), through the basic equations for the CARS effect discussed in the theoretical section, determine the shape of the resonant CARS spectrum. Experience in this laboratory has demonstrated that temperature determination from

experimental CARS spectra requires fitting to computer-generated spectra (Refs. 2, 3, 14). The possible exception might be for hydrogen CARS spectra, where, because of the large vibration-rotation interaction, $\alpha_e = 2.933 \text{ cm}^{-1}$, the Q-branch transitions are well separated and temperature can be found from relative peak heights. However, hydrogen is present in abundance in combustion systems only for special cases. A more useful CARS probe, present in large quantity in all air-supported combustion, is the nitrogen molecule.

CARS NITROGEN THERMOMETRY

In addition to the nearly ubiquitous presence of nitrogen, the spectroscopic parameters, including the Raman linewidth, needed for accurate CARS spectral modelling, are quite well known. That the N_2 vibrational CARS spectrum provides an excellent basis for thermometry can be appreciated through examination of the computer calculated temperature dependence of the N_2 spectrum shown in Fig. 6. These calculations, carried out by Hall (Ref. 3), correspond to multiplex (broadband Stokes) CARS employing a 0.8 cm^{-1} bandwidth ω_1 , a 150 cm^{-1} bandwidth Stokes ω_2 , and a 1 cm^{-1} instrumental slit function. Clearly, these spectra exhibit pronounced temperature sensitivity, particularly at higher temperatures, and show much spectral detail even though the instrumental resolution is not particularly high. These spectra all correspond to the "strong line" case. It is assumed that nitrogen is present at 70%, hence, there is little contribution from the nonresonant susceptibility background although its inclusion in the calculations is important for accurate thermometry. Some notable features should be pointed out. At room temperature a single narrow peak, without structure at this resolution, is observed. This peak broadens with increasing temperature and shows resolved Q-branch transitions corresponding to $Q(J = 20)$ to $Q(J = 40)$ at about 1000 K. The peaks observed correspond to even-J Q-branch transitions; the odd-J transitions, are reduced in intensity by one-fourth (nuclear statistical factors are squared in CARS, because χ is squared). A second vibrational band, a "hot band," $v=1$ to $v=2$, becomes noticeable above 2000 K, but is not shown in Fig. 6. For the moderate resolution conditions stated (and readily achieved) for Fig. 6, vibrational CARS thermometry would be most accurate for measurements above $\sim 1000 \text{ K}$. Given better instrumental resolution, and lasers of smaller bandwidth (both requiring greater cost and effort), more spectral detail would be observable at lower temperatures, which would increase the accuracy of CARS measurement at lower temperatures. In contrast, under conditions of poorer spectral resolution, when the fine structure is lost, temperature still can be found from the width of the fundamental and/or the relative strength of the hot band. From the preceding discussion, it is seen that vibrational CARS thermometry can be applied over a wide range of temperature with a varying degree of accuracy.

As an example of the type of accuracy that can be achieved with CARS N_2 thermometry, experiments were performed at UTRC in premixed flat flame burners (Refs. 14,15). Comparison of the CARS determined temperatures was made with radiation-corrected thermocouples (in turn calibrated by sodium line reversal). Figure 7 shows a scanned, broadband N_2 CARS spectrum

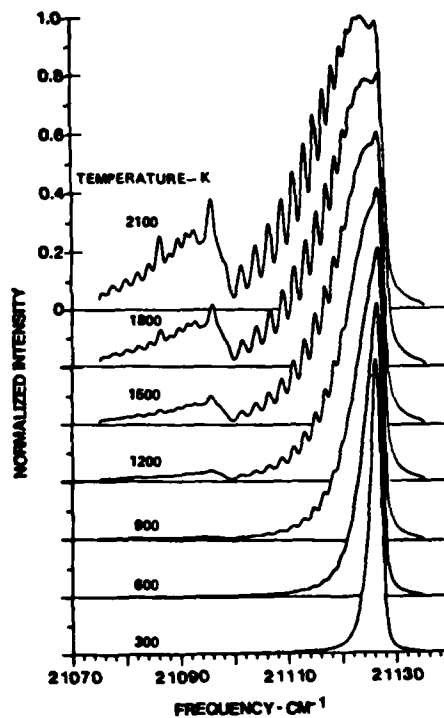


Fig. 6. Temperature variation of the CARS spectrum of N_2 for a pump linewidth of 0.8 cm^{-1} , a Stokes bandwidth of 150 cm^{-1} and a 1 cm^{-1} slit width.

taken in a clean (non-sooting) methane/air flame at a point where the temperature, measured by the thermocouple, was determined to be 2110 K. The dotted curve is the computer model, least mean squares fit to the experimental spectrum; the best fit temperature is $2104 \text{ K} \pm 9 \text{ K}$. This corresponds to an accuracy of better than 1.0%. In order to achieve this type of accuracy for the theoretical fit, very accurate spectral constants for the N_2 vibrational-rotational energy levels are required. In particular, the Raman linewidths, which enter into the expression for the resonant susceptibility equation (5), must be known as a function of temperature and J-state. Fortunately, accurate measurements of the Raman linewidths of N_2 have been obtained by Rahn and co-workers (Ref. 16) at 300 K and 1700 K using high resolution stimulated Raman gain spectroscopy. Equally important, a theoretical model for Raman linewidths, developed by Bonamy and colleagues (Ref. 17), is in good agreement with the experimental values. This model, anchored by the experimental points, permits extrapolation to higher temperatures for estimates of the Raman linewidths, with an error probably less than 20%. Moreover, the T and J dependence of the linewidth is weak at higher temperatures. The sensitivity of the CARS determined temperature to the Raman linewidth has been examined by Eckbreth and Hall (Ref. 1). At 2100 K, it is estimated that the temperature error is less than 25 K (hence, $\sim 1\%$) for a 20% error in the Raman linewidths. Thus, the sensitivity to linewidth is not large, and extrapolated values should be quite adequate.

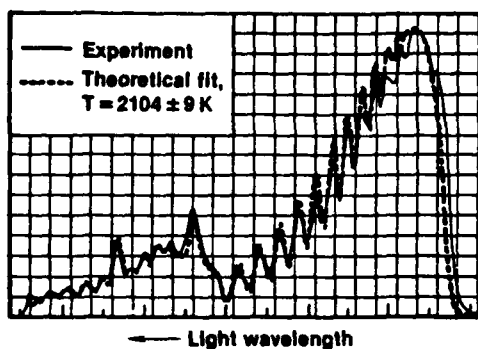


Fig. 7. Comparison of experimental (solid line) and theoretical least squares fit (dashed) N_2 CARS spectra at a measured temperature of 2110°K.

To illustrate the application of CARS thermometry under adverse conditions, measurements in a highly sooting flame will be described (Ref. 3). BOXCARs, with a spatial resolution of about 0.3 by 1.0 mm, was employed in a laminar propane/air diffusion flame. The axial and radial variation of temperature in this flame are shown in Figs. 8, 9, respectively. The quality of the sooting flame CARS spectra is equivalent to that obtained from clean flames. The significance of CARS temperature measurements in the highly luminous, sooting flame is that the CARS method succeeds where conventional Raman methods would fail because laser-induced particulate incandescence (Ref. 18) would swamp the weak Raman signal. In contrast, the CARS signal, which is completely collected, is sufficiently intense to determine temperature from a single, 10^{-8} second pulse. An example of single shot CARS spectra will be presented under the section dealing with applications.

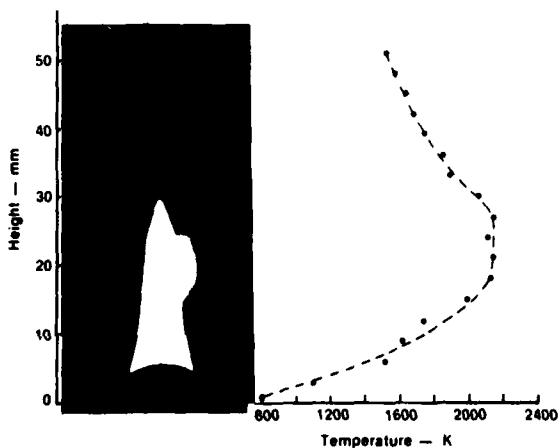


Fig. 8. Axial temperature profile determined in a laminar propane diffusion flame.

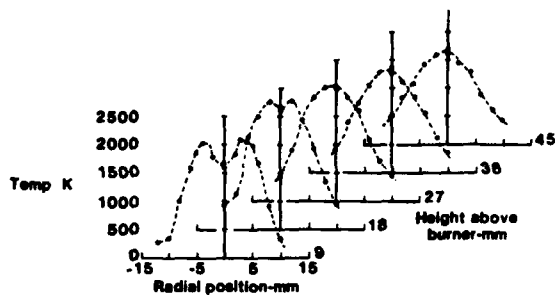


Fig. 9. Radial temperature profiles determined by CARS in a laminar propane diffusion flame.

PRESSURE EFFECTS IN N_2 THERMOMETRY

To achieve maximum usefulness as a diagnostic tool, CARS must be extended to pressures much higher than one atmosphere. Combustion at high pressure is important in such devices as gas turbines, internal combustion engines (especially diesels), and rockets. The pressure encountered in such systems ranges from a few tens of atmospheres to well over 100 atmospheres. If the theoretical CARS analysis used to explain one atmosphere CARS flame spectra were employed at high pressure, it would predict that the overall bandwidth of the spectrum would increase linearly with pressure. The unmodified theory would also predict that the $1 \rightarrow 2$ "hot band" would merge with the fundamental band, and therefore would be lost as a sensitive indicator of temperature.

The effect of pressure on N_2 CARS spectra has been investigated experimentally and theoretically over the pressure range of one to 100 atmospheres (Ref. 19). A similar study has been performed by Roland and Steele (Ref. 20) for pressure up to 30 atmospheres. The room temperature studies of Hall, Eckbreth, and Verdieck show experimentally that, after an initial narrowing of the Q-branch band over the first five to ten atmospheres, the width of the band remains constant with increasing pressure to 100 atmospheres. Figure 10 shows collinear CARS Q-branch spectra of nitrogen at one and 100 atmospheres scanned with a monochromator spectral width of $\sim 0.4 \text{ cm}^{-1}$. The dotted line, the theoretical fit, demonstrates the excellent agreement of the computer model modified to include "collision-induced band narrowing". In simple terms, collisional narrowing of the band occurs when the collision frequency (a function of pressure) becomes comparable to the spacing between individual Q-branch transitions. When this happens, the molecule moves rapidly through many J states and appears to spend, on the average, most of the time in a most probable J-state, defined by the Boltzmann distribution. The phenomenon has also been observed in NMR (Ref. 21), and Raman spectroscopy (Ref. 22). For greater detail on the quantum mechanical treatment of collisional narrowing in CARS spectra, the interested reader may consult (Refs. 1 and 19). Figure 11 illustrates more dramatically the importance of collisional narrowing by a comparison of a collision-narrowed line with a line calculated not including narrowing. Note that for the latter case a very broad line, $\sim 10 \text{ cm}^{-1}$, results.

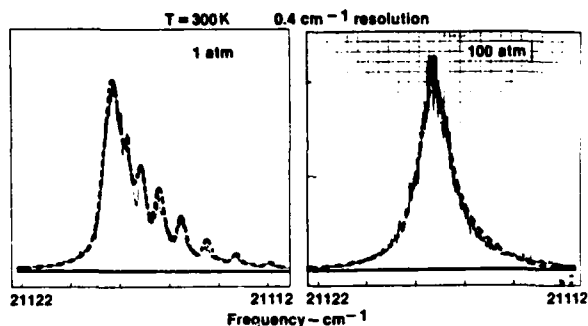


Fig. 10. CARS signatures of 300°K N_2 at one and one hundred atmospheres pressure. The solid line is the experimentally-scanned spectrum in each case, the dashed line the theoretical prediction.

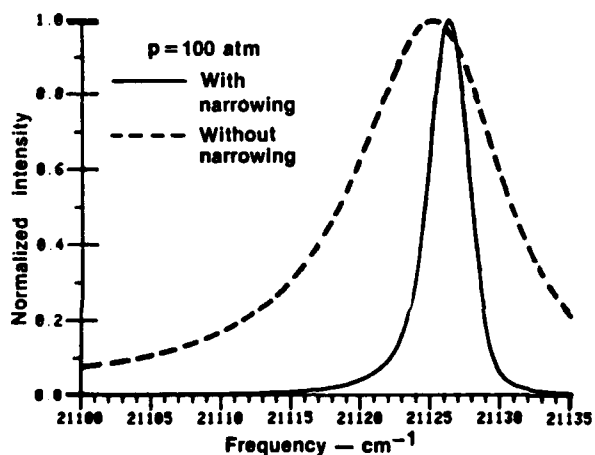


Fig. 11. Comparison of calculated 100 atm signature with and without collisional narrowing - with narrowing, --- without narrowing.

The effect of high pressure on high temperature CARS spectra has been initiated at UTRC; some results are shown in Fig. 12 (Ref. 23). Experimental results are shown at ~ 1600 K for pressures of ~ 8 and 28 atmospheres. The model predicted spectra are presented for comparison. It is noted that although the rotational structure collapses over this pressure change, the hot band persists; hence, the potential for temperature measurements at high pressure still exists. Obviously the area of high pressure, high temperature CARS spectra must be investigated more carefully and thoroughly in order to assess CARS diagnostics for the several important high pressure applications listed earlier.

PURE ROTATIONAL CARS THERMOMETRY

Pure rotational CARS may offer advantages over vibrational-rotational CARS at high pressures, and also at low temperatures (under 1000 K, at low pressures). The reason for this is that the pure rotational lines have better spectral separation, $4B$; where B is the rotational constant. In N_2 , this amounts to 8 cm^{-1} . Pure rotational CARS presents the

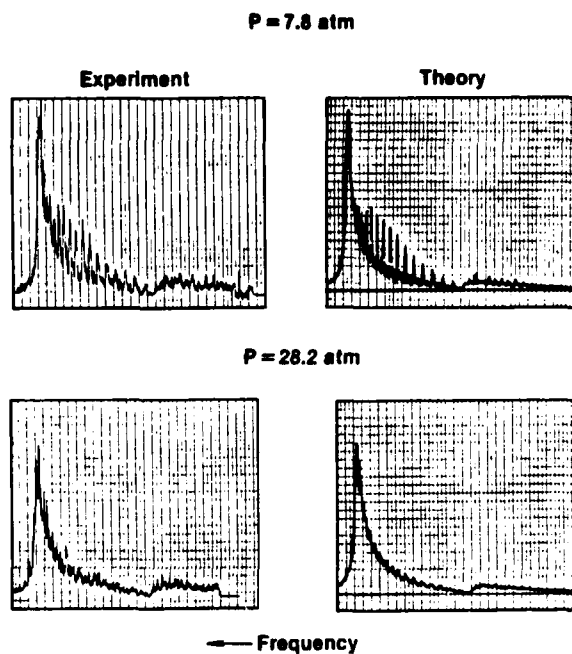


Fig. 12. High pressure CARS spectra for N_2 at 1600°K.

same classic problem that pure rotational Raman spectroscopy does; the frequency shifts from the incident radiation are small, and the CARS radiation is difficult to separate spectrally from the input beams. One method, employed in conventional Raman spectroscopy is to employ a double (or triple) monochromator. In this laboratory the necessary spectral separation of the CARS beam is achieved by the complete spatial separation of the beams, without a dispersing optic, through use of the three-dimensional phase-matching technique called "folded BOXCARs" (Ref. 6), discussed earlier in the experimental section. Referring back to Fig. 5, it can be seen that the CARS beam, ω_3 , emerges well separated angularly from the input beams. In this manner, the pure rotational CARS spectrum of room air (one atmosphere, 300°K) was recorded by spectrally scanning the isolated ω_3 beam (Fig. 10). This experimental spectrum is in good agreement with the theoretical model (Ref. 6).

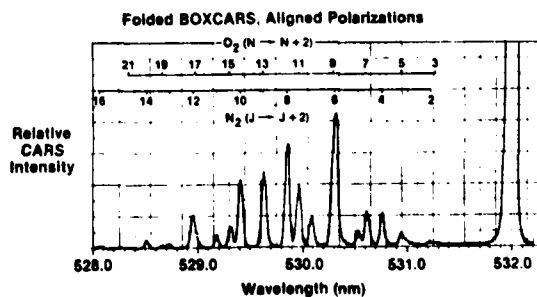


Fig. 13. Pure rotational CARS spectra of air.

CARS THERMOMETRY WITH OTHER MOLECULES

At UTRC, several other molecules of interest to combustion science have been examined for CARS thermometry and concentration measurements. CARS spectra have been obtained for hydrogen, oxygen, carbon monoxide, carbon dioxide, water, and methane. Space does not permit a discussion of all of these; hydrogen, water, and carbon dioxide CARS spectra are selected for discussion with application to temperature measurement.

Computed CARS spectra of hydrogen at four different temperatures are illustrated in Fig. 14. The vibrational-rotational interaction, α , is much larger in hydrogen (2.993) than in nitrogen (0.0187); therefore, the spectrum is simple (few lines), and quite spread out (over nearly 200 cm^{-1}). The alternation in intensity due to nuclear spin statistics is quite apparent. Recall that ortho/para forms of hydrogen bear statistical weights of 3:1; however, in CARS spectroscopy, population differences are squared (because χ is squared), therefore, the intensity contrast between adjacent lines is quite large, and hence useful for temperature measurements. For comparison, experimental CARS spectra for H_2 recorded on an OMA and taken in a H_2/air diffusion flame, are presented in Fig. 15. The temperatures listed were obtained from comparison of the peak height ratios of Q(1), Q(3), and Q(5) transitions. As a practical application, temperature profiles of a slot-shaped H_2/air diffusion flame were determined from H_2 CARS spectra, and also from O_2 CARS spectra (O_2 CARS spectral temperatures are obtained in manner analogous to that for N_2), and are displayed in Fig. 16. The CARS derived temperatures are in fairly good agreement with a radiation-corrected thermocouple. A detailed discussion of all aspects of the hydrogen CARS studies is found in Ref. 24.

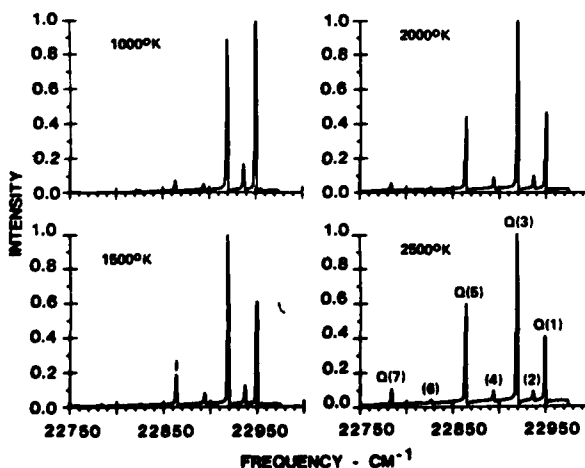


Fig. 14. Theoretical CARS spectra of H_2 over the temperature range $1000^\circ\text{K} \leq T \leq 2000^\circ\text{K}$.

Because water is a major product of air supported combustion of hydrogen-containing fuels, it can serve as a thermometric probe molecule, if present in sufficient abundance. Moreover, the measurement of

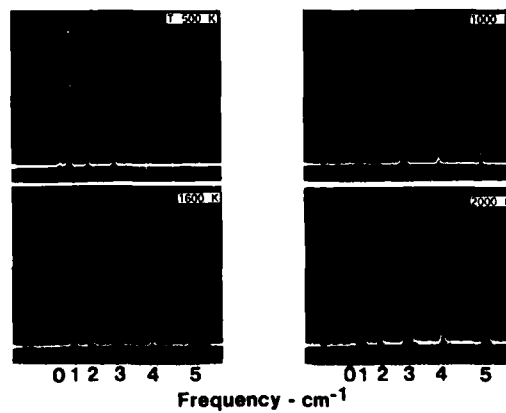


Fig. 15. CARS spectra of H_2 in H_2/air diffusion flame at temperatures determined from relative strengths of indicated Q-branch transitions. Frequency scale corresponds to 0.60 cm^{-1} per dot.

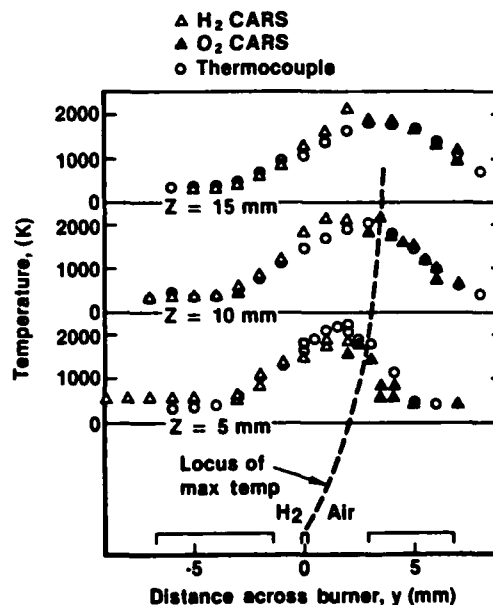


Fig. 16. Temperature measurements in a flat H_2/air diffusion flame. Symbols: circles, radiation-corrected thermocouple; open triangles, H_2 CARS; and solid triangles, O_2 CARS. Dotted curve is locus of maximum temperature.

water concentration as a function of distance in a combustion system could yield chemical kinetic information and a better understanding of the combustion process.

The water molecule is an asymmetric top with three vibrational modes, of which the ν_1 symmetric stretch is strongly Raman allowed, with a Raman shift of 3657 cm^{-1} . Because it is an asymmetric top, the rotational structure is complex and the rotational energy levels cannot be expressed in closed form. However, the structure of the Q-branch of the ν_1 mode is tractable, and Hall, et al. (Ref. 25) have modelled the CARS spectrum. Figure 17 displays the comparison

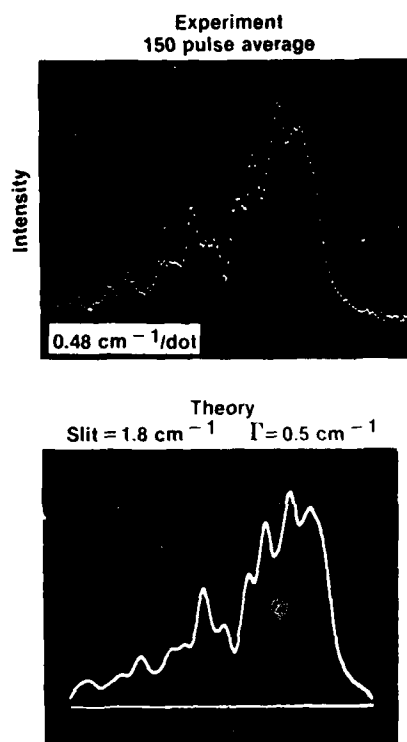


Fig. 17. Comparison of calculated CARS spectrum of pure H_2O with spectrum measured in a heated cell at $773^{\circ}K$.

between computed and experimental CARS spectra of water in a static, heated cell at $773^{\circ}K$. Because Raman linewidth data were not available for this calculation, a value of 0.5 cm^{-1} , independent of J was selected on the basis of the good agreement achieved between the calculated and experimental aspects. A similar comparison of theory and experiment is shown in Fig. 18 for H_2O in a $1700^{\circ}K$ premixed methane/air flame. Because of the higher

temperature, the assumed Raman linewidth was estimated to be 0.2 cm^{-1} . In these calculations, nearly one thousand vibrational-rotational Q-branch transitions were included in the computed spectrum. Because the shape of the water spectrum is quite sensitive to temperature, the water molecule may offer the potential for thermometry over a wide range of temperature.

The other major product of hydrocarbon combustion is carbon dioxide. CO_2 , a linear triatomic molecule, has three normal vibrational modes, a symmetric stretch (ν_1), an antisymmetric stretch (ν_3), and doubly-degenerate bend, (ν_2). Moreover, an accidental degeneracy of ν_1 and $2\nu_2$, the prototype case of Fermi resonance, mixes these two states and makes both transitions from the ground state Raman active. Not only these two states are in Fermi resonance, but several other combinations, occurring up the vibrational state ladder, are also in Fermi resonance which makes the problem of calculating CO_2 vibrational energy levels difficult. In spite of this complexity, theoretical CARS spectra for CO_2 have been calculated by Hall (Ref. 26).

BOXCARS spectra of CO_2 have been obtained by Eckbreth (Ref. 1) in several propane-air and CO-air flames, as shown in Fig. 19 where a measured thermo-couple temperature is given for each spectrum. The experimental signature displays a fundamental band at a Raman shift of about 1388 cm^{-1} , assigned to the transition between the ground vibrational state and the first symmetric stretch state. A number of hot bands, originating in vibrationally excited initial states, appear at larger shifts. The relative strength of the hot bands is seen to be moderately sensitive to temperature, making the molecule potentially attractive for thermometry.

Figure 20 compares the experimental CO_2 CARS spectrum at $1520^{\circ}K$ with a theoretical spectrum based on the isolated line approximation (Ref. 26). As can be seen, the agreement is fairly good, except for the highest hot bands. In the theoretical calculation, vibrational energy levels, rotational constants, and polarizability matrix elements were computed following the treatment of Courtoy (Ref. 27). This basically involves diagonalizing the system Hamiltonian for each set of near resonance states. It was found, however,

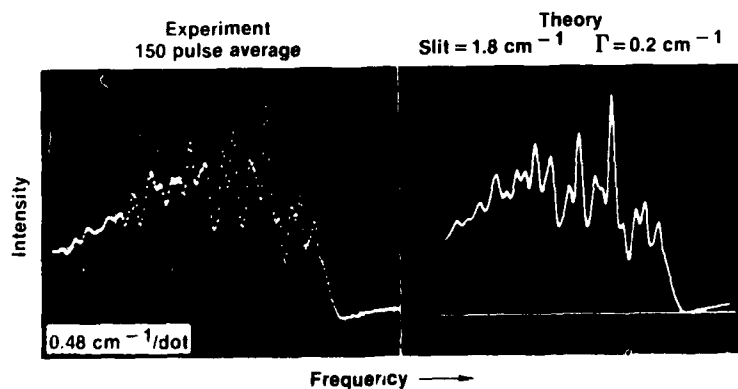


Fig. 18. Comparison of experimental and theoretical CARS spectra of water vapor in a flame at $1700^{\circ}K$. A best-fit pressure-broadened linewidth $\Gamma = 0.19\text{ cm}^{-1}$ was inferred for all transitions in the calculation.

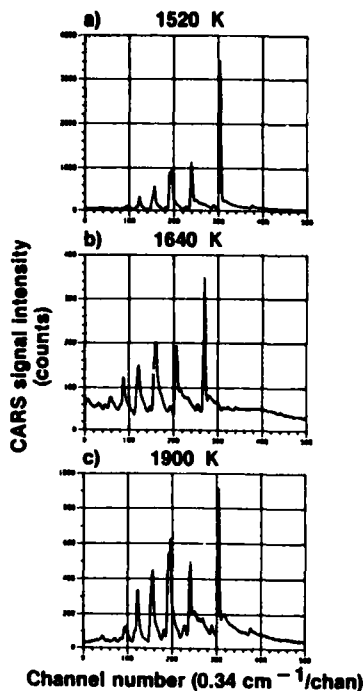


Fig. 19. Experimental carbon dioxide spectra at selected temperatures.

and better agreement with experiment resulted from the use of tabulated values for the rotational constants (Ref. 28). Similar agreement was obtained with the other experimental spectra of Fig. 19. Further investigations, mainly theoretical, will be needed before CO₂ CARS can be regarded as a reliable diagnostic tool. For example, the calculations display some sensitivity to assumed Raman linewidth, and more information concerning the magnitude of these quantities is needed. Also, the high degree of line overlap within each band may make the isolated line approximation questionable even at one atmosphere pressure.

CARS CONCENTRATION MEASUREMENTS

Although this review is intended to deal primarily with CARS temperature measurements, species concentration measurements from CARS will be included for completeness. CARS measurements of species

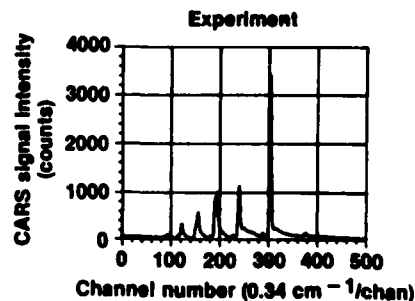
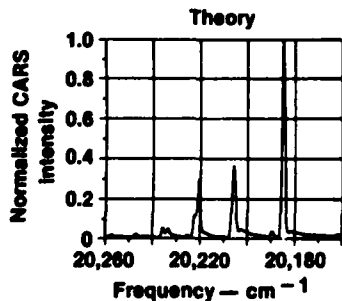


Fig. 20. Comparison of experimental and calculated CARS carbon dioxide spectra.

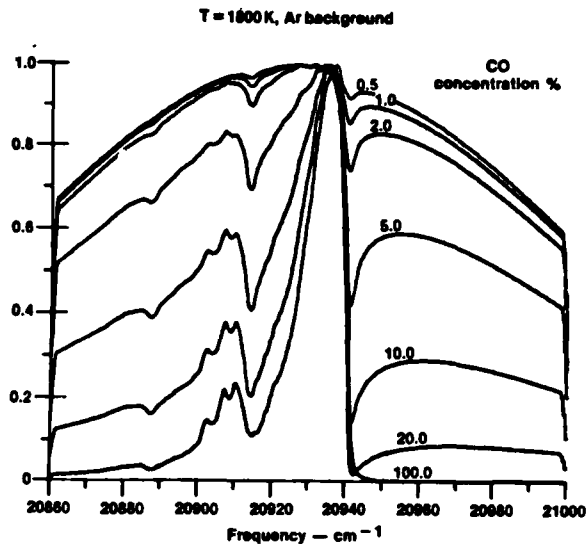


Fig. 21. Computed CARS spectral behavior of CO at various concentrations at 1800°K.

concentration in combustion are made in either of two quite different ways; from the absolute intensity of the CARS signal, or in certain concentration ranges, from the shape of the spectrum. The latter case, which will be presented here, results when the resonant and nonresonant contributions are comparable and the weak signal limit applies, shown in Fig. 2. This behavior can be better understood by reference to Fig. 21, which displays a set of model predicted spectra of carbon monoxide at 1800 K. The concentration values range from 0.5 percent to 100 percent; however, the useful range extends to ~ 30 percent at the high end. Beyond this value some sort of reference is required to scale the intensity. Below ~ 0.5 percent level, the resonant signal disappears into the baseline.

Spectral shape fitting for concentration measurements has been demonstrated experimentally in CO, as illustrated by the two spectra in Fig. 22. The upper portion is the experimental CARS spectrum (dotted line) of a 2.1 percent CO (in argon) calibrated gas mixture at 300 K. The thin solid line is the computer generated CARS spectrum calculated for the same concentration, and is in excellent agreement. The bottom part of Fig. 22 displays a similar comparison for CO in a CH₄/O₂/Ar

flame doped with CO. The flame temperature was 2100 K. The theoretical spectrum was calculated for 3.6 percent CO, which was determined with a quartz microprobe and NDIR CO detector. Again the agreement is good. For more detailed information on CO concentration measurements, including a discussion of other CARS methods, the reader may consult Ref. 29. Concentration measurements by the CARS spectral shape fitting technique have been applied to oxygen (Ref. 30) and nitrogen (Ref. 3). Spectral fitting could be used for measuring water vapor concentrations as well.

Before closing the discussion of concentration measurement by spectral shape, it must be emphasized that both the temperature, and the nonresonant susceptibility, must be known in order to determine the concentration of the desired species. Because the nonresonant susceptibility changes little (10-15%) through the air fed combustion reaction going from reactants to products, intelligent estimates can be made for $\chi^{(2)}$, if the location, and temperature at that point, are known. From the experiments shown above, it is clear that concentration measurement by spectral shape fitting is a viable technique, easily applied, where appropriate.

PRACTICAL APPLICATIONS OF CARS THERMOMETRY

In this section some illustrations of CARS measurements, mainly temperature measurements, in industrial scale combustion devices are listed. A detailed description of CARS measurements performed at UTRC on a gas turbine test combustor concludes this final section.

Apparently the first application of CARS measurements on a practical, large-scale combustion device was performed by Taran and co-workers at ONERA

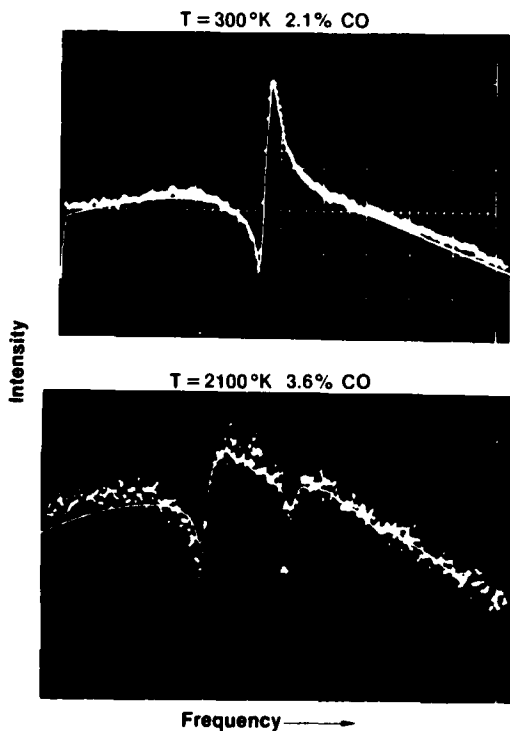


Fig. 22. Comparison of experimental and computed (solid line) CARS spectra at 300°K (2.1% CO) and 2100°K (3.6% CO).

in 1978 (Ref. 31). Temperature and concentration measurements of N_2 and CO_2 were made in a simulated turbomachine combustor burning kerosene. More recently this group has made measurements in a commercial gas turbine combustion can. Similar measurements at Wright-Patterson AFB have been carried out in a large scale diffusion flame which was stabilized with a bluff body (Ref. 32).

CARS measurements in an internal combustion engine have been made by Stenhouse et al. (Ref. 33). The CARS input laser pulses were synchronized with the engine cycle to generate the CARS spectrum in time steps, and could be positioned at known points on the engine cycle. More recently, workers at Ford Motor Company Research have measured temperature and carbon monoxide concentration in a research scale, single cylinder engine (Ref. 34). A special type of non-collinear phase matching was employed which achieved a spatial resolution of ~ 2 mm along the beam and $100 \mu m$ transverse to the beam. Single pulse, 10^{-8} second, CARS spectra were obtained, from which temperature was determined. CARS measurements also have been made in a commercial diesel engine (Ref. 35) at Komatsu Corporation. Further measurements in internal combustion engines using CARS are scheduled at many laboratories throughout the world.

In experiments at UTRC, Eckbreth (Ref. 7) made CARS measurements in a 0.5 m diameter combustion tunnel fitted with a variety of burners, one of which was a gas turbine (JT-12) combustor. CARS temperature measurements (using BOXCARS) from nitrogen were made in the primary zones of flames and in the exhaust. Both gaseous (propane) and liquid (Jet A) fuels were used.

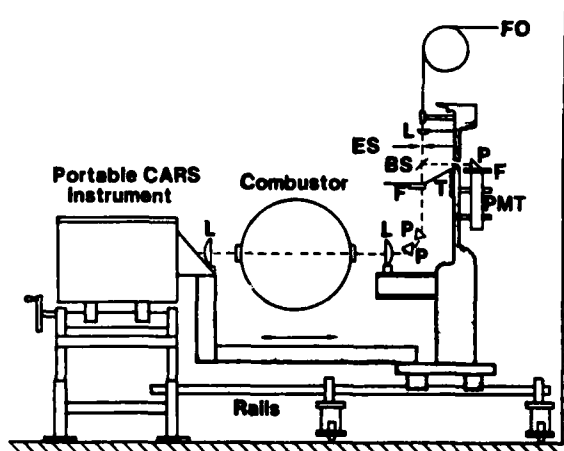


Fig. 23. Cross-section through combustor test tunnel indicating the CARS transmitter on the left and CARS receiving optics on the right. Abbreviations are defined in the text.

The experimental scheme is shown in cross-section in Fig. 23. The pump and Stokes lasers, along with the requisite optics, are contained on a one by two meter optical pallet placed near the test tunnel. Lenses focus and collect the BOXCARS beams through the tunnel windows. It should be noted that the flame in the test combustor is so luminous that most conventional optical methods would fail. The emergent laser beams are manipulated in a receiver which spectrally disperses the beams, and traps the

unwanted ω_1 and ω_2 frequencies. A reference PMT detects a small fraction of the CARS signal and serves to monitor the optical alignment of the input optics. The CARS beam is focussed into a fiber optic (20 m long) and piped out to a control room. The control room furnishes a much quieter environment for delicate instrumentation, such as the spectrometer, and the optical multichannel analyzer which is subject to microphonics.

As examples of CARS measurements from this experiment, Fig. 24 displays averaged N_2 CARS system at two different locations downstream of the burner exit face. These CARS spectra correspond to 100-150 laser pulses, or to a 10-15 second average. The spectrum at $x = 6$ cm was made in the fuel spray, hence, the relatively cool temperature. The second location, at 39 cm, is in the flame, and is much hotter. Figure 25 demonstrates that temperature can be determined in a highly luminous, noisy combustion system, from a single, 10^{-8} second, pulse spectrum. Comparison is made with a 130 pulse average spectrum. The single pulse spectrum displays photon statistical noise (shot noise); however, it is of sufficiently good quality to allow instantaneous temperature measurement. The single shot measurement capability, together with the high spatial resolution of BOXCARs, fulfills an obvious need for studies in highly turbulent, inhomogeneous combustion systems.

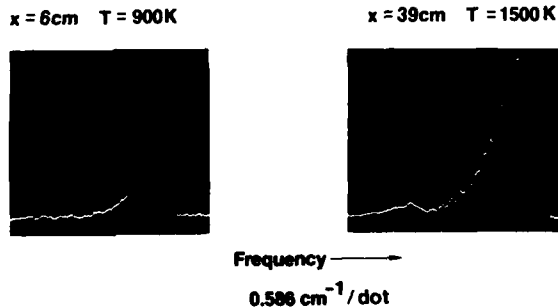


Fig. 24. Spatial variation of temperature from averaged CARS spectra of N_2 in swirl burner with Jet A fuel.

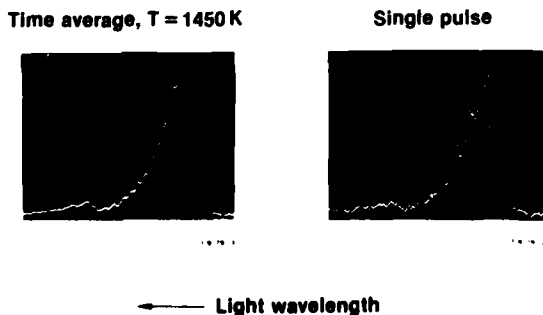


Fig. 25. Comparison of averaged and single pulse N_2 CARS spectra in swirl burner with refractory back wall fueled with Jet A at an overall equivalence ratio of 0.8.

At the UTRC CARS Laboratory, in East Hartford, a multipurpose portable CARS apparatus is being assembled for use at the Government Products Division (GPD) of Pratt & Whitney Aircraft. When complete, measurements will be made in the exhaust of a production run 1130 (a modified F-100) gas turbine engine. In addition to N_2 temperature measurements, the concentration of water, carbon dioxide, and oxygen will be determined, as well as some measure of total unburned hydrocarbons. These measurements are scheduled to take place before the end of 1981.

The application of CARS diagnostics to both research scale and production line combustion devices is increasing rapidly. Academic, government, and industrial research laboratories are, or soon will be, performing measurements in internal combustion engines, gas turbine combustors, furnaces, chemical process streams, and propellant burning strands. The equipment necessary for CARS is commercially available, and special methods for employment near noisy environments can be developed, as illustrated by the previous discussion. The capabilities of the CARS technique will be further improved by experimental modification, and more importantly, from advances in computer data processing (including better modelling of spectra). Considering the great amount of knowledge that conventional diagnostic methods have provided, CARS should increase our understanding of fundamental and applied combustion processes even further.

Acknowledgements

The authors wish to thank the Environmental Protection Agency, the Army Research Office, the Air Force Office of Scientific Research, NASA, and the Office of Naval Research for supporting portions of research carried out at UTRC.

References

1. A. C. Eckbreth and R. J. Hall, "Coherent Anti-Stoke Raman Spectroscopy (CARS): Application to Combustion Diagnostics" to appear in *Laser Applications (Vol. V)*, ed. by R. K. Erf; Academic Press.
2. R. J. Hall, *Combust. Flame*, **35**, 47, (1979).
3. A. C. Eckbreth and R. J. Hall, *Combust. Flame*, **36**, 87 (1979).
4. J. J. Barrett and R. F. Begley, *Appl. Phys. Lett.*, **27**, 129 (1975).
5. A. C. Eckbreth, *Appl. Phys. Letts.*, **32**, 421 (1978).
6. J. A. Shirley, R. J. Hall and A. C. Eckbreth, *Opt. Letts.*, **5**, 380 (1980).
7. A. C. Eckbreth, *Combust. Flame*, **39**, 133 (1980).
8. A. C. Eckbreth and R. J. Hall, *Combust. Sci. and Tech.*, **25**, 175 (1981).
9. R. L. Farrow, R. E. Mitchell, L. A. Rahn and P. L. Mattern, AIAA Paper No. 81-0182, AIAA, New York, New York.
10. T. W. Hansch, *Appl. Opt.* **11**, 895 (1972).

11. M. G. Littman, *Opt. Letts.*, 3, 138 (1978).
12. F. J. Duarte and J. A. Piper, *Opt. Comm.*, 35, 100 (1980).
13. The Optical Multichannel Analyzer is Manufactured by the PAR Company; OMA is a registered trademark.
14. R. J. Hall, *Appl. Spectrosc.*, 34, 700 (1980).
15. A. C. Eckbreth and R. J. Hall, *Opt. Eng.*, 20, 494 (1981).
16. L. A. Rahn, A. Owyong, M. E. Colvin, and M. L. Koszykowski, "The J Dependence of Nitrogen "Q" Branch Linewidths," Proc. of VII International Conference on Raman Spectroscopy, Ottawa, Canada (1980).
17. J. Bonamy, L. Bonamy, D. Robert, *J. Chem. Phys.*, 67, 4441 (1977).
18. A. C. Eckbreth, *J. Appl. Phys.*, 48, 4473 (1977).
19. R. J. Hall, J. F. Verdick and A. C. Eckbreth, *Opt. Comm.*, 35, 69 (1980).
20. C. M. Roland and W. A. Steele, *J. Chem. Phys.*, 73, 5924 (1980).
21. N. Bloembergen, E. M. Prucell and R. V. Pound, *Phys. Rev.*, 73, 679 (1948).
22. A. D. May, J. C. Stryland and G. Varghese, *Can. J. Phys.*, 48, 2331 (1970).
23. J. A. Shirley, R. J. Hall, J. F. Verdick and A. C. Eckbreth, New Direction in CARS Diagnostics for Combustion, AIAA Paper No. 80-1542 (1980).
24. J. A. Shirley, R. J. Hall and A. C. Eckbreth, "Investigation of the Feasibility of CARS Measurements in Scramjet Combustion," Technical Report R79-954390-8 under Contract NASI-15491.
25. J. A. Shirley, R. J. Hall and A. C. Eckbreth "Investigation of the CARS Spectrum of Water Vapor," Proceedings of Laser 1980 International Conference, New Orleans (1980).
26. R. J. Hall and A. C. Eckbreth, *Opt. Eng.*, 20, 494 (1981).
27. C. P. Courtoy, *Can. J. Phys.*, 35, 608 (1957).
28. L. S. Rothmann and W. S. Benedict, *Appl. Opt.*, 17, 2605 (1978).
29. A. C. Eckbreth and R. J. Hall, *Comb. Sci. and Tech.*, 25, 176 (1981).
30. J. A. Shirley, R. J. Hall and A. C. Eckbreth, Proceedings of 16th JANNAF Meeting, CPIA Publication 309, 487 (1979).
31. B. Attal, M. Pealat and J-P. E. Taran, CARS Diagnostics at Combustion, AIAA Paper No. 80-0282.
32. G. L. Switzer, L. P. Goss, W. M. Roguemore, R. P. Bradley and P. W. Schreiber, AIAA Paper No. 80-0353, AIAA, New York.
33. I. A. Stenhouse, D. R. Williams, J. B. Cole and M. D. Swords, *Appl. Opt.*, 18, 3819 (1979).
34. D. Klick, K. A. Marko and L. Rimai, *Appl. Optics*, 20, 1178 (1981).
35. K. Kajiyama, Komatsu Ltd., Hiratsaka, Japan, Private Communication.

R82-954566-F

APPENDIX G

APPLICATION OF THE ROTATIONAL DIFFUSION MODEL TO GASEOUS N_2 CARS SPECTRA

APPLICATION OF THE ROTATIONAL DIFFUSION MODEL TO GASEOUS N₂ CARS SPECTRA

Robert J. HALL

United Technologies Research Center, East Hartford, Ct., USA

and

Douglas A. GREENHALGH

Engineering Sciences Division, AERE Harwell, Oxfordshire, UK

Received 22 October 1981

A theoretical model of CARS intensities based on Gordon's rotational diffusion model has been found to give good agreement with 300 K N₂ spectra over the pressure range one to 100 atmospheres. The model requires only that the isolated pressure-broadened linewidths be known and greatly simplifies the task of calculating CARS spectra for overlapping transitions.

Coherent anti-Stokes Raman spectroscopy (CARS) has come to prominence in recent years because of its promise as a versatile diagnostic tool [1-4]. The application of CARS to combustion research in particular is an area of great current interest, with the technique proving useful for thermometry and species concentration measurements [5-8]. The ability to model CARS spectra for molecules of interest in combustion (e.g. N₂, CO, CO₂, H₂O, ...) is an important aspect of the process of extracting diagnostic information from experimental spectra, because of unique spectral interference effects that preclude simplified data reduction in most cases [9]. One important problem in the theory of gas-phase CARS is the effect of pressure on predicted spectra. Experimentally, it is most common to probe vibrational Q-branch transitions; for most of the molecules of interest, the splitting of adjacent lines due to vibration-rotation interaction is relatively small, giving rise to appreciable line overlap even at modest gas pressures. When there is strong line overlap, the overall band contour is no longer adequately described in terms of isolated lines undergoing ordinary pressure broadening. It is then necessary to account for the phenomenon of collisional narrowing, which causes a coalescence or collapse of adjacent transitions toward a frequency center of gravity determined by the most

populous rotational state [10-14]. This effect is analogous to narrow bandwidth detection of an emitter which is rapidly switching between discrete frequencies with no change of phase. Diatomic Q-branch frequencies are separated by $2\alpha_e J$, where α_e is the vibration-rotation interaction constant. If the mean time between inelastic molecular collisions is of the order of $(2\alpha_e J)^{-1}$, the transition frequency of the molecule will appear to switch rapidly during the radiation process, and the detector will record an averaged signal in which the individual Q-branch frequencies have merged or blended together.

The pressure-induced narrowing effect has been modelled for CARS, and good agreement with experiment has been obtained for 300 K N₂ over the pressure range one to 100 atm [15]. As is well known from theoretical studies of overlapping spectral lines, it is necessary to specify not only the isolated pressure-broadened linewidths, but also an off-diagonal transition rate matrix for line amplitudes whose elements sensibly give the rates of collisional energy transfer between rotational energy levels [10-14]. Unless these off-diagonal linewidth parameters can be measured or calculated from first principles, however, unknown parameters will have to be introduced into the calculation. Also, these theoretical approaches re-

quire at each frequency the inversion of a complex matrix (sometimes called the "G-matrix") [13,14] resulting in cumbersome calculation for conditions requiring the inclusion of large numbers of rotational states.

We report here a simpler calculation of gaseous N_2 CARS spectra based on Gordon's extended J -diffusion model of rotational motion [16,17]. The analysis draws on Brueck's [18] application of Gordon's model to the lineshapes of two-photon resonances in liquids. The rotational diffusion theory has primarily been applied to liquid phase infrared and Raman spectra [16, 17]; however, because it is based on a gas-like rather than a structure-dominated view of the liquid state, it can with equal validity be applied to the gaseous state. It is an impact theory in which the times during which intermolecular torques act on a molecule are assumed to be short compared to the time for free rotation of the molecule, with free rotation assumed between collisions. Strong collisions are assumed in which both the magnitude and orientation of the rotational angular momentum are randomized with each collision. Thus, the values of the rotational quantum numbers after a collision are unrelated to those before, with the magnitude of the angular momentum assumed to be redistributed in accordance with the Boltzmann distribution.

Vibrational CARS signals for the molecules of interest are generated mainly by the isotropic part α of the polarizability tensor, which is sensitive only to the magnitude of the angular momentum and not to its orientation. Brueck has derived the third-order electric susceptibility in these approximations using a density matrix formulation which properly accounts for vibration-rotation interaction. The off-diagonal vibrational density matrix element ρ_{10} (the temperature is assumed to be so low that the influence of hot bands can be neglected) is assumed to be a function of the rotational angular frequency ω_r as well as time, and its equation of motion

$$\partial \rho_{10}(\omega_r, t) / \partial t = -(i/\hbar) [H_0 + h(t), \rho]_{10} - \frac{1}{T_v} \rho_{10} - \frac{1}{\tau_J(\omega_r)} \{ \rho_{10} - f(\omega_r) \langle \rho_{10} \rangle \} \quad (1)$$

is solved to first order with the perturbation interaction energy $h(t) = -\frac{1}{2} \alpha E^2$ and a collision term that randomizes the distribution of angular frequency. In eq. (1) H_0 is the unperturbed molecular hamiltonian;

T_v is a characteristic time for vibrational processes; $\tau_J(\omega_r)$ is a characteristic time between angular momentum randomizing collisions; $f(\omega_r)$ is the thermal distribution of angular velocity, and $\langle x \rangle = \int d\omega_r x(\omega_r)$. The mixing of fields with frequencies ω_1 and ω_2 by the third-order susceptibility will give rise to a CARS frequency component in the macroscopic polarization $\rho^{(3)}$ given by

$$P^{(3)} = N \alpha_{10} \langle \rho_{10} \rangle E_1, \quad (2)$$

where N is the number density of Raman-active molecules, and from this the vibrationally resonant third order susceptibility may be defined as

$$\chi_{01}^{(3)} = (N \alpha_{10}^2 / \hbar) \langle f(\omega_r) \rangle / (\omega_1 - \omega_2 - \omega_{01}(\omega_r) - i/\tau_J(\omega_r)) \times \{ 1 + i \langle [f(\omega_r) / \tau_J(\omega_r)] / (\omega_1 - \omega_2 - \omega_{01}(\omega_r) - i/\tau_J(\omega_r)) \rangle \}^{-1}, \quad (3)$$

where $\omega_{01}(\omega_r)$ is the Q -branch transition frequency; the vibrational broadening (T_v) term has been neglected, and the dependence of the angular momentum randomizing rate on ω_r (rotational quantum number) has been retained. The Boltzmann population factor $f(\omega_r)$ in the numerator should strictly be the population difference between the upper and lower Q -branch energy levels, but the difference between the two quantities will be small for modest temperatures. If the temperature is sufficiently high that the populations of higher vibrational states cannot be neglected, then the resonant contribution to $\chi^{(3)}$ can be represented as a sum of contributions from all significant bands:

$$\chi^{(3)} = \sum_v \chi_{v,v+1}^{(3)} \quad (4)$$

with

$$\chi_{v,v+1}^{(3)} = \frac{N \alpha_{v,v+1}^2}{\hbar} \frac{\langle \Delta f'_v(\omega_r) / D_v(\omega_r) \rangle}{1 + i \langle [f(\omega_r) / \tau_J(\omega_r)] / D_v(\omega_r) \rangle}, \quad (4)$$

where $\Delta f'_v(\omega_r)$ is now the population difference factor with $f'_v(\omega_r)$ normalized to unity for all vibrational and rotational states, and $D_v(\omega_r) = \omega_1 - \omega_2 - \omega_{v,v+1}(\omega_r) - i/\tau_J(\omega_r)$. The above formulation is based on the assumptions that vibrationally inelastic energy transfer will be relatively slow, and that neither the rotational Boltzmann factor f nor the angular momentum randomizing frequency $(\tau_J)^{-1}$ will have a significant dependence on vibrational state. In the ab-

sence of vibrational effects, the angular momentum redistribution frequency $\tau_J(\omega_r)^{-1}$ is equivalent to the pressure-broadened halfwidth. Similar formulations of the Gordon rotational diffusion theory have been given by Lynden-Bell [19], Eagles and McClung [20], and Temkin and Burshstein [21].

Given $\chi^{(3)}$, the predicted CARS spectral density is given by the convolution of $|\chi^{(3)}|^2$ with the spectral profiles of the pump and Stokes sources [9,22]. Numerical calculations were performed using eq. (3) to simulate the pressure variation of the 300 K N_2 CARS spectrum reported in [15]. For these calculations the N_2-N_2 Raman linewidths measured by Rahn and Owyong [23] were scaled linearly with pressure to give $\tau_J(\omega_r)^{-1}$. Because these widths have a significant dependence on rotational quantum number, it was not possible to obtain an analytic expression for $\chi^{(3)}$ as was done by Brueck, and the integrations over ω_r required in eq. (3) were performed using explicit summations over the discrete rotational states [21]. Comparison of the rotational diffusion model with the experimental data of [15] presents a good test for the theory because, with the transition linewidths $\tau_J(\omega_r)^{-1}$ known, the problem is completely specified, and there are no adjustable parameters.

A comparison of the signature bandwidths predicted by eq. (3) with the experimental data of [15] is shown in fig. 1. As explained in [15], the various symbols denote the results of different series of broadband experiments taken over a period of several weeks, and the assignment of bandwidth to each signature is prone to a subjective error in reading of peak height and full width at half maximum that is estimated to be $\pm 0.1 \text{ cm}^{-1}$. Bearing this in mind, the comparison between experiment and theory is seen to be quite satisfactory, with agreement to within the experimental error. The theory predicts a slight minimum in the vicinity of 2 atmospheres, a gradual increase in the bandwidth to about 20 atmospheres, and then a steady contraction out to 100 atmospheres. The theory does tend to the low side of the experimental data at the higher pressures; this may indicate the presence of a small vibrational dephasing contribution. Also shown in the figure is the bandwidth predicted on the basis of isolated line theory, that is, neglecting the $\langle \rangle$ term in the denominator of eq. (3). At 100 atm, the predicted isolated line bandwidth exceed 10 cm^{-1} , emphasizing the very significant role that collisional narrow-

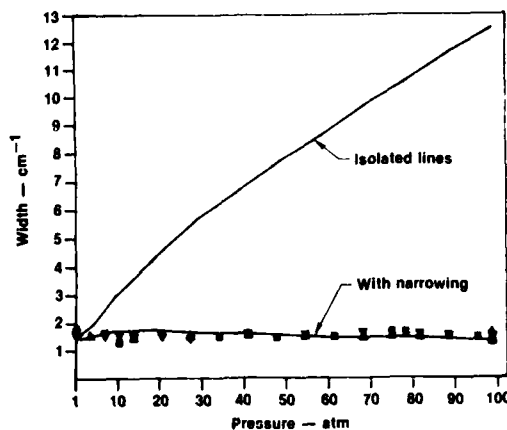


Fig. 1. Bandwidth (FWHM) of 300 K N_2 CARS signature versus pressure. Symbols denote experimental points [15]; solid lines denote theoretical calculations for an assumed overall resolution of 0.4 cm^{-1} .

ing plays at higher pressures.

Scatter in the data presented in fig. 1 precludes a detailed verification of the predicted bandwidth variation at low pressures. However, the initial contraction of the bandwidth at 2–4 atmospheres, with a subsequent increase out to approximately 20 atmospheres, does seem to be confirmed qualitatively by the experiments of Roland and Steele [24], in which the spectrum of 300 K N_2 was examined using tuned, narrow-band sources for pressures up to 33 atm.

In view of the fact that the theoretical spectra contain no adjustable parameters, the overall agreement exhibited in fig. 1 is gratifying. Use of eq. (3) to model collisional narrowing effects in CARS spectra offers great computational advantages, because the calculation of $\chi^{(3)}$ is only slightly more involved than in the isolated line approximation and therefore requires practically no extra computation expense. It will be interesting to see whether the rotational diffusion theory is also applicable to the gas-phase CARS spectra of other molecules of interest; for molecules such as H_2O and CO_2 in particular, whose spectra are comprised of very large numbers of transitions, the rotational diffusion theory would make possible narrowing calculations that would otherwise be very costly.

References

- [1] S. Druet and J.P. Taran, Chemical and biological applications of lasers, ed. C.B. Moore (Academic Press, New York, 1979) p. 187.
- [2] J.W. Nibler and G.V. Knighten, Topics in current physics, Vol. III, ed. A. Weber (Springer-Verlag, Heidelberg, 1979) Ch. 7.
- [3] A.C. Eckbreth, P.A. Bonczyk and J.F. Verdick, Prog. Energy Combust. Sci. 5 (1979) 253.
- [4] A.B. Harvey, Chemical applications of nonlinear Raman spectroscopy (Academic Press, New York, 1981).
- [5] A.C. Eckbreth, Combust. Flame 39 (1980) 133.
- [6] A.C. Eckbreth and R.J. Hall, Comb. Sci. and Tech. 25 (1981) 175.
- [7] B. Attal, M. Pealat and J.P.E. Taran, CARS diagnostics of combustion, AIAA paper No. 80-0282 (1980).
- [8] I.A. Stenhouse, D.R. Williams, J.B. Cole and M.D. Swords, Appl. Optics 18 (1979) 3819.
- [9] R.J. Hall, Combust. Flame 35 (1979) 47.
- [10] M. Baranger, Phys. Rev. 111 (1958) 494; 112 (1958) 855.
- [11] A.C. Kolb and H. Griem, Phys. Rev. 111 (1958) 514.
- [12] R.G. Gordon, J. Chem. Phys. 45 (1966) 1649.
- [13] V. Alekseyev, A. Grasiuk, V. Ragulsky, I. Sobelman and F. Faizulov, IEEE J. Quant. Electr. QE-4 (1968) 654.
- [14] A.D. May, J.C. Stryland and G. Vargese, Can. J. Phys. 48 (1970) 2331.
- [15] R.J. Hall, J.F. Verdick and A.C. Eckbreth, Optics Comm. 35 (1980) 69.
- [16] R.G. Gordon, J. Chem. Phys. 44 (1966) 1830.
- [17] R.E.D. McClung, Adv. Mol. Relaxation and Interaction Processes 10 (1972) 83.
- [18] S.R.J. Brueck, Chem. Phys. Lett. 50 (1977) 516.
- [19] R.M. Lynden-Bell, Mol. Phys. 31 (1976) 1653.
- [20] T.E. Eagles and R.E.D. McClung, J. Chem. Phys. 59 (1973) 435.
- [21] S.I. Temkin and A.I. Burshtein, JETP Letters 24 (1976) 86; Chem. Phys. Lett. 66 (1979) 52.
- [22] M.A. Yuratich, Mol. Phys. 38 (1979) 625.
- [23] L.A. Rahn, A. Owyong, M.E. Coltrin and M.L. Koszykowski, The J -dependence of nitrogen Q -branch linewidths, Proc. VIIth Intern. Conf. on Raman spectroscopy, Ottawa, Canada (1980).
- [24] C.M. Roland and W.A. Steele, J. Chem. Phys. 73 (1980) 5919.

R82-954566-F

APPENDIX H

SOME APPLICATIONS OF GAS PHASE CARS SPECTROSCOPY

Some Applications of Gas Phase CARS Spectroscopy

J. F. Verdleck, R. J. Hall, J. A. Shirley, and A. C. Eckbreth
United Technologies Research Center, East Hartford, CT 06108

CARS (coherent anti-Stokes Raman spectroscopy) is a unique nonlinear optical technique made possible with high power lasers. It is a spectroscopic method which obeys Raman selection rules but is a much stronger effect than conventional Raman spectroscopy. Equally important, the CARS radiation emerges from the sample as a laser-like beam which may be completely collected, thus providing good discrimination against incoherent interfering radiation. For these reasons, CARS is finding numerous applications involving small volume, highly dilute samples such as biochemical substances in solution, or gas phase samples. The application of the CARS spectroscopic technique as a diagnostic method for measuring temperature and species concentrations in combustion systems of various types will be described in this paper.

Problems in Combustion Diagnostics

Combustion diagnostics is a fascinating and rewarding, yet very challenging, area for spectroscopic analysis. Although non-spectroscopic methods, such as mass spectrometry and gas chromatography, have contributed significantly to our understanding of combustion processes, spectroscopic methods offer several advantages over probe sampling methods. Some of the advantages of spectroscopic techniques are: (1) remote operation, (2) rapid measurement, (3) combustion process is not disturbed, (4) good spatial precision is possible, and (5) very high temperature capability. Each of these advantages will be illustrated by several CARS applications described below.

The advantages just listed apply equally well for CARS spectroscopic measurement of temperature. It should be emphasized, that in combustion, the single most important parameter to measure is the temperature. Given the initial conditions and the temperature at a point in a combusting system, the products, heat release, and other parameters can be estimated quite well. For this reason, highly accurate, spatially precise measurements of temperature are a necessity in understanding and controlling combustion processes. It is noted that thermocouple probes are limited to temperatures below ~ 2500 K. In contrast, spectroscopic methods have much higher limits, up to several thousand degrees for the case of nitrogen vibrational thermometry, as will be explained in detail. Moreover, spectroscopic temperature measurement is more accurate than thermocouple probe thermometry be-

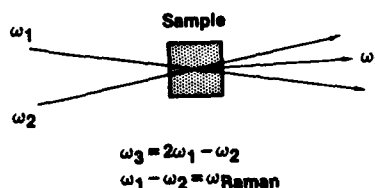


Figure 1. Basic Coherent Anti-Stokes Raman Spectroscopy (CARS) Process.

cause of the corrections which must be applied to thermocouples, namely, radiative and conduction corrections.

To gain an appreciation of why a powerful, wide-ranging technique such as CARS is required for combustion diagnostics, it is useful to list some examples of combustion systems which are investigated. Combustion devices can range from simple candle or Bunsen burner type flames to controlled detonations which occur in rockets or gun barrels. In between these extremes are home heating and industrial furnaces, gasoline and diesel engines, and gas turbine engines (both airborne and ground-based). These extremes represent very wide ranges of temperature and pressure. In an energy-scarce society, equally concerned about its environment, it is essential to design our combustion systems to be energy efficient and as nearly pollution free as we can. Reliable diagnostic methods are required to gain the knowledge necessary to achieve these goals, and CARS can help attain that knowledge. For more detailed discussions of these types of CARS applications, the reader may check references (1-3).

CARS Essentials: Experimental

An introduction to the CARS technique is made by first describing the CARS experiment and the apparatus required. The CARS theory will be described in the following section. CARS is a coherent, nonlinear-optical process in which light waves of different frequencies, ω_1 and ω_2 , are mixed together in a material medium (liquid, gas, or solid) to generate a new frequency, ω_3 , which appears in a coherent, laser-like beam. This is shown by the simple sketch of Figure 1. When the frequency difference between the two input frequencies corresponds to a Raman-active molecular vibration or rotation

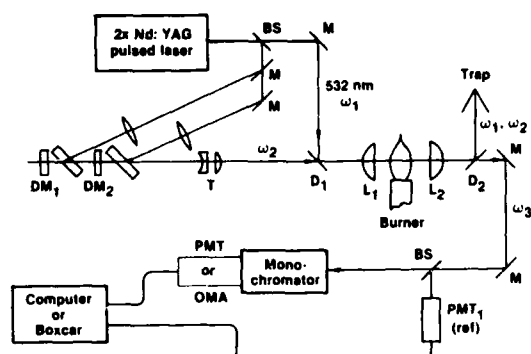


Figure 2. CARS experimental arrangement for flame measurements.

(or electronic transition), then the CARS effect is strong and easily detected. Because the CARS process is a coherent nonlinear-optical process, laser beams are required to provide the proper phase of waves in space and time, and the intensity to enhance the nonlinear aspect of the process. Usually, high-peak power pulsed lasers are employed to generate CARS, but lower power cw lasers have been used in a few cases (4).

At the United Technologies Research Center (UTRC), CARS experiments are based upon a frequency-doubled neodymium:YAG laser, hereafter simply referred to as 2X Nd:YAG. The frequency-doubled output occurs in the visible at 532 nm and is used for one of the CARS input frequencies, ω_1 . The second CARS frequency, ω_2 , is generated from a dye laser driven by a portion of the 2XNd:YAG beam. Thus, the dye laser pulses are nearly synchronous with the 2XNd:YAG pulses. The 2XNd:YAG pulses are ~ 10 nanoseconds (10^{-8} sec) in duration and occur at a repetition rate of 10 Hz. The high repetition rate is advantageous because it permits high data rate acquisition, and for adjusting optics for critical alignment of the CARS input beams. The peak power in a 2XNd:YAG pulse is ~ 10 MW; the average power is ~ 2 W.

The arrangement of the lasers is shown in Figure 2. A portion of the 2XNd:YAG radiation (532 nm) is picked off with a beamsplitter to pump the oscillator and amplifier stages of the dye laser. The 532 nm radiation is ideally suited to pumping laser dyes in the 550–700 nm range, particularly rhodamine type dyes which can exhibit conversion efficiencies of more than 30%. The dye lasers are of quite simple construction, utilizing either spectrophotometer cells or homemade dye cells. The dye solution flows through the cells to prevent heat buildup and subsequent optical distortion of the laser beam. The 532 nm is directed nearly parallel to the dye laser optical axis (defined by the dye laser mirrors DM₁ and DM₂). This so-called end pumping (or axial pumping) yields good dye laser beam quality and good conversion efficiency. The purpose of the Galilean telescope (negative lens-positive lens pair, T) in the dye laser beam is to insure that the dye beam will focus at the same region as the 532 nm beam.

The two laser beams are combined on a dichroic (two-color) mirror, D₁. In this case the dye laser frequency, ω_2 , also termed the Stokes frequency, passes through the dichroic mirror while the 532 nm beam, or pump frequency, ω_1 , is reflected by it. This type of configuration is called collinear phase matching and will be compared to other beam configurations below. The collinear beams are focused (by lens L) through the flame or combustion system of interest and recollimated by a similar lens. The newly generated CARS frequency, ω_3 ($=2\omega_1 - \omega_2$), can be separated from the ω_1 and ω_2 frequencies by use of

• Spectrum

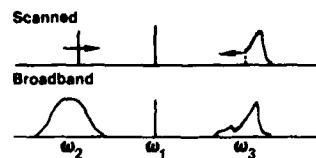


Figure 3. Generation of CARS spectra.

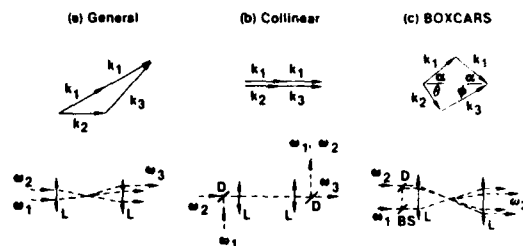


Figure 4. CARS phase-matching techniques.

another dichroic, D₂, which transmits blue light, but not green (532 nm), or dye laser light (yellow to red). Dispersing prisms can also be used to isolate the CARS beam. The CARS beam is then directed to a monochromator for spectral analysis, from which temperature and concentration information is extracted as described in the theoretical section below. A portion of the CARS beam is picked off by a beam splitter and detected by a photomultiplier-filter combination (PMT-1). The detector serves as a monitor of the total (spectrally wideband) CARS signal. This monitor can be used as a normalizing signal and is also used to adjust optical components for maximum CARS signal.

Spectral analysis of the CARS signal is obtained by scanning with a monochromator and processing the output photomultiplier signal, PMT-2 in Figure 2, with a laser triggered electronic gate, a so-called boxcar averager. A more useful alternative is to employ an optical multichannel analyzer (OMA)¹ which can capture the entire CARS spectrum, with gain, from each laser shot. This information is sent to a computer for storage, analysis, and display. This latter technique offers the potential for measuring temperature and concentration from a single, 10 nanosecond, laser pulse. Both methods of spectral analysis are in use at UTRC and have been described in several references (3, 5–6). Several examples of CARS spectra are given below.

It must be mentioned that the method of generating CARS spectra described here is called "broadband CARS" or sometimes "multiplex CARS." It is only one of several different techniques. One other method, used for high resolution CARS spectroscopy (8, 9) makes use of a tunable, narrowband dye laser. The CARS spectrum is generated by combining the ω_1 and ω_2 laser frequencies, and while tuning ω_2 , detect the amplitude changes in the CARS signal (whose frequency, ω_3 , is changing). These two methods are contrasted pictorially in Figure 3. For combustion diagnostics, the broadband CARS method appears more suitable because it generates a complete spectrum with each laser pulse. Single-shot thermometry, with the aid of an OMA¹ and computer, is then possible, as mentioned previously.

For the broadband CARS method, the dye laser is operated wideband, that is, with appropriate mirrors which generate laser output which has a large bandwidth (full width at half maximum) of ~ 100 cm⁻¹, or greater. The center of this spectral band should be located at $\omega_2 = \omega_1 - \omega_{\text{RAM}}$, where ω_{RAM} corresponds to the desired Raman frequency shift. The desired frequency is obtained by appropriate dye selection and concentration adjustment.

¹ OMATM, Optical Multichannel Analyzer, is a registered trademark of PAR Co., Princeton, N. J.

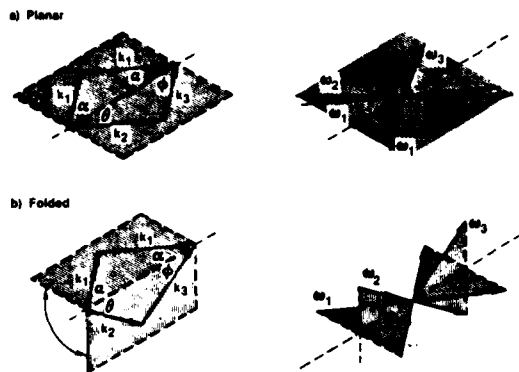


Figure 5. Illustration of folded BOXCARS geometry.

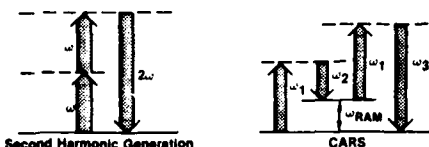


Figure 6. Comparison of nonlinear optical processes.

The CARS effect requires that the proper relationship exists between the input frequencies, ω_1 , ω_2 , and the CARS frequency, ω_3 , namely: $\omega_3 = 2\omega_1 - \omega_2$. This is a conservation of energy requirement. A similar conservation of linear momentum requirement demands that the laser beams travel in certain directions with respect to each other. Satisfying these directional requirements is known as phase-matching. The relationships which must be satisfied for maximum CARS generation are shown in Figure 4. The wave-vector k_i has magnitude $\omega_i n_i / c$ (n_i is the refractive index at frequency ω_i), and direction given by the propagation direction of the laser beam. Note that the phase-matching condition is a vector sum as illustrated in Figure 4a. In gases, the refractive index varies little with frequency which means that the collinear condition, Figure 4b, satisfies the phase matched condition. Although it is the easiest configuration to implement and yields high intensity CARS signals, collinear operation can suffer from poor spatial resolution. The reason for this is that the ω_1 and ω_2 input beams interact and generate CARS over a considerable sample length, dependent upon the focal length of the lens used. For example, a 10-cm lens yields a sample length of ~ 0.07 cm, whereas a 100-cm lens (which might be mandatory for some cases) yields a sample length of 7.3 cm (3). Clearly this length is much too large and could sample both hot and cold regions of a combusting system.

Recognizing this, Eckbreth (9) has shown how a phase-matched, crossed-beam configuration leads to excellent spatial resolution, because CARS is generated only from the region of beam crossing. The method has been termed BOXCARS, Figure 4c, from the shape of the phase matching diagram. Resolution of a millimeter or less is easily achieved, even for relatively shallow angles between input beams. BOXCARS has been employed in this laboratory to map out the temperature distribution, including both the axial and radial variation, in a conventional diffusion flame (10). It is not mandatory to confine phase matching to a plane. One type of three-dimensional phase matching, illustrated in Figure 5, is called "folded BOXCARS" for obvious reasons. An outstanding advantage of folded BOXCARS is that the ω_3 CARS beam is completely separated from the ω_1 and ω_2 beams without using a dichroic mirror or a prism. This allows one to examine very small Raman shifts such as found in rotational

CARS spectroscopy. Folded BOXCARS has been utilized at UTRC for nitrogen and air rotational CARS spectra in flames (11). Several other phase matching schemes for CARS exist (12, 13) which are not discussed here because of space limitations.

CARS Essentials: Theoretical

In this brief section an elementary presentation of CARS theory is given which provides a basis for temperature and concentration measurements. More complete descriptions of the theory may be found in references 14-16.

Perhaps an appropriate place to begin is to draw a comparison with a nonlinear optical process which may be familiar, namely second-harmonic generation (frequency doubling). This second-order (because it is quadratic in laser intensity) effect converts laser radiation of frequency ω into radiation of frequency 2ω . One way of explaining this effect is to state that two photons are absorbed simultaneously and a single photon of twice the initial energy is emitted. The absorption and emission occurs through "virtual energy states;" real energy states are not directly involved. Figure 6a presents this explanation pictorially. Figure 6b shows the more complicated third-order process of CARS. CARS involves the mixing of three light waves of frequency ω_1 , ω_1 , and ω_2 to generate a fourth beam at frequency ω_3 . The intensity of the CARS beam is given by

$$I_3 = KI_1^2 I_2 |\chi^{(3)}| z^2 \quad (1)$$

The third-order dependence of laser intensity is readily seen (I_1 , I_2 , and I_3 are the intensities at frequencies, ω_1 , ω_2 , and ω_3 , respectively). $\chi^{(3)}$ is the third-order nonlinear susceptibility, a macroscopic parameter which relates the electric fields of the incoming light waves to the polarizations (charge distortion) in the macroscopic medium. $\chi^{(3)}$ depends on both nuclear and electronic motions of the molecules which compose the medium (liquid, solid, or gas). The term z is an interaction length over which the nonlinear process is strongly generated. K is a constant.

$\chi^{(3)}$ can be separated into the terms shown in eqn. 2.

$$\chi^{(3)} = \chi' + i\chi'' + \chi^{nr} \quad (2)$$

The first two terms account for the resonant portion of the susceptibility which relates to nuclear motion; hence, is resonant with certain (Raman active) vibrational-rotational frequencies. χ^{nr} accounts for the electronic contribution from all molecular species present.

The resonant susceptibility depends upon individual molecular transitions in a complicated fashion given by eqn. (3).

$$\chi' + i\chi'' = \frac{K_2}{\omega_2^4} N \Delta_j \left(\frac{\partial \sigma}{\partial \Omega} \right) \left(\frac{1}{2\Delta\omega_j - i\Gamma_j} \right) \quad (3)$$

K_2 is a constant, ω_2 is the Stokes frequency, N the molecular number density, Δ_j is a population difference factor (essentially the Boltzmann factor from which temperature is obtained), $(\partial \sigma / \partial \Omega)_j$ is the differential Raman scattering cross-section, $\Delta\omega$ is the detuning from resonance (i.e., $\omega_1 - \omega_2 - \omega_{\text{Ram}} = 0$ at resonance), and finally, Γ_j is the Raman linewidth of the j th transition. Several important points should be made about eqn. 3. As mentioned parenthetically, temperature information is contained in the Δ_j term; concentration from the number density N . In order to extract this information, it is mandatory to interpret experimental CARS spectra by direct comparison with computer generated model spectra. This further implies that all the molecular data, Raman cross-sections, linewidths (including temperature and quantum number dependences) should be known. Note that when $\Delta\omega_j = 0$, the resonant portion of $\chi^{(3)}$ is measured; hence, one is dealing with all the terms of eqn. (4)

$$|\chi^{(3)}|^2 = (\chi')^2 + 2\chi'\chi'' + (\chi'')^2 + (\chi^{nr})^2 \quad (4)$$

AD A124 304

CARS DIAGNOSTICS OF HIGH PRESSURE COMBUSTION(U) UNITED
TECHNOLOGIES RESEARCH CENTER EAST HARTFORD CT
J H STUFFLEBEAM ET AL. NOV 82 R82-954886-F

2/2

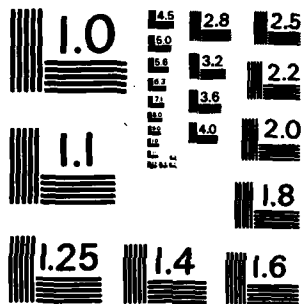
UNCLASSIFIED

ARO-16124.6-CH DAAG29-79-C-0008

F/G 21/2

NL

			■ ■ ■ ■	■ ■	■ ■ ■ ■							END DATE FILMED 3 83 DTIC
--	--	--	---------	-----	---------	--	--	--	--	--	--	---------------------------------------



MICROCOPY RESOLUTION TEST CHART
NATIONAL BUREAU OF STANDARDS-1963-A

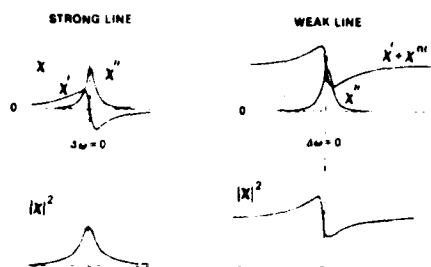


Figure 7 Limiting cases of CARS spectra

This equation is best understood by referring to Figure 7 where the strong line and weak line limits for CARS spectra are depicted. In the strong line limit, χ'' is negligible compared to the resonant portion, χ' , and the spectrum reflects the character of (χ') . In the weak limit χ'' cannot be neglected and contributes a background baseline upon which the resonant CARS contribution appears as a modulation. The limit where the modulation can just be observed gives the limit of detection of the desired species in the particular environment which yields that non-resonant background (contributed by all species present).

The non-resonant background is generally considered a nuisance, and techniques have been designed to suppress or eliminate it (discussed below). However, in many cases of interest in combustion, the shape of the CARS signal against the χ'' background provides for easily interpreted concentration measurements, without the need of intensity measurements. Examples of this method will be shown later.

CARS Spectra: Temperature Measurements

In this section, CARS spectra, both experimental and computer model predicted, will be presented for several different molecules. The emphasis is given to nitrogen CARS spectra because nitrogen is present, in quantity, in air-supported combustion. Moreover, the necessary spectroscopic constants are known quite accurately for nitrogen. The change in the spectral shape with temperature will be demonstrated for nitrogen and other molecules as well. The effect of high pressure on CARS spectra will be treated briefly and illustrated with experimental results. Applications of CARS temperature measurements in real combustion systems will be demonstrated by an example from this laboratory.

Figure 8 shows a set of computer-generated spectra of nitrogen for typical experimental conditions over a temperature range of 300 to 2100 K, taken in 300 K increments (17). The 300 K room temperature spectrum is a narrow line with peak at $\sim 21126 \text{ cm}^{-1}$, exhibiting no rotational structure at moderate resolution. As the temperature increases, rotational structure begins to appear. The CARS spectrum shown here is for the Q-branch ($\Delta J = 0$), $v = 0$ to $v = 1$ transition. At about 1200 K the hot band ($v = 1$ to $v = 2$) transition begins to appear. At 1500°, the hot band has a peak height of about 0.1 of the fundamental, and reaches about 0.4 of the fundamental at 2100°. Clearly, there is considerable change in the CARS spectrum with temperature, and from this change the temperature in a combusting system could be "eyeballed" to about $\pm 100^\circ$. As Figure 9 demonstrates, if a least square computer fit to the experimental data is made, temperature can be measured to better than 1% precision. What is shown in Figure 9 is the computer least squares fit (dotted line) superimposed on an experimental CARS spectrum (solid line) from a premixed CH_4/Air flame, whose temperature was independently measured by sodium line reversal (18). The agreement is excellent.

CARS has been used to determine temperatures in highly sooting flames (10). These measurements are significant,

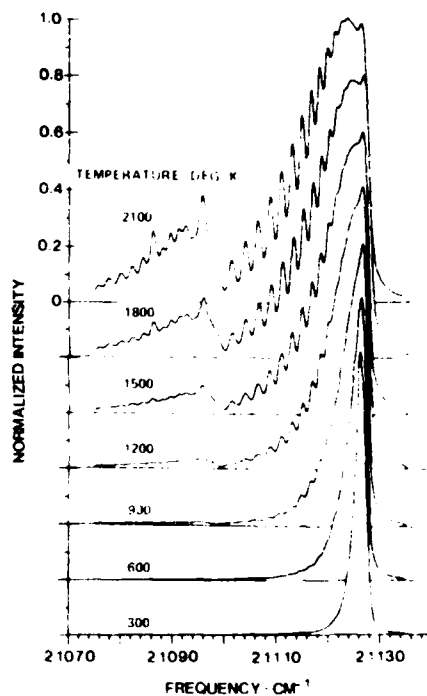


Figure 8 Variation of nitrogen CARS spectra with temperature

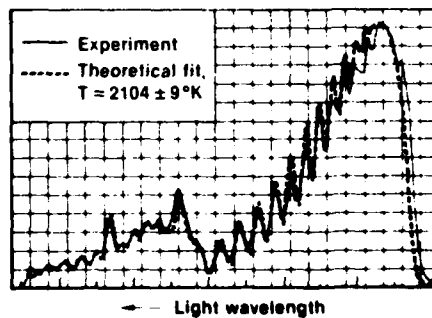


Figure 9 Comparison of experiment and theory for N_2 at 2100 K

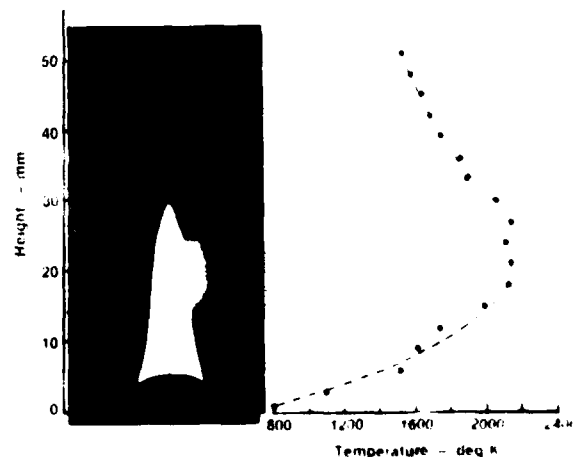


Figure 10 CARS temperature measurement along axis of flame

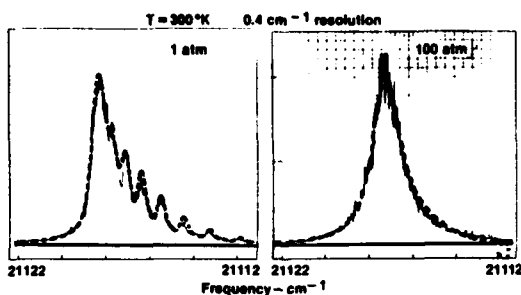


Figure 11. CARS spectra of nitrogen at 1 and 100 atm.: solid line; experimental, dotted line; theoretical.

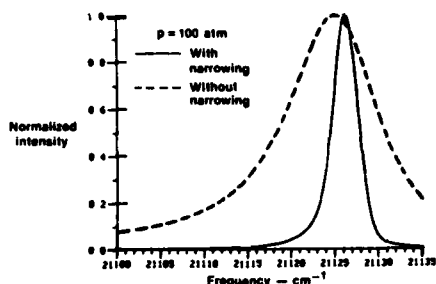


Figure 12. Model illustration of CARS linewidth with and without collisional narrowing.

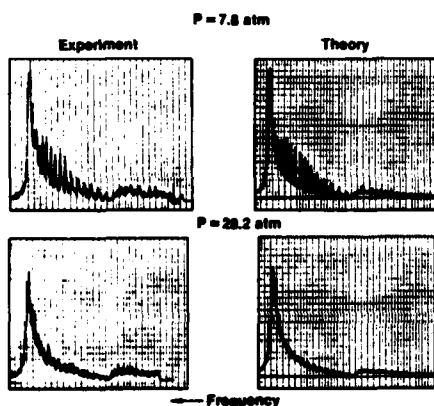


Figure 13. Pressure variation of high temperature CARS spectra.

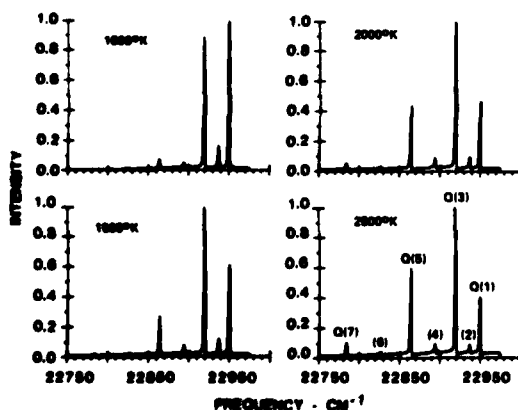


Figure 14. Hydrogen CARS spectra as a function of temperature: model predictions.

because practical combusting systems often operate under sooting conditions which preclude conventional optical techniques, such as spontaneous Raman scattering. Figure 10 shows the axial variation of temperature in a sooty propane laminar diffusion flame as found by the BOX-CARS method. The spatial resolution in these experiments was about 0.3 mm by 1.0 mm, which, as the temperature profile demonstrates, is necessary for exploring flame structure.

Pressure Effects in Nitrogen CARS Thermometry

In order to achieve maximum utility as a diagnostic tool, it is necessary to extend CARS measurements into the high pressure regime. Examples of important practical combustion systems which operate at elevated pressures are internal combustion engines (both gasoline and diesel), gas turbine engines and rockets. The pressure encountered in such systems ranges from a few atmospheres to well over 100 atm. If the theoretical CARS analysis which has been used to successfully explain one atmosphere CARS flame spectra were employed at very high pressure it would predict that the overall bandwidth of the spectrum would increase linearly with pressure. It would also predict that the $l = 2$ "Hot" band would merge with the fundamental band and therefore would be lost as a sensitive indicator of temperature.

The effect of pressure on N_2 CARS spectra has been investigated experimentally and theoretically over the pressure range of one to 100 atm. (6). A similar study has been performed by Roland and Steele (19) for pressures up to 30 atm. The experimental studies of Hall, Verdieck, and Eckbreth show that after an initial narrowing of the Q-branch band over the first five to ten atmospheres, the width of the band remains constant with increasing pressure to 100 atm, the width of the band remains constant with increasing pressure to 100 atm. Figure 11 shows scanned CARS Q-branch spectra at one and 100 atm. The solid line in Figure 11 is the experimental spectrum obtained from collinear CARS, scanned with a monochromator with spectral width of $\sim 0.4 \text{ cm}^{-1}$. The dotted line represents the theoretical fit of the computer model. The collapse of the resolved rotational structure to the symmetric band is termed "collision-induced band narrowing" or "motional narrowing." It is a phenomenon observed in NMR (20) and in Raman spectroscopy (21). Figure 12 illustrates the importance of collisional narrowing through theoretical comparison of a collision-narrowed line with one calculated without narrowing. For the latter case a very broad line, $\sim 10 \text{ cm}^{-1}$, results. The effect of pressure on high temperature has also been investigated, some results of which are shown in Figure 13 (2). Experimental results are shown for $\sim 1600 \text{ K}$ for pressures of ~ 8 and $\sim 28 \text{ atm}$, along with model spectra. It is noted that although the high J rotational structure collapses between these pressures, the "hot" band persists; hence, the potential for temperature measurement still exists. High pressure, high temperature CARS spectra must be examined more thoroughly in order to assess CARS diagnostics for high pressure applications.

CARS Spectra of Other Molecules

Several other molecules of interest to combustion studies have been examined in this laboratory; CARS spectra have been recorded for hydrogen, oxygen, carbon monoxide, water, carbon dioxide, and methane (22-23). Of these, hydrogen and water CARS spectra will be discussed with regard to temperature measurement.

Computed CARS spectra of hydrogen are shown in Figure 14 for four temperatures. Because the vibrational-rotational constant, α , is so large in hydrogen ($\alpha = 2.993$, compared to $\alpha = 0.0187$ for nitrogen), the spectrum is simple (few lines), and quite spread out (over nearly 200 cm^{-1}). The alternation in intensity due to nuclear spin statistics is quite apparent. Recall that the ortho/para forms of hydrogen bear statistical weights of 3:1. Because population differences get squared in

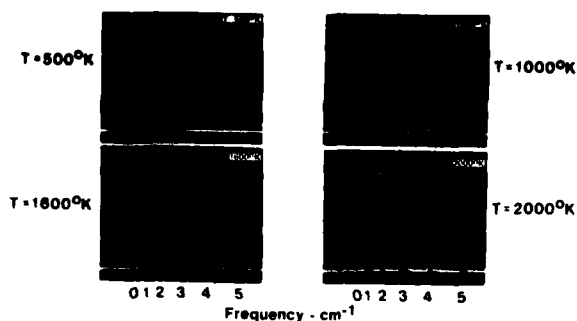


Figure 15. Experimental hydrogen CARS spectra versus temperature.

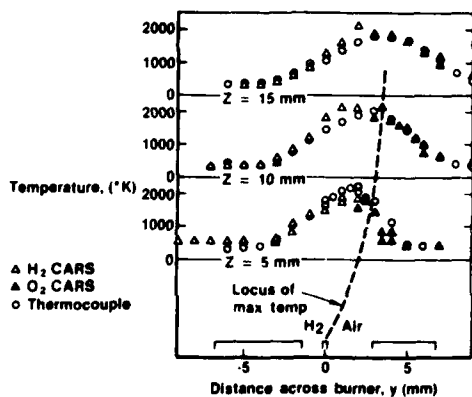


Figure 16. CARS mapping of temperature in a H_2/O_2 flame.

a CARS spectrum (as χ is squared), the difference in adjacent lines is quite dramatic in CARS spectra. For this reason, H_2 should serve as a good thermometric probe molecule. Experimental CARS spectra for H_2 are shown in Figure 15, as recorded with an OMATM. The spectra were recorded from an H_2 /Air diffusion flame, with temperatures found from comparison of peak height ratios of $Q(1)$, $Q(3)$, and $Q(5)$. Temperature profiles of a slot shaped H_2 /Air diffusion flame were obtained from H_2 and O_2 CARS spectra (O_2 CARS spectral temperatures are obtained in a fashion similar to that for N_2) and are displayed in Figure 16. The CARS-derived temperatures are compared with a radiation-corrected thermocouple. The agreement is quite good. A detailed discussion of the hydrogen CARS studies is found in reference 22.

Water is a major product of air-supported combustion of hydrogen-containing fuels, and thus is available as a thermometric probe molecule, if present in sufficient quantity. Measurement of water concentration as a function of distance could yield chemical kinetic information and a better understanding of the combustion process.

H_2O is an asymmetric top molecule with three vibrational modes, of which the ν_1 symmetric stretch is strongly Raman allowed, with a Raman shift of 3657 cm^{-1} . Because it is an asymmetric top, the rotational structure is complex and the rotational energy levels cannot be expressed in closed form. However, the structure of the Q-branch of the ν_1 is not too complex and the H_2O CARS spectrum has been modeled by Hall et al., (23). Figure 17 shows the comparison between computed and experimental CARS spectra of water in a heated cell at 500 C. Raman linewidth data were not available for this calculation. An assumed value of 0.5 cm^{-1} , independent of J , produced the good agreement shown. A similar comparison for H_2O in a 1700 K premixed methane/air flame

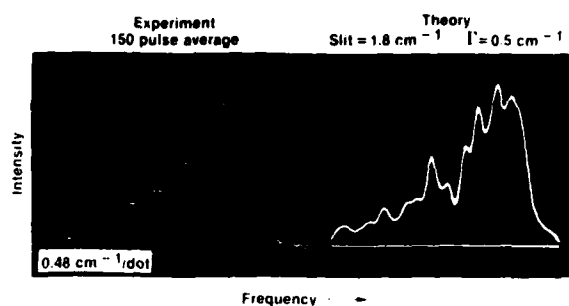


Figure 17. CARS water spectra at 773 K

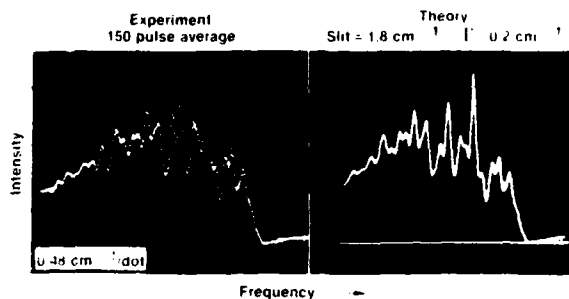


Figure 18. CARS water spectra at 1700 K

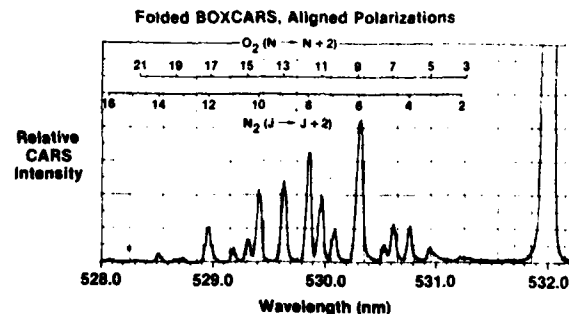


Figure 19. Rotational CARS spectrum of air using folded BOXCARS

is shown in Figure 18. Here the Raman linewidth was assumed to be 0.2 cm^{-1} . In these calculations, nearly one thousand vibrational-rotational Q-branch transitions were included to produce the computed spectrum shown. Because the shape of the CARS water spectrum is quite sensitive to temperature, the water molecule offers the potential for combustion thermometry over a wide range of temperature.

Pure Rotational CARS Spectroscopy

Pure rotational CARS may offer advantages over vibrational-rotational CARS at high pressure because adjacent rotational lines are better separated (by 8 cm^{-1} in N_2), than in the Q-branch spectrum. For the same reason—well-resolved spectral lines—rotational CARS may offer advantages at low temperatures, say, below 800 K.

Pure rotational CARS presents the classic problem that pure rotational Raman spectroscopy does; the frequency shifts are small, and the CARS radiation is difficult to separate spectrally from the input beams. One method used in conventional Raman is to employ a double (or triple) monochromator. At UTRC, the spectral separation of the CARS beam is achieved by complete spatial separation of the beams through use of the three-dimensional phase-matching method,

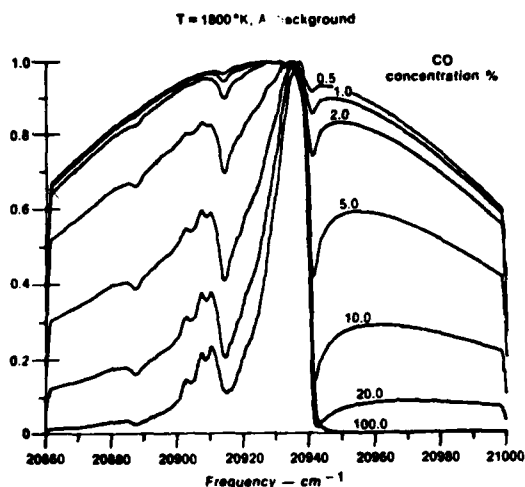


Figure 20. Concentration variation of CO CARS spectra at 1800 K, model calculation.

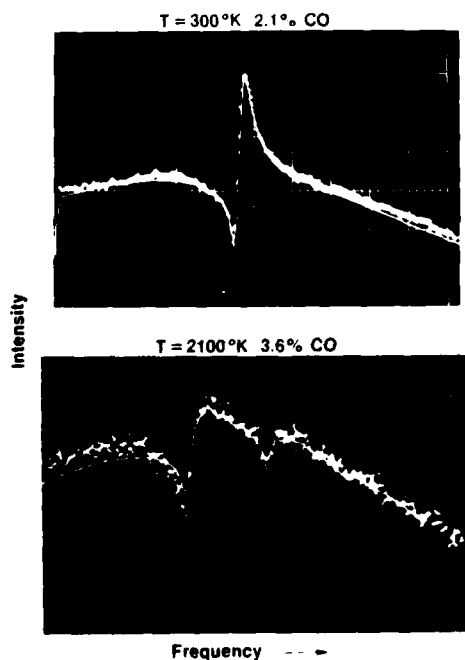


Figure 21. Theory/experiment comparison for CO CARS spectra at two different temperatures and different concentrations.

"folded BOXCARS" (12), described earlier. Referring back to Figure 5, it can be seen that the CARS beam, ω_3 emerges well separated angularly from the input laser beams and is isolated easily from them by simply masking and trapping. In this manner, the CARS pure rotational spectrum of room air (300 K, and 1 atm.) was obtained by scanning the ω_3 radiation (Fig. 19). This experimental spectrum is in good agreement with model calculations (11).

Species Concentration Measurements by CARS

CARS measurements of species concentration in combustions systems are made by either of two quite different methods; from the absolute intensity of the spectrally-integrated resonant CARS signal, or in certain concentration ranges, from the shape of the spectrum. The latter case, which

will be discussed here in detail, results when the resonant signal interferes with the background. At very low concentrations, each method fails because the resonant CARS signal is completely dominated by the nonresonant signal. However, there are CARS techniques which have demonstrably reduced or suppressed the nonresonant background. One of the most useful of these methods is polarization-sensitive CARS, which yields nearly complete elimination of the background. But a price must be paid for the background suppression, one which can reduce the resonant signal considerably. The background suppression techniques usually employ integrated intensity measurements to make concentration determinations. Because the absolute strength of the signal is difficult to measure, reference cells (which furnish a calibration) must be employed. This adds considerable experimental difficulty. For these reasons, the method of concentration measurement based upon spectral shapes is emphasized in this paper. Both methods have been evaluated critically in a recent paper by Eckbreth and Hall (24).

Concentrations from Spectral Shapes

CARS offers the unique capability of measuring species concentration, over a limited range, solely from the shape of the CARS spectrum. This remarkable situation applies in the weak signal limit (Fig. 7) where the resonant and nonresonant contributions are comparable. This behavior is best understood by reference to Figure 20, which displays a computer-generated set of carbon monoxide CARS spectra at 1800 K. The concentration ranges from 0.5% to 100%; however, the useful range over which measurements can be made is probably only to 30% at the high end. Beyond this value some sort of reference is required to scale the intensity. Below 0.5% the resonant signal disappears into the baseline.

As an example of spectral shape fitting for concentration measurement, the experimental CARS spectrum of 2.1% CO, in argon at 300 K, is shown as the dotted line in Figure 21. The thin solid line is the computer-generated CARS spectrum for the same concentration. The agreement is quite good. A similar comparison is shown also in Figure 21 for the case of CO in a CH_4/O_2 -Ar flame doped with CO. The flame temperature was 2100 K. The experimental CARS spectrum is compared with a theoretical spectrum for 3.6% CO, a value determined by a quartz microprobe and NDIR CO detector (24). Again the agreement is good. Similar measurements by the spectral shape method have been made for measuring low concentrations of water vapor as well. Before closing the discussion of concentration measurement by spectral shape, it must be pointed out that the temperature, and the nonresonant susceptibility must be known for a determination of concentration of the desired species. Because the nonresonant susceptibility changes little (10-15%) from reactants to products, intelligent estimates can be made for χ'' in a combustor, knowing the location and temperature at that location. From the experiments shown, it is clear that concentration measurement by spectral shape fitting is a viable technique, and, where applicable, should enjoy numerous applications.

Background Suppression

In the most general case, CARS is the mixing of three input beams which can have three different frequencies and three different polarizations. Usually, two input frequencies are chosen to be the same frequency ω_1 . Often the polarizations are selected to be parallel as well. However, because the resonant and nonresonant susceptibilities have different responses to certain choices of input polarizations, it is possible to dramatically reduce the nonresonant CARS signal by use of a polarization analyzer in the CARS beam. Figure 22 illustrates this technique applied to CO in a CO/air-Ar flame. On the left is shown the BOXCARS signal using aligned polarizations (polarizations of all three input beams parallel).

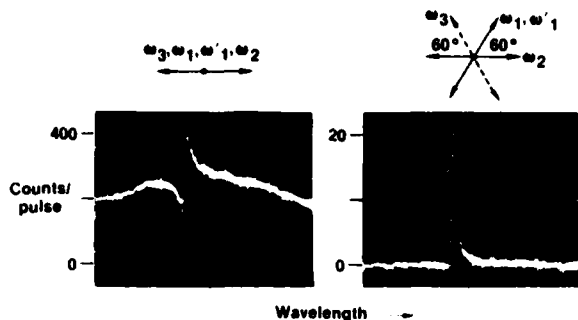


Figure 22. Polarization orientation suppression of background susceptibility.

BOXCARS Setup in Jet Burner Stand

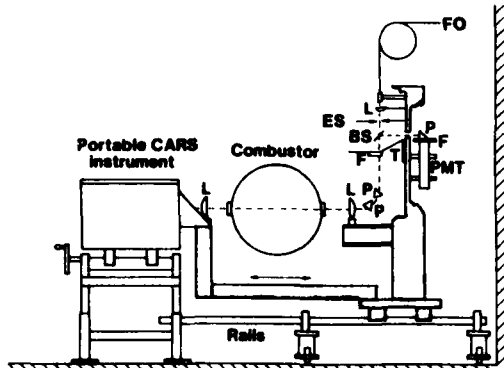


Figure 23. Experimental scheme for CARS measurements in a combustor.

A signal of the "weak signal" type is obtained as discussed in the previous section. In contrast, if the polarizations of the input beams are arranged in the pattern shown, the resultant signal is of the "strong signal" limit. The nonresonant contribution is now small compared to the resonant contribution. Earlier it was stated that a price must be paid for this background suppression. Because of this signal loss, polarization suppression of the nonresonant background will be less useful than the spectral shape method when the signal is weak, i.e., photon limited. For strong CARS signals, polarization background suppression is a useful method and has been applied successfully by several workers (25, 26).

Practical Applications

Several applications of CARS in practical combustion devices, mainly CARS temperature measurements, are listed. A detailed description of CARS measurements at UTRC on a gas turbine test combustor is illustrated in some detail.

Apparently, the first application of CARS measurements on a combustion device was performed by Taran and co-workers at ONERA in 1978 (27). Temperature and concentration measurements of N_2 and CO_2 were made in a simulated turbo machine combustor burning kerosene. More recently, this group has made measurements in a gas turbine combustion can (28). Similar measurements at Wright-Patterson AFB have been performed in a bluff-body stabilized diffusion flame (29).

In experiments at UTRC, Eckbreth (30) used BOXCARS to make measurements in a 50-cm diameter combustion test tunnel fitted with a variety of burners, one of which was a gas turbine (JT-12) combustor. CARS temperature measurements from N_2 were made in the primary zones of flames and in the exhaust. Both gaseous (propane) and liquid fuels (Jet A) were used.

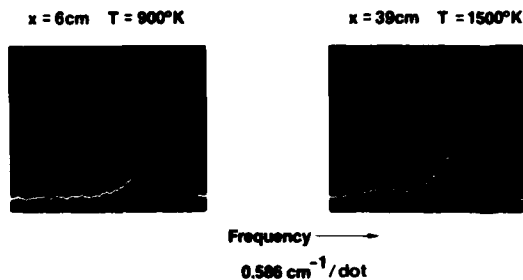


Figure 24. CARS temperature measurements in a swirl burner with Jet A fuel.

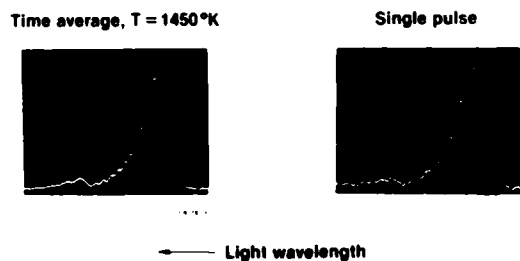


Figure 25. Comparison of single pulse CARS N_2 spectrum with averaged spectrum in the swirl burner.

The experimental layout is shown in cross-section in Figure 23. The CARS lasers, along with the necessary optics, are contained in a box which is placed near the test combustor tunnel. Lenses focus and collect the BOXCAR beams through the tunnel windows. (It should be noted in passing that the flame in the test tunnel is extremely luminous, so luminous that most conventional optical methods would fail.) The laser beams are manipulated in a receiver which spectrally disperses the beams and isolates the CARS signal. A reference PMT observes a small fraction of the CARS signal and serves to monitor optimal alignment of optics. The CARS signal is piped out to a nearby control room through a 20-m long fiber optic. The control room furnishes a much quieter environment for delicate instrumentation, such as the spectrometer and the optical multichannel analyzer (which can be very micro-ponic).

As examples of CARS measurements, Figure 24 displays averaged CARS N_2 spectra at two locations downstream of the burner exit face. These CARS spectra were averaged on the OMATM for 10–15 sec which corresponds to 100–150 laser pulses. The spectrum at $X = 6$ cm was made through the fuel spray; hence, the relatively cool temperature, the second location is much hotter. Figure 25 demonstrates that temperature can be determined from a 10^{-8} sec, single pulse spectrum. Comparison is made with a 130 pulse averaged spectrum. Although the single pulse spectrum displays photon statistics noise (shot noise), it is of sufficiently good quality to allow instantaneous temperature measurement.

In the UTRC CARS Laboratory, in East Hartford, a multipurpose portable CARS apparatus is being assembled for use at the Government Products Division (GPD) of Pratt & Whitney Aircraft. When complete, measurements will be made in the exhaust of a production run 1130 (a modified F-100) gas turbine engine. In addition to N_2 temperature measurements, the concentration of water, carbon dioxide, and oxygen will be determined, as well as some measure of total unburned hydrocarbons. These measurements are scheduled to take place before the end of 1981.

CARS measurements in an internal combustion engine have been made by Stenhouse et al. (32). The CARS input laser

pulses were synchronized with the engine cycle to generate the CARS spectrum in time steps, but at a known point relative to the engine cycle timing. Both nitrogen and propane CARS spectra were obtained and the temperature determined.

More recently, workers at Ford Motor Company Research have measured temperature and carbon monoxide concentration in a research scale, single-cylinder engine (33). A special type of noncollinear phase matching was employed which achieved a spatial resolution of ~ 2 mm along the beam and $100 \mu\text{m}$ transverse to the beam. Single pulse, 10^{-8} second, CARS spectra were obtained, from which temperature was determined. CARS measurements also have been made in a commercial diesel engine (34) at Komatsu Corporation. Further measurements in internal combustion engines using CARS are scheduled at many laboratories throughout the world.

Interest in CARS measurements in practical combustion devices is increasing rapidly as illustrated by the many laboratories throughout the world applying CARS to internal combustion engines, furnaces, gas turbine combustors, and propellant burning for propulsion and ballistics. The equipment necessary for CARS is commercially available, and the technique can be engineered for application in noisy environments, as illustrated by the previous discussion. The capabilities of the CARS technique will be improved by experimental modifications and from increased computer data processing development (including better modeling of spectra). Based upon comparison with conventional diagnostic methods, CARS should greatly increase our understanding of fundamental and applied combustion processes.

Acknowledgment

The authors would like to thank NASA Langley, the Army Research Office, Project SQUID, the Air Force Aeronautical System Division, and the Environmental Protection Agency for supporting various portions of this work.

Literature Cited

- (1) Eckbreth, A. C., Bonczyk, P. A., and Verdieck, J. F., *Prog. Energy Combust. Sci.*, **5**, 253 (1979).
- (2) Shirley, J. A., Hall, R. J., Verdieck, J. F., and Eckbreth, A. C., *New Directions in CARS Diagnostics for Combustion*, AIAA Paper No. 80-1542, 1980.
- (3) Hall, R. J. and Eckbreth, A. C., Coherent Anti-Stokes Raman Spectroscopy (CARS): Application to Combustion Diagnostics. In "Laser Applications," Ed. R. K. (Editor), Academic Press, New York, 1981.
- (4) Barrett, J. J. and Begley, R. F., *Appl. Phys. Lett.*, **27**, 129 (1975).
- (5) Eckbreth, A. C., Bonczyk, P. A., and Verdieck, J. F., Investigation of CARS and Laser-Induced Fluorescence for Practical Combustion Diagnostic. Report EPA-600/7-80-091, May 1980.
- (6) Hall, R. J., Verdieck, J. F., and Eckbreth, A. C., *Opt. Comm.*, **35**, 69 (1980).
- (7) Farrow, R. L., Mitchell, R. E., Rahn, L. A., and Mattern, P. L., AIAA Paper No. 81-0182, AIAA, New York, 1981.
- (8) Attal, B., Schnepf, O. G., and Taran, J. P. E., *Opt. Comm.*, **24**, 77 (1978).
- (9) Eckbreth, A. C., *Appl. Phys. Lett.*, **32**, 421 (1978).
- (10) Eckbreth, A. C., and Hall, R. J., *Combust. Flame*, **36**, 87 (1979).
- (11) Shirley, J. A., Hall, R. J., and Eckbreth, A. C., *Opt. Lett.*, **5**, 380 (1980).
- (12) Marko, K. A. and Rimai, L., *Opt. Lett.*, **4**, 211 (1979).
- (13) Laufer, G. and Miles, R. B., *Opt. Comm.*, **28**, 250 (1979).
- (14) Nibler, J. W., Shaub, W. M., McDonald, J. R., and Harvey, A. B., Coherent Anti-Stokes Raman Spectroscopy, in Durig, J. R., (Editor), "Vibrational Spectra and Structure," Vol. 6, Elsevier, Amsterdam, 1977, pp. 173-225.
- (15) Druet, S., and Taran, J. P. E., Chemical and Biological Applications of Lasers. Moore, C. B., (Editor), Academic Press, New York, 1979.
- (16) Nibler, J. W. and Knighten, G. V., Coherent Anti-Stokes Raman Spectroscopy, in Topics in Current Physics, Weber, A., (Editor), Springer Verlag, 1979, Ch. 7.
- (17) Hall, R. J., *Combust. Flame*, **35**, 47, (1980).
- (18) Hall, R. J., *Appl. Spectr.*, **34**, 47 (1980).
- (19) Roland, C. M. and Steele, W. A., *J. Chem. Phys.*, **73**, 5924 (1980).
- (20) Bloembergen, N., Purcell, E. M., and Pound, R. V., *Phys. Rev.*, **73**, 679 (1948).
- (21) May, A. D., Stryland, J. C., and Varghese, G., *Can. J. Phys.*, **59**, 1706 (1973).
- (22) Shirley, J. A., Eckbreth, A. C., and Hall, R. J., Investigation of the Feasibility of CARS Measurements in Scramjet Combustion. Technical Paper R79-954390-8, under Contract NAS1-15491, 1979.
- (23) Shirley, J. A., Hall, R. J., and Eckbreth, A. C., Investigation of the CARS Spectrum of Water Vapor. Proceedings of the Lasers '80 Int. Conference, New Orleans, 1980.
- (24) Eckbreth, A. C. and Hall, R. J., *Combust. Sci. and Tech.*, **25**, 175 (1981).
- (25) Rahn, L., Zych, J., and Mattern, P. L., *Opt. Comm.*, **39**, 249 (1979).
- (26) Farrow, R. L., Mattern, P. L., and Rahn, L. A., Crossed-Beam, Background Free CARS Measurements in a Methane Diffusion Flame. Sandia Laboratories Report SAND80-8640, 1980.
- (27) Attal, B., Pealat, M., and Taran, J. P. E., CARS Diagnostics of Combustion. AIAA Paper No. 80-0282, 1980.
- (28) Taran, J. P. E. (1981): ONERA, Chatillon, France. Private Communication.
- (29) Switzer, G. L., Gross, L. P., Roquemore, W. M., Bradley, R. P., and Schreiber, P. W., AIAA Paper No. 80-0353, AIAA, New York, 1980.
- (30) Eckbreth, A. C., *Combust. Flame*, **39**, 133 (1980).
- (31) Stanhouse, I. A., Williams, D. R., Cole, J. B., and Swords, M. D., *Appl. Opt.*, **18**, 3819 (1979).
- (32) Klick, D., K. Marko, A., and Rimai, L., *Appl. Opt.*, **20**, 1178 (1981).
- (33) Kajiyama, K., Komatsu Ltd., Hiratsuka, Japan. Private Communication.

R82-954566-F

APPENDIX I

ROTATIONAL DIFFUSION THEORY CALCULATIONS OF HIGH PRESSURE N₂ AND CO₂ CARS BANDSHAPES

ROTATIONAL DIFFUSION THEORY CALCULATIONS OF HIGH
PRESSURE N₂ AND CO₂ CARS BANDSHAPES*

Robert J. Hall

United Technologies Research Center
East Hartford, Connecticut 06108

One important problem in vibrational CARS spectroscopy concerns the pressure dependence of signatures which consist of closely spaced Q-branch transitions. As the pressure and degree of line overlap increase, an interference effect termed collisional narrowing arises which manifests itself as a blending or coalescence of the various transitions into a band whose width is substantially less than one would expect on the basis of isolated, pressure-broadened lines [1].

Collisional narrowing has its origins in inelastic energy transfer between rotational sublevels, and there is one model of collisional interactions which does not involve adjustable parameters and for which the calculation of polarized Q-branch spectra is particularly simple; namely, the Gordon "extended J-diffusion" model [2]. In this picture of molecular interactions, collisions are presumed to be so strong that a molecule loses memory of its initial rotational state, with the collisions leading to thermal randomization of the magnitude and orientation of the rotational angular momentum.

Brueck [3] has applied the Gordon model to the problem of polarized two-photon resonances in fluids through an analysis that properly accounts for the effect of vibration-rotation interaction. By solving the equation of motion for the density operator with a collision term reflecting the basic assumption about angular momentum thermalization, the vibrationally resonant CARS susceptibility can be shown for one vibrational band to be given by: [3]

$$\chi_{01}^{(3)} = \frac{N\alpha_{10}^2}{\hbar} \left[\sum_J \frac{\Delta f_J}{(\omega_1 - \omega_2 - \omega_J - i(\frac{1}{T_v} + \frac{1}{\tau_J}))} \right] \left[1 + i \sum_J \frac{f_J}{\tau_J (\omega_1 - \omega_2 - \omega_J - i(\frac{1}{T_v} + \frac{1}{\tau_J}))} \right]^{-1} \quad (1)$$

where N is the number density of Raman active molecules; α_{10} the polarizability matrix element; Δf_J the population difference factor for the transition ($\sum f_J = 1$); T_v a characteristic time for vibrational dephasing and relaxation processes; ω_1 and ω_2 the pump and Stokes frequencies, respectively; and ω_J and τ_J the frequency and angular momentum random-

ization time respectively for transition Q(J). The T_v term has been neglected in these calculations.

The dependence of N_2 and CO_2 vibrational CARS spectra on pressure has been investigated experimentally by measurements in a high pressure test cell; details of the experimental apparatus are given in [4]. Figure 1 presents a comparison of the measured N_2 signature bandwidths at $300^\circ K$ with those calculated from the rotational diffusion theory (Eq. 1) for pressures up to 100 atm. Also shown is a calculation based upon isolated line theory, that is, setting the denominator in Equation 1 equal to unity. Good agreement has also been obtained at higher temperatures ($\sim 1600^\circ K$, ~ 30 atm.).

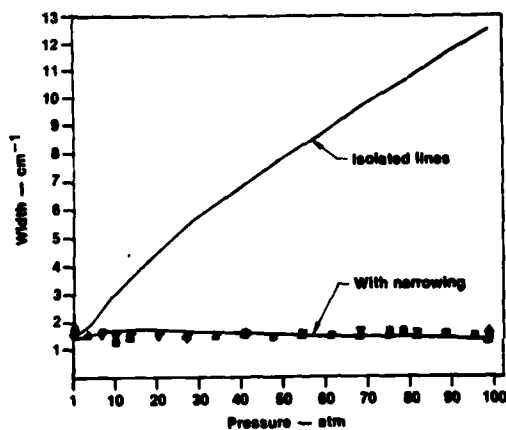


Figure 1. Bandwidth of $300^\circ K$ N_2 CARS Signature vs. Pressure. Resolution $.4 \text{ cm}^{-1}$. From [5] With the permission of North Holland Publ. Co.

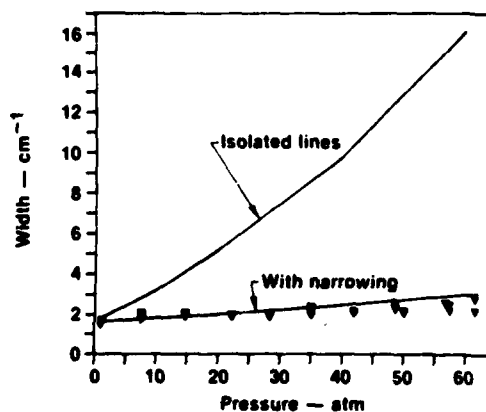


Figure 2. Bandwidth of $300^\circ K$ CO_2 CARS Signature vs. Pressure. Resolution 1.7 cm^{-1} .

The CARS spectrum of the 1388 cm^{-1} ν_1 mode of CO_2 has also been investigated experimentally in the test cell at $300^\circ K$. The measured CO_2 bandwidths show a slight increase with pressure out to the highest pressure recorded, ~ 60 atm (Figure 2), with the predicted bandwidth from the rotational diffusion theory in good agreement. The significant role played by collisional narrowing can be seen by considering the width of the spectrum that would be expected on the basis of isolated lines.

*The experimental portions of the research were sponsored by the Army Research Office under Contract DAAG29-79-C-0008.

REFERENCES

1. M. Baranger, Phys. Rev., 111, 494, (1958); 112, 855 (1958).
2. R.G. Gordon, J. Chem. Phys., 44, 1830 (1966).
3. S.R.J. Brueck, Chem. Phys. Lett., 50, 516 (1977).
4. R.J. Hall, J.F. Verdick, and A.C. Eckbreth, Opt. Comm., 35 69 (1980).
5. R.J. Hall and D.A. Greenhalgh, Opt. Comm., in Press.

ATE
LME
8